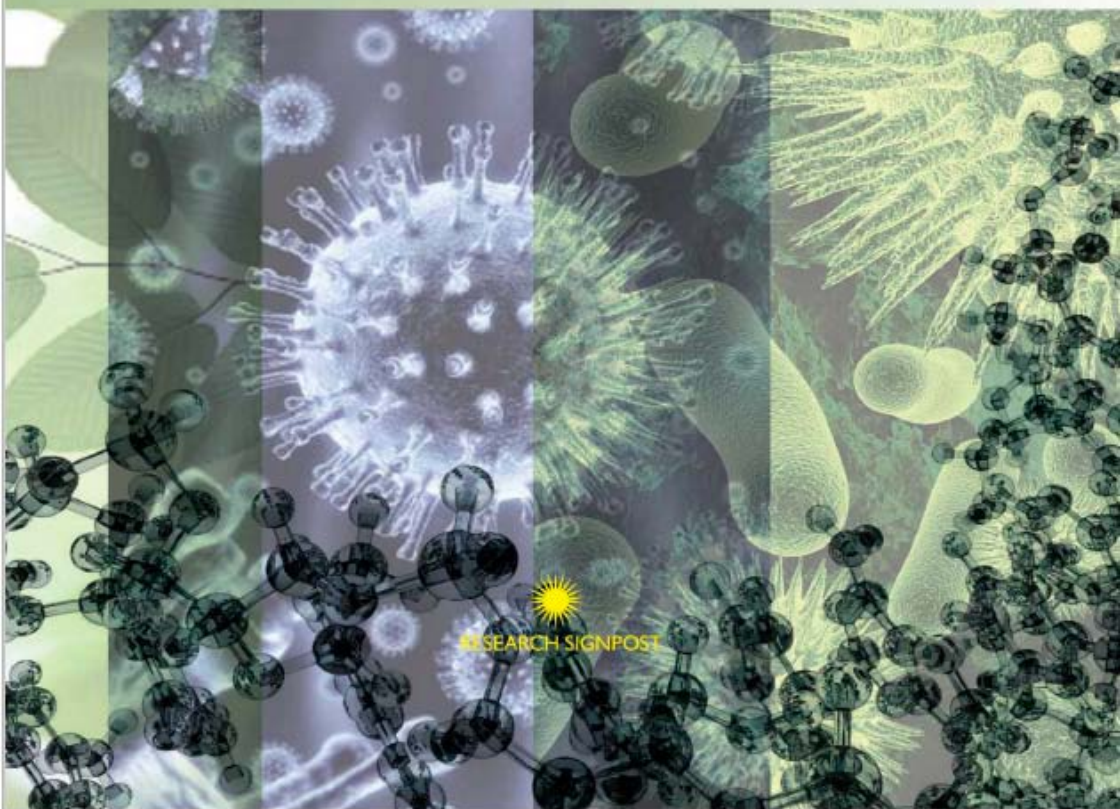


RECENT ADVANCES IN PHARMACEUTICAL SCIENCES

VOL. VII

Editors

Diego Muñoz-Torrero, Montserrat Riu, Carles Feliu



Recent Advances in Pharmaceutical Sciences VII

Editors

Diego Muñoz-Torrero

Montserrat Riu

Carles Feliu

Faculty of Pharmacy and Food Sciences, University of Barcelona, Spain



Research Signpost, T.C. 37/661 (2), Fort P.O., Trivandrum-695 023
Kerala, India

Published by Research Signpost

2017; Rights Reserved
Research Signpost
T.C. 37/661(2), Fort P.O.,
Trivandrum-695 023, Kerala, India

E-mail IDs: signpost99@gmail.com;
rsignpost@gmail.com

Websites: <http://www.reassign.com>
<http://www.trnres.com>
<http://www.signpostejournals.com>
<http://www.signpostebooks.com>

Editors

Diego Muñoz-Torrero
Montserrat Riu
Carles Feliu

Managing Editor

Shankar G. Pandalai

Publication Manager

A. Gayathri

Research Signpost and the Editors assume no responsibility
for the opinions and statements advanced by contributors

ISBN: 978-81-308-0573-3

Preface

The E-book series Recent Advances in Pharmaceutical Sciences reports research contributions from different areas of the multidisciplinary field of Pharmaceutical Sciences. This seventh volume consists of nine chapters, mainly dealing with the fields of botany, physiology, food science, biochemistry & molecular biology, plant physiology, microbiology, parasitology, pharmacology, and medicinal chemistry.

Chapter 1 reports on ethnobotanical prospections on the interface between the two most relevant plant uses, namely food and medicinal applications. Despite the greater difficulty to find information about folk functional foods, compared with collecting data on medicinal or food uses separately, the reported results show promise for the design and development of new commercial nutraceuticals, and even afford good prospects for ethnoveterinary uses. Chapter 2 elaborates on the hypothesis that some probiotic bacteria derived from a neonatal source, such as breast milk or from baby faeces, can enhance the immune response and the anti infective capacity of the organism. Through three particular representative studies, the Authors discuss the beneficial effect of early life probiotics on the immune development and prevention against rotavirus infections, the leading cause of severe diarrhoea among infants and young children. Nutrimetabolomics has been proposed as a tool for assessing the changes in metabolome associated with food consumption and/or the effects of a dietary intervention. Chapter 3 summarizes the most relevant results of recent research on the identification of biomarkers related to food ingestion (biomarkers of intake), and their potential association with health (biomarkers of effect), through the application of an untargeted HPLC-QToF-MS metabolomics approach in nutritional studies, highlighting the greater predictive ability of dietary exposure through multimetabolite biomarker models than that of individually evaluated single metabolites, and the usefulness of combined models to improve accuracy during the evaluation of dietary intake.

Chapter 4 describes the design and use of repair-polypurine reverse Hoogsteen hairpins (PPRHs) and editing-PPRHs as a new methodology either to correct a point mutation or to edit a genomic fragment of the dihydrofolate reductase gene in Chinese Hamster Ovary (CHO) cells. The Authors provide evidences that repair-PPRHs and editing-PPRHs represent a powerful tool for gene therapy to correct disorders caused by point mutations and an alternative method to the use of site specific nucleases for efficient editing, devoid of off-target effects caused by

nucleases and non-homologous end joining effects stimulated after a DNA double strand break. Amaryllidaceae plants are not only known for their ornamental flowers, but also for the medicinal value conferred by their exclusive group of alkaloids. Chapter 5 reviews the structural determinants that are responsible for the antitumor, antiparasitic, and anticholinesterasic activity of the Amaryllidaceae alkaloids. Chapter 6 reports on the application of cryo-electron tomography techniques to the study of the Antarctic cold-adapted bacterium *Pseudomonas deceptionensis* MIT, which has revealed the existence of a novel cytoplasmic structure, the “stack”. This novel structure consists of a set of stacked oval discs, variable in number, surrounded by a lipid bilayer, which are located close to the cell membrane and to DNA fibers and might play a role in chromosome dynamics. Ingestion of undercooked snails, parasitized by *Brachylaima* (Trematoda) metacercariae, can cause brachylaimiasis, a parasitic disease with a mortality rate 5-10%. Chapter 7 describes a strategy to circumvent this food-borne disease, based on the use of feeding stuff supplemented with praziquantel. β -Amyloid peptide is widely regarded as the main culprit of Alzheimer’s disease, the main neurodegenerative disorder and one of the major causes of mortality in developed countries. Chapter 8 provides an overview of the different therapeutic approaches and anti-Alzheimer drug candidates that are under development, mostly designed to hit β -amyloid biology, with the potential to modify the natural course of the disease. The M2 proton channel protein, essential for the viability of the influenza A virus, is a key target to tackle this major threat to human health. Unfortunately, most of influenza virus isolates are now resistant to the M2 proton channel blocker amantadine, due to the appearance of mutations V27A, S31N, and L26F. Chapter 9 describes the design and synthesis of novel classes of polycyclic small molecules that are purported to inhibit the wild-type and the mutant M2 channels.

We hope that this seventh volume will be of interest for all the scientific community, especially for those interested in pharmaceutical, medical, biological, and chemical sciences.

Dr. Diego Muñoz-Torrero
Dr. Montserrat Riu
Dr. Carles Feliu
Faculty of Pharmacy
and Food Sciences
University of Barcelona
Spain

Contents

Chapter 1

Medicinal and food plants in ethnobotany and ethnopharmacology:
Folk functional foods in Catalonia (Iberian Peninsula) 1
*Joan Vallès, Ugo D'Ambrosio, Airy Gras, Montse Parada,
Montse Rigat, Ginesta Serrasolses and Teresa Garnatje*

Chapter 2

Immunomodulatory role of probiotics in early life 19
*Maria J. Rodríguez-Lagunas, Ignasi Azagra-Boronat, Sandra Saldaña-Ruiz
Malen Massot-Cladera, Mar Rigo-Adrover, Anna Sabaté-Jofre,
Àngels Franch, Margarida Castell and Francisco J. Pérez-Cano*

Chapter 3

Dietary exposure biomarkers in nutritional intervention
and observational studies to discover biomarkers of intake
and disease risk through an HPLC-QToF-MS metabolomics approach 35
*Mar Garcia-Aloy, Rafael Llorach, Mireia Urpi-Sarda, Rosa Vázquez-Fresno
Olga Jáuregui and Cristina Andres-Lacueva*

Chapter 4

Polypurine Reverse Hoogsteen Hairpins as a tool for gene repair and editing 51
Carles Ciudad, Anna Solé, Alex J. Félix and Véronique Noé

Chapter 5

Research in natural products: Amaryllidaceae ornamental plants
as sources of bioactive compounds 69
*Laura Torras-Claveria, Luciana Tallini, Francesc Viladomat,
and Jaume Bastida*

Chapter 6

Deciphering the stack, a novel bacterial structure, by (cryo-) transmission electron microscopy and (cryo-) electron tomography 83
Lidia Delgado, Carmen López-Iglesias and Elena Mercadé

Chapter 7

Development of a strategy for the administration of praziquantel to the terrestrial edible snail *Cornu aspersum* parasitized by *Brachylaima* sp. Metacercariae 101
Laia Gállego and Mercedes Gracenea

Chapter 8

Strategies against β -amyloid protein as therapeutics in Alzheimer's disease 115
Jaume Folch, Miren Ettcheto, Oriol Busquets, Elena Sánchez-López, Rubén Darío Castro-Torres, Carlos Beas-Zarate, Mercè Pallàs, Jordi Olloquequi, Daniela Jara, M.L. Garcia, Carme Auladell and Antoni Camins

Chapter 9

Fighting the Influenza A virus. New scaffolds and therapeutic targets 133
Marta Barniol-Xicota and Santiago Vázquez



Research Signpost
Trivandrum
Kerala, India

Recent Advances in Pharmaceutical Sciences VII, 2017: 1-17 ISBN: 978-81-308-0573-3
Editors: Diego Muñoz-Torrero, Montserrat Riu and Carles Feliu

1. Medicinal and food plants in ethnobotany and ethnopharmacology: Folk functional foods in Catalonia (Iberian Peninsula)

Joan Vallès¹, Ugo D'Ambrosio^{1,2}, Airy Gras¹, Montse Parada^{1,2}
Montse Rigat^{1,2}, Ginesta Serrasolses^{1,2} and Teresa Garnatje²

¹Laboratori de Botànica (UB), Unitat Associada al CSIC, Facultat de Farmàcia i Ciències de l'Alimentació, Av. Joan XXIII s/n, 08028 Barcelona, Catalonia, Spain; ²Institut Botànic de Barcelona (IBB-CSIC-ICUB), Passeig del Migdia s/n, 08038 Barcelona, Catalonia, Spain

Abstract. Ethnobotanical studies have focused with particular intensity -especially in industrialized countries- on food and medicinal plant properties and management claimed by informants. Nevertheless, the uses on the interface between both areas have not been addressed to the same proportion, although they have a very important place both in ethnological and in health issues. We present in this paper the results of ethnobotanical prospections carried out in Catalonia regarding folk functional foods and nutraceuticals. A total amount of 1,888 use reports from 195 taxa, belonging to 64 botanical families, corresponding to this category have been collected and analyzed. The most quoted taxa are *Thymus vulgaris*, *Allium sativum*, *Ruta chalepensis* and *Sambucus nigra*, the most cited families are Lamiaceae, Rosaceae, Rutaceae, Amaryllidaceae, Asteraceae and Apiaceae. Aerial parts of the plants are by an ample margin the most used, and alcoholic

Correspondence/Reprint request: Prof. Joan Vallès, Laboratori de Botànica (UB), Unitat Associada al CSIC Facultat de Farmàcia i Ciències de l'Alimentació, Av. Joan XXIII 27-31, 08028 Barcelona, Catalonia, Spain
E-mail: joanvalles@ub.edu

beverages are the most common way of preparation of the products, closely followed by the direct ingestion of raw materials. The results obtained in ethnobotanical prospections related to the folk functional food (FFF) concept are numerous and robust enough to appear as promising for new commercial nutraceutical products development.

Introduction

Ethnobotanical and ethnopharmacological studies are very abundant all over the World, including not only developing areas, a priori richer in folk knowledge about biodiversity and its management, but in industrialized areas such as North America and Western Europe as well. In these investigations, food and medicinal information occupies a preeminent place in the ranking of popular uses, usually being the two first ones, whereas other plant uses, such as, to give two examples, artisanal or dyeing ones, are less commonly preserved, particularly in developed regions [1, 2, and references therein]. The interface of those two more relevant uses is particularly attractive, although it has scarce attention in ethnobotany. In the present paper we contribute data on folk functional foods or nutraceuticals in Catalonia (NE Iberian Peninsula) coming from ethnobotanical prospections carried out in this area.

1. Ethnobotany and ethnopharmacology

Ethnobotany, a term coined in 1895 and published the following year [3], is a multiapproach discipline placed on the interface of human and natural sciences [4], which deals with plant knowledge, use and management by human groups. It is a branch of ethnobiology, together with ethnozoology, ethnoecology or ethnomycology (the latter dealing with folk knowledge on fungi, and most frequently merged with ethnobotany). On the one hand, it belongs to the domains of economic botany (together with industrial botany, for instance) and ethnosciences (at the same level as popular chemistry in cooking, as an example). On the other hand, the ethnobotanical corpus of popular wisdom is an important part of the traditional ecological knowledge [5]. Finally, it has a non-negligible component of citizen science, since people are at the basis of research, although, logically, conducted by scientists, and has relevant issues linked both to primary and secondary education [2, 6, 7]. Ethnobotanical data linked to aspects of health (mostly medicine, but also food in many respects) are included in the field of medical or

pharmaceutical ethnobotany, which has a close and intimate relationship with ethnopharmacology, a term coined in 1967, sharing some aspects with pharmacognosy and phytotherapy [2]. Ethnopharmacology shows a larger reach than pharmaceutical ethnobotany, since it comprises not only knowledge on plants and fungi, but on animals and on mineral products as well, and it addresses also pharmacological issues. Ethnobotany in general, has, in its turn, a larger scope than ethnopharmacology, dealing not only with medicinal and associate uses, but with any popular knowledge on plants. In any case, both disciplines share a significant part of aims, methods, results and their derivatives. Pharmaceutical ethnobotanical and ethnopharmacological approaches have been considered as forming a platform for new drug design and development [8]. In this respect, one of the recipients of 2016's Nobel Prize for Medicine or Physiology was recognized for her development of antimalarial plants from traditional Chinese medicine ethnobotanical evidence [9]. The medicinal uses of food plants, and the leads they can achieve and generate, clearly fall within this common area of ethnobotany and ethnopharmacology.

2. Functional foods, nutraceuticals and their popular knowledge and management

The borders between the concepts of food and medicine have always been diffuse. Already Hippocrates (5th and 4th centuries BC) stated that food can be medicine and medicine can be food for human beings [10]. Consistently with this idea, the concept of nutraceutical (also spelled nutriceutical) arose in 1979 to define foods providing health benefits, both for preventing or treating diseases [11, 12]. Other terms, such as medicinal food or pharmafood or functional food (the latter, appearing in 1993 [13], quite extended) have also been used as synonyms or quasi-synonyms of nutraceuticals to indicate any kind of food with physiological functional properties in the human organism [14]. Commercially and according to health products legislation (and, again, in some cases with no total coincidence in the concept but, in any case, quite related), the term 'nutritional supplement' alludes to foods or food derivatives with these properties as well. Probably one of the oldest-dated and most popular commercialized functional food or nutraceutical product is milk with added omega-3 and omega-6 acids (those coming from salmonids and related cold-water fishes), having protective properties against cardiovascular troubles and hypercholesterolemia [15]. Quite recently, the term 'superfood' was coined to mean "a food (such as salmon, broccoli, or

blueberries) that is rich in compounds (such as antioxidants, fiber, or fatty acids) considered beneficial to a person's health" (Merriam-Webster dictionary, <http://www.merriam-webster.com/dictionary/superfood>, accessed October 10, 2016). Irrespective of legal and trade considerations, this term has a very similar sense to the nutraceuticals' concept. All these terms and the high number of food products put on the market with direct or indirect allusions to medicinal properties account for the relevance of this concept that make the link between nutrition and medicine [11]. Independent of logical pros and cons [16], a large experience exists of marketing such products, either as drugs or -more frequently because it is easier or cheaper due to legal dispositions-, as food supplements [17].

Despite the concept of nutraceutical (and the above-mentioned associated terms) having been early addressed by ethnobiologists [14, 18] and a compilation of health foods existing [19], research on plant-based nutraceuticals with ethnobotanical approaches is still scarce. Nevertheless, apart from seminal Etkin's works [14, 18], several authors have addressed this question in Mediterranean territories [20, 21] as well as in North America

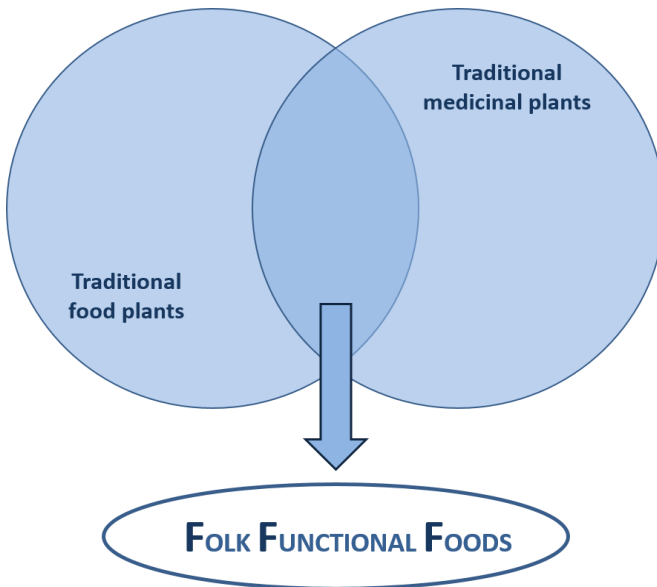


Figure 1. Folk functional foods and their relationships with traditionally-used medicinal and food plants.

[22, 23]. According to these and other examples, as well as our own data from previous ethnobotanical prospections in Catalan-language territories, we proposed the term ‘folk functional food’ (hereafter FFF) to name the concept of popular medicinal knowledge and use of food plants [24] (Fig. 1). This concept was less restrictive than the same one used by Pieroni & Quave [25], who distinguished three levels in medicinal uses of food plants and reserved FFF for taxa eaten because they are healthy in general terms. We believe that this concept is basically equivalent to the term ‘salutiferous’ and that the idea of FFF encompasses more uses than this one (Fig. 1). Later, the term ‘traditional functional food’ was coined [26] with the same sense as our FFF. In this paper, FFF will be specifically addressed in depth on the basis of our data from ethnobotanical prospections in several regions of Catalonia.

3. Methodology

The area considered is constituted by Catalonia, located in the northeastern Iberian Peninsula. The territories where ethnobotanical studies have been performed, going from sea level to high mountain, are shown in Fig. 2.

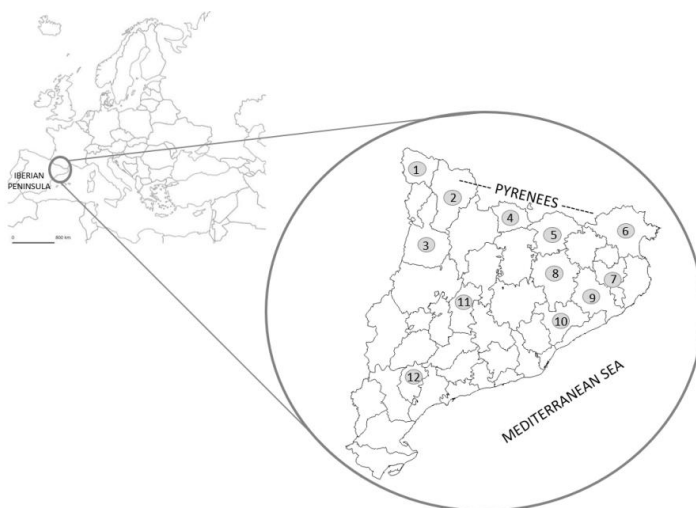


Figure 2. Studied areas: Vall d’Aran (1), Pallars (Pallars Sobirà, 2; Pallars Jussà, 3), Cerdanya (4), Ripollès (5), Alt Empordà (6), Gironès (7), Guillerics (8, 9), Gallecs (10), Vall del Tenes (10), Montseny (8, 9, 10), Segarra (11), Ulldemolins (12).

The ethnobotanical research was carried out between 1987 and 2016, not at the same time in all the regions, but overlapping in many of them. The informants were selected in each area starting with some of them known by the interviewers (in each studied region at least one interviewer was closely linked to the territory concerned) and then according to a snowball model [27]. Most informants were middle-aged to elderly people, who were born in the studied area or have lived there a very significant part of their lives, and a large number of them have primary studies and professions linked to agricultural and cattle raising activities.

The basic survey method was the semistructured interview [28], consisting of general, but subject-oriented conversations, after prior informed consent from the interviewees. Interviews were developed avoiding asking direct questions, which could influence, direct or bias the informants' responses. The interviews were developed in the Catalan language, except in Vall d'Aran, where they were carried out in the Occitan language (locally called Aranese); in all cases the language was common to interviewers and interviewees.

All plants quoted in each territory were collected and identified using the *Flora manual dels Països Catalans* [29]. For botanical families, Angiosperm Phylogeny Group criteria were used ([30], <http://www.mobot.org/MOBOT/research/APweb>, accessed October 10, 2016). A voucher for each taxon in each territory was prepared and deposited at the herbarium BCN, of the *Centre de Documentació de Biodiversitat Vegetal, Universitat de Barcelona*.

Once finished, the interviews were transcribed and the results entered to our research team's database. Analyses performed consisted of descriptive statistics (percentages, mean, standard deviations, ranges) for botanical variables (species, families, part used and mode of preparation). Indexes accounting for the consistency and reliability of the data collected have been calculated: percentage of taxa and uses quoted by at least three independent informants [31, 32] and the informant consensus factor (F_{IC} [33]; number of use reports minus number of taxa divided by number of use reports minus 1).

4. Results and discussion

Use reports, data reliability, taxa, and families

A total of 1,888 use reports (hereafter UR) were collected for 195 taxa belonging to 64 botanical families. The results obtained show a high

consistency and reliability. On the one hand, a total of 79 taxa, representing a 40.51%, have at least one use (and in some cases, more than one) quoted by three or more independent informants, which is a criterion for reliability of ethnobotanical data [31, 32]. On the other hand, the F_{IC} , accounting for the consistency (and non-dispersion) of the information reported by the informants, is very high (0.90, out of a maximum of 1.00), suggesting a solid corpus of popular knowledge on FFF and a high relevance of such uses in the territories studied. The high values of these indexes concerning this use category (FFF) agree with the results obtained, in the same cultural and geographical area, in other use categories (medicinal, food, and other uses) [34, and references therein].

Apart from the species level, the 195 taxa include 23 subspecies and five varieties, and four entities have only been determined to the generic level. All taxa but two fungal species belong to plants, with no representative of algae and bryophytes, and only one of pteridophytes. The 18 most quoted species, roughly representing half of the UR (50.05%), are listed in Table 1. Eleven out of these 18 top taxa are included in the “Dictionary of Nutraceutical and Functional Foods” [35]. This means, on the one hand, that a significant number of the plants most used as FFF in Catalonia is consistent with the state-of-art of the subject at global level. On the other hand, this also means that a not less relevant number of such taxa have not (or have only scarcely) been considered to date as functional foods (at least at global and commercial levels), but do have their properties, claimed at popular level, so that they could constitute a good target for further research focused on new nutraceutical product development.

Thymus vulgaris occupies a preeminent first position in this ranking, followed by *Allium sativum*, *Ruta chalepensis* and *Sambucus nigra*. The first and fourth of these taxa are always among the top ones in pharmaceutical ethnobotanical studies in the area considered and, in general, in the Mediterranean region [24, and references therein]. In addition, the soup prepared with *Thymus vulgaris* is a very typical dish of traditional (and now even gastronomic) cuisine [36]. The other two taxa, although being relevant in such studies, are not in the very first places. This may be due to the fact that both taxa are specifically considered as FFF: *Allium sativum*, the only species quoted as FFF in the 12 areas prospected, is frequently consumed as food and medicine at the same time, and *Ruta chalepensis* is particularly used, in very small amounts, to flavor drinking chocolate and to give medicinal properties to this food.

Table 1. Plant taxa most quoted as folk functional foods in the territories considered. AE: Alt Empordà, CE: Cerdanya, GA: Gallecs, GI: Gironès, GU: Guillerries, MO: Montseny, PA: Pallars, RI: Ripollès, SE: Segarra, UL: Ulldemolins, VA: Vall d'Aran VT: Vall del Tenes. Asterisk (*) after the scientific name indicates the reference of the taxon in the “Dictionary of Nutraceuticals and Functional Foods” [35].

Taxon (herbarium voucher)	Vernacular Catalan (and Occitan-Aranese, when reported) names	Use reports	Medicinal uses	Territories
<i>Thymus vulgaris</i> L.* (BCN 25023)	farigola, timó (timonet)	116	Anticephalalgic. Antidysmenorrhoeal. Digestive. Gastrointestinal antiseptic and anti-inflammatory. Tonic, reinforcing, vitamin	AE, CE, GA, GI, GU, MO, PA, RI
<i>Allium sativum</i> L.* (BCN 24708)	all (alh)	90	Antialgic. Antihelmintic. Antihypertensive. Antirheumatic. Cardiotonic. Digestive. Hematocathartic. Hipolypemiant. Internal antiseptic. Resolutive. Salutiferous. Vasotonic	AE, CE, GA, GI, GU, MO, PA, RI, SE, UL, VA, VT
<i>Ruta chalepensis</i> L. (BCN 24980)	ruda	77	Antidiarrhoeal. Antidysmenorrhoeal, Antihelmintic. Anti-nauseous. Digestive. Gastrointestinal antiseptic and anti-inflammatory. Labour and post-labour coadjuvant. Sedative. Tranquillizer	AE, CE, GI, GU, MO, PA, RI
<i>Sambucus nigra</i> L. (BCN 24984)	bonarbre, saüc (saüquèr)	77	Antidysmenorrhoeal. Digestive. Gastrointestinal antiseptic and anti-inflammatory. Refreshing	AE, CE, GI, GU, MO, RI
<i>Mentha spicata</i> L.* (BCN 24930)	herba-sana, menta (menta)	68	Antidysmenorrhoeal, Antihelmintic. Anti-nauseous. Digestive. Gastrointestinal antiseptic and anti-inflammatory. Refreshing	AE, CE, GA, GI, MO, RI
<i>Citrus limon</i> (L.) Burm.* (BCN 27241)	llimoner (limon)	58	Anticatarral. Antidiarrhoeal. Antidysmenorrhoeal. Antihypertensive. Digestive. Gastrointestinal antiseptic and anti-inflammatory. Hematocathartic. Internal antiseptic	AE, CE, GA, GI, GU, MO, PA, RI, SE, VA, VT

Table 1. Continued

<i>Hyssopus officinalis</i> L. (BCN 24906)	hisop	56	Antidiarrhoeal. Antidysmenorrhoeal. Antinauseous. Digestive. Gastrointestinal antiseptic and anti-inflammatory. Labour and post-labour coadjuvant	CE, GU, MO, PA,
<i>Rosa canina</i> L. (BCN 20772)	gavarrera, roser de pastor (garrauèr)	56	Digestive. For child weakness (<i>enaiguament</i>). Tonic, reinforcing, vitamin	CE, GU, VA
<i>Cydonia oblonga</i> Mill. (BCN 24758)	codonyer (codonhèr)	52	Antidiarrhoeal. Digestive. Gastrointestinal antiseptic and anti-inflammatory. Refreshing	AE, CE, GA, GI, MO, PA, RI
<i>Gentiana lutea</i> L. (BCN 24893)	gençana, genciana (jançana)	46	Antianorectic, aperitive. Hematocathartic. Tonic, reinforcing, vitamin	CE, RI, VA
<i>Oryza sativa</i> L.* (BCN-Etno 16)	arròs	38	Antidiarrhoeal	AE, CE, GA, PA, RI, SE
<i>Allium cepa</i> L.* (BCN 27279)	ceba (ceba)	35	Cardiotonic. Diuretic. Hematocathartic. Laxative	AE, CE, GA, GU, MO, PA, RI, SE, VA
<i>Taraxacum officinale</i> Weber in Wiggers* (BCN 25015)	pixallits, xicoina (chicòia)	34	Antianorectic, aperitive. Antipelochemic. Hematocathartic	AE, CE, GI, MO, PA, RI, VA
<i>Juniperus communis</i> L.* (BCN 24910)	ginebre, ginebró (gimbros)	30	Digestive. For child weakness (<i>enaiguament</i>). Salutiferous	AE, CE, GU, MO, RI
<i>Daucus carota</i> L.* (BCN 46847)	carrota, pastanaga, safranòria (carròta)	28	Antidiarrhoeal. Visual restaurative	AE, CE, GA, MO, PA, RI, VT
<i>Juglans regia</i> L.* (BCN 24908)	noguer, noguera (escarèr)	28	Antidysmenorrhoeal. Digestive. Hypolipemiant	AE, GA, GU, MO, PA, RI
<i>Mentha pulegium</i> L. (BCN 113598)	poliol, poniol	28	Antidysmenorrhoeal. Refreshing	AE, GU, MO, UL
<i>Prunus domestica</i> L.* (BCN 46834)	pruner, prunera	28	Laxative	AE, CE, GA, PA, RI, VT

Apart from two families of fungi, one of ferns and two of gymnosperms, the remaining 59 are angiosperms. The most cited families (Fig. 3) were Lamiaceae (412 UR), Rosaceae (233 UR), Rutaceae (162 UR); Amaryllidaceae (133 UR), Asteraceae (130 UR), and Apiaceae (125 UR). Percentages are shown in Fig. 3. Most of these families appear in the top of the ranking in practically all ethnobotanical works performed in Catalonia dealing with pharmaceutical, food or other uses [34, and references therein], because they are big families (Asteraceae, for instance, is the largest one in plants) with a relevant presence in the Mediterranean region. Conversely, two of the families (Rutaceae and Amaryllidaceae) do not occupy the first positions in such rankings, although they have a non-negligible presence. The intense and specific nutraceutical uses of *Citrus limon* and *Allium sativum* (see Table 1), respectively belonging to those two families, may explain this situation. In Amaryllidaceae, Rutaceae and Apiaceae families, the UR are concentrated in a few species (4, 6, and 10, respectively), whereas in the Rosaceae, Lamiaceae and Asteraceae the number of species is higher (22, 24, and 26, respectively). Some of these families (Asteraceae, Lamiaceae, Rosaceae, Rutaceae) are quoted as top ones in FFF in other territories, and well-known for their chemical composition justifying their nutraceutical properties [26, and references therein].

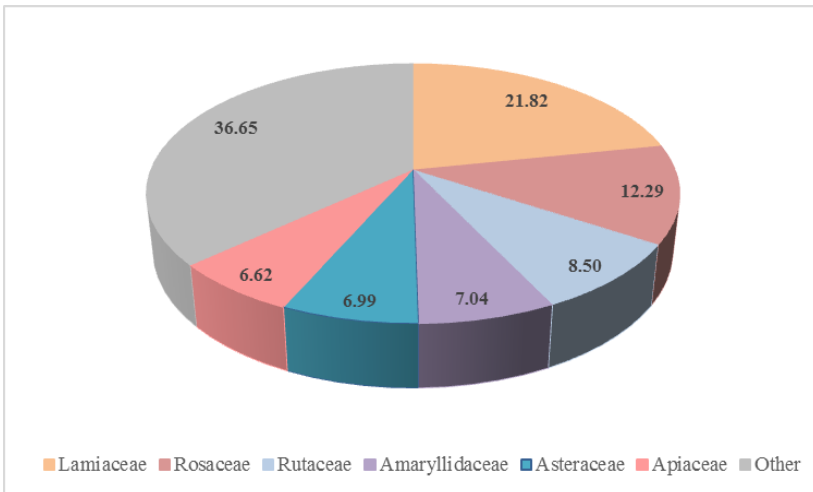


Figure 3. Main families providing plant folk functional foods in the studied areas.

Parts of plants used and preparation forms

The parts of plants employed for nutraceutical purposes are presented in Fig. 4.

Aerial part is largely dominating. Apart from the complete aerial part itself, some aerial organs, such as fruits, leaves and flowers complete this more easily available part of the plant. The use of the flowered aerial part of *Thymus vulgaris*, with more than 100 UR (see Table 1), make this part of the plant particularly important. Plants used as salads help to complete this first position in the ranking. Some subterranean parts (roots and tubers, very typically consumed in food plants) occupy a discrete, but not at all null, place.

The modalities of preparation of the plant products claimed as FFF are presented in Fig. 5, and Fig. 6 illustrates a few examples of some of the commonest forms.

Alcoholic beverages received almost one third (29.61%) of the UR. This basically comes from liqueurs or different kind of wines, which are often used for different purposes, such as aperitive or digestive. Among those, *ratafia*, a very typical Catalan liqueur including *Juglans regia* unripe fruits, along with a number of other plant taxa, overpassing 50 in

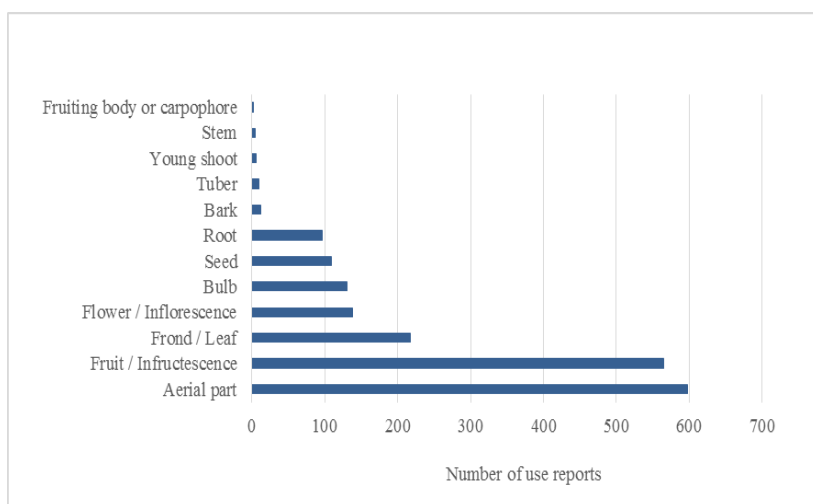


Figure 4. Plant (and fungal) parts used as folk functional foods in the studied areas.

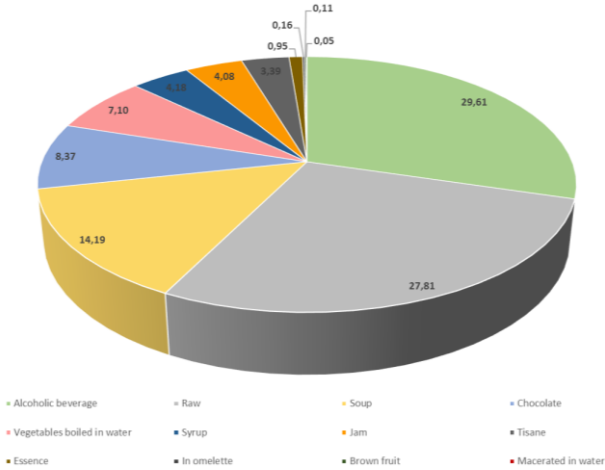


Figure 5. Preparation forms of folk functional foods in the studied areas.



Figure 6. Examples of four out of the five most quoted preparation forms of folk functional foods in the studied areas. A. First step of *ratafia* (a digestive and antidysmenorrhoeal liqueur) preparation, with abundant *Juglans regia* and other taxa. B. Salad of *Taraxacum dissectum*, diuretic and hematocathartic. C. Boiled leaves of *Chenopodium bonus-henricus*, blood depurative. D. Soup with *Thymus vulgaris*, digestive and antidiarrhoeal.

some cases [37], predominates. The other highly relevant form is just the one without preparation (apart from cleaning): raw plant consumption, most often linked to their use as salads, represents more than a quarter (27.81%) of the UR. Hot, drinking chocolate is an also relatively common (and rather original) vehicle (8.37% of UR) for different plant taxa that confer it functional activities. Conversely, tisane, one of the major preparation or administration forms in pharmaceutical ethnobotany and folk phytotherapy, shows a very low occurrence (3.39% of UR) among FFF. This can be explained by the fact that nutraceutical uses are predominantly linked to plant consumption as food, and tisane is perceived by the informants more as a specific medicine than an alimentary product.

Nutraceutical uses

The main types of uses of the plants claimed to constitute FFF by our informants are presented in Table 2, which contains the main uses, representing 73.09% of the total.

Table 2. Number and percentage of use reports of the kinds of nutraceutical uses in the areas studied.

Nutraceutical uses	Use reports	%
Antidysmenorrhoeal	262	13.88
Digestive	220	11.65
Gastrointestinal antiseptic and anti-inflammatory	219	11.60
Antidiarrhoeal	167	8.85
Hematocathartic	129	6.83
Refreshing	96	5.08
Anti-nauseous	79	4.18
Laxative	73	3.87
For child weakness (<i>enaiguament</i>)	49	2.60
Tonic, reinforcing, vitamin	47	2.49
Antianorectic, aperitive	39	2.07
Other uses	508	26.91

The most frequent nutraceutical property, by far, is the one linked to troubles of the digestive system: digestive itself, gastrointestinal antiseptic and anti-inflammatory, antidiarrhoeal, anti-nauseous, and laxative. This is consistent with the fact that digestive use is one of the commonest in pharmaceutical ethnobotanical prospections [38, and references therein], and also with the idea that, in general, phytotherapeutic uses are basically addressed to mild and chronic diseases [39], among which gastrointestinal ones are important. Nevertheless, stronger uses, such as blood depurative or appetite stimulating, are relevant too. Indeed, the first position (if we do not associate all digestive system troubles) is occupied by the antidysmenorrhoeal use. This is mostly linked to the classical and considerable consumption of the liqueur called *ratafia*, in general terms considered as digestive, by women having troubles in menstruation. Another use with a high number of reports is related to a degraded physical state of children due to psychological reasons. The Catalan word *enaiguament* (textually meaning flooding) designates the state of children when they feel themselves not well attended by their parents when a smaller child is born. This syndrome, consisting on a general organic weakness, is treated with food with functional properties.

Some nutraceutical properties have less UR, but are not uninteresting and deserve a comment. Antioxidant, a very relevant function in commercial nutraceuticals, has received only two UR, indicating that this relatively recent medical concept is not yet present in traditional thinking. Another property quite usual in dietary supplements and nutraceutical products collected 24 UR, far from the top ones in the ranking (Table 2): salutiferous (sometimes expressed as panacea and equivalent to what is usually called adaptogenic in phytotherapy); this means that most FFF in the studied area are addressed to specific troubles rather than to general health maintenance.

5. Conclusion

This paper represents a first approach to the FFF in several areas covering different biogeographical regions of Catalonia. Tradition (in classical plants for the territory, such as *Thymus vulgaris*) and innovation (in plants such as *Actinidia chinensis*, which appeared on the food market in Catalonia not a lot of years ago, but is already used as medicine) go together to configure an interesting field of folk knowledge and ethnobotanical research. The search for information concerning FFF is not

as simple as that for collecting data on medicinal or food uses separately, since some concepts applied to food, such as salutiferous, are not easy to follow. Nevertheless, the results obtained in ethnobotanical prospections related to the FFF concept are both numerous and robust enough to appear as promising and interesting for the design and development of new commercial nutraceutical products. In addition, only human-directed nutraceutical properties have been addressed here, and we believe that it would be worth investigating the same topic in an ethnoveterinary context.

Acknowledgements

The authors are first grateful to their informants, who accepted to share with them their wisdom on biodiversity management. Antoni Agelet, Clara Aliu, Bea Almeida, M. Àngels Bonet, Jordi Camprubí, Núria Llurba, Joan Muntané, Dolors Raja, Mònica Roldán and Anna Selga are thanked for their contributions to field work, Samuel Pyke (Barcelona's Botanical Garden) for the revision of the English language, and Esperança Carrió for her advice after reading the first version of this manuscript. This work was supported by the Catalan government (projects 2005ACOM00024, 2009ACOM00012, 2009ACOM00013, 2009SGR439, 2014SGR514), and the Spanish government (project CSO2014-59704-P).

References

1. Pardo-de-Santayana, M., Pieroni, A., Puri, R. K. 2010, The Ethnobotany of Europe, Past and Present. In Pardo-de-Santayana, M., Pieroni, A., Puri, R. K. (Eds.) Ethnobotany in the new Europe. People, Health and Wild Plant Resources, Berghahn Books, New York and Oxford.
2. Heinrich, M., Jäger, A. K. (Eds.) 2015, Ethnopharmacology, Willey Blackwell, Oxford.
3. Harshberger, J. W. 1896, *Bot. Gaz.*, 21, 146.
4. Barrau, J. 1971, *Bull. Soc. Bot. France*, 118, 237.
5. Turner, N. J., Luczaj, L. J., Migliorini, P., Pieroni, A., Dreon, A. L., Sacchetti, L. E., Paoletti, M. G. 2011, *Crit. Rev. Plant Sci.*, 30,198.
6. Mueller, M., Tippins, D., Bryan, L. 2012, *Democr. Educ.*, 20, 1.
7. Vallès, J., Garnatje, T. 2015, *Mètode - Sci. Stud. J.*, 86, 22.
8. Heinrich, M., Gibbons, S. 2001, *J. Pharm. Pharmacol.*, 53, 425.
9. Tu, Y. Y. 2011, *Nature Med.*, 10, XIX.
10. Arai, S., Vattem, D. A., Kumagai, H. 2016, Functional foods – History and concepts. In Vattem, D. A., Maitin, V. (Eds.) Functional foods, nutraceuticals

- and natural products. Concepts and applications. DEStech Publications, Lancaster.
11. Blesalski, H. K. 2001, Nutraceuticals: the link between nutrition and medicine. In Krämer, K., Hoppe, P. P., Packer, L. (Eds.) Nutraceuticals in health and disease prevention. Marcel Dekker, New York.
 12. López, R., Medina, I. (eds.) 2009, La alimentación en el siglo XXI. Consejo Superior de Investigaciones Científicas, Madrid.
 13. Swinbanks, D., O'Brien, J. 1993, *Nature*, 346, 180.
 14. Etkin, N. L., Johns, T. 1998, "Pharmafoods" and "nutraceuticals": paradigm shifts in biotherapeutics. In Prendergast, H. D. V., Etkin, N. L., Harris, D. R., Houghton P. J. (Eds.) Plants for food and medicine. Royal Botanic Gardens, Kew.
 15. Hebeisen, D. F., Hoeflin, F., Reusch, H. P., Junker, E., Lauterburg, B. H. 1993, *Int. J. Vitam. Nutr. Res.*, 63, 229.
 16. Espín, J. C., García, M. T., Tomás-Barberán, F. A. 2007, *Phytochemistry*, 68, 2986.
 17. Bombardelli, E., Bombardelli, V. 2005, *Fitoterapia*, 76, 495.
 18. Etkin, N. L. 1996, *Int. J. Pharmacogn.*, 34, 313.
 19. Vaughan, J. G., Judd, P. A. 2003, The Oxford book of health foods. Oxford University Press, Oxford.
 20. Heinrich, M., Leonti, M., Nebel, S., Peschel, W. 2005, *J. Physiol. Pharmacol.*, 56, suppl. 1, 5.
 21. Heinrich, M., Müller, W. E., Galli, C. 2006, Local Mediterranean food plants and nutraceuticals. Karger, Basel.
 22. Cavender, A. 2006, *J. Ethnopharmacol.*, 108, 74.
 23. Turner, N. J., Tallio, W. R., Burgess, S., Kuhnlein, H. V. 2013, The Nuxalk food and nutrition program for health revisited. In Kuhnlein, H. V., Erasmus, B., Spigelski, D., Burlingame, B. (Eds.) Indigenous Peoples' food systems & well-being: interventions & policies for healthy communities, FAO, Rome, 177.
 24. Rigat, M., Bonet, M.À., Garcia, S., Garnatje, T., Vallès, J. 2009, *Ecol. Food Nutr.*, 48, 303.
 25. Pieroni, A., Quave, C. 2006, Functional foods or food medicines? On the consumption of wild plants among Albanians and Southern Italians in Lucania. In Pieroni, A., Leimar Price, L. (Eds.), Eating and healing. Food Product Press - Haworth Press, Binghamton.
 26. Valossi, M., Scirè, A. S. 2012, *Nutrafoods*, 11, 85.
 27. Goodman, L. A. 1961, *Ann. Math. Stat.*, 32, 148.
 28. Pujadas, J. J., Comas, D., Roca, J. 2004, Etnografía. Universitat Oberta de Catalunya, Barcelona.
 29. Bolòs, O. de, Vigo, J., Masalles, R. M., Ninot, J. M. 2005, Flora manual dels Països Catalans. 3rd ed. Ed. Pòrtic, Barcelona.
 30. Angiosperm Phylogeny Group - APG IV. 2016, *Bot. J. Linn. Soc.*, 181, 1.
 31. Le Grand, A., Wondergem, P. A. 1987, *J. Ethnopharmacol.*, 21, 109.
 32. Johns, T., Kokwaro, J. O., Kimanani, E. K. 1990, *Econ. Bot.*, 44, 369.
 33. Trotter, R. T., Logan, M. H. 1986, Informant consensus: a new approach for identifying potentially effective medicinal plants. In Etkin, N. L. (Ed.) Plants in

- Indigenous Medicine and Diet, Behavioural Approaches, Redgrave Publishing Company, Bredford Hills, New York.
34. Gras, A., Garnatje, T., Bonet, M., Carrió, E., Mayans, M., Parada, M., Rigat, M., Vallès, J. 2016, *J. Ethnobiol. Ethnomed.*, 12, 23.
 35. Eskin, N. A. M., Tamir, S. 2006, Dictionary of Nutraceutical and Functional Foods, CRC Press Taylor & Francis Group, Boca Raton.
 36. Vallès, J., Garnatje, T., Carrió, E., Parada, M., Rigat, M. 2013, Identidad propia e identidad con medios adoptados. Plantas de siempre y plantas nuevas en la cultura alimentaria del área lingüística catalana. In Imaz, M., Álvarez, P. (Eds.) Identidad a través de la cultura alimentaria, Comisión Nacional para el Conocimiento y Uso de la Biodiversidad, México, D.F.
 37. Vallès, J., Bonet, M. À., Agelet, A., Selga, A. 2004, “Quaranta dies en alcohol a sol i serena”... y el sabor embotellado: la “ratafia”, licor catalán de plantas aromáticas. In Garrido, A. (Ed.) El sabor del sabor: hierbas aromáticas, condimentos y especias, Publicaciones de la Universidad de Córdoba, Córdoba, 255.
 38. Parada, M., Carrió, E., Bonet, M. À., Vallès, J. 2009, *J. Ethnopharmacol.*, 124, 609.
 39. Barnes, J. 2003, *British J. Clin. Pharmacol.*, 55, 226.



Research Signpost
Trivandrum
Kerala, India

Recent Advances in Pharmaceutical Sciences VII, 2017: 19-34 ISBN: 978-81-308-0573-3
Editors: Diego Muñoz-Torrero, Montserrat Riu and Carles Feliu

2. Immunomodulatory role of probiotics in early life

Maria J. Rodríguez-Lagunas, Ignasi Azagra-Boronat, Sandra Saldaña-Ruíz
Malen Massot-Cladera, Mar Rigo-Adrover, Anna Sabaté-Jofre, Àngels Franch
Margarida Castell and Francisco J. Pérez-Cano

*Department of Biochemistry and Physiology, Faculty of Pharmacy and Food Science
University of Barcelona, Barcelona, Spain*

*Institute of Research in Nutrition and Food Safety (INSA), University of Barcelona
Santa Coloma de Gramanet, Spain*

Abstract. The immune response in early life, as well as the anti-infective capacity of the organism, can be enhanced by some probiotic bacteria, especially those of importance in this neonatal period. The potential effect of these particular strains associated with early life, either isolated from breast milk or from baby faeces, on the immune system should be evaluated by *in vitro* and *in vivo* models of health or infection status before their introduction to babies, for example, in infant formulas.

Correspondence/Reprint request: Dr. Francisco J Pérez-Cano, Physiology Section, Department of Biochemistry and Physiology, Faculty of Pharmacy and Food Science, University of Barcelona, Av. Joan XXIII 27–31 Barcelona, 08028, Spain. E-mail: franciscoperez@ub.edu

Introduction

In the last few years, interest in the mutualism between hosts and their microbiota has increased considerably. The intestinal microbiota affects the human physiology by enhancing the epithelial barrier and immune functions, among others, both directly and indirectly. These beneficial effects are especially relevant in early life, when the immune system is still immature [1]. For this reason, it is important to develop strategies to modulate the intestinal environment and microbiota composition and functionality, which in turn may modulate the mucosal immune system, and therefore the systemic immunity.

Among the dietary strategies used to enhance the anti-infective response of neonates, the use of probiotics is the most studied. It is known that probiotics are exogenous micro-organisms that interact with various cellular components within the intestinal environment and have a positive impact on the host's health as defined by the International Scientific Association for Probiotics and Prebiotics (ISAPP) in 2013 [2], based on the initial one suggested by experts in the World Health Organization (WHO) in 2001 and in the Food and Agriculture Organization (FAO) [3]. This concept is supported by several other organizations such as the Codex, the Institute of Food Technologists (IFT), the World Gastroenterology Organization (WGO) and the European Food Safety Authority (EFSA).

The probiotics themselves or their metabolites are responsible for the effects on the immune system. Probiotics can be recognized by the immune cells through pattern-recognition receptors specific to microbial components, such as peptidoglycan or lipoteichoic acid [4]. This direct recognition triggers inflammatory or anti-inflammatory responses, depending on the specific strain [5]. Moreover, probiotics might induce intestinal epithelial cells to secrete an array of cytokines, therefore influencing immune function indirectly [6].

Mechanisms of immunomodulation include the induction of mucus production, short chain fatty acid (SCFA) synthesis, macrophage activation, stimulation of cytokine and secretory IgA production, and elevated production of peripheral immunoglobulins, among others (Fig. 1). During infancy, probiotic interventions could be helpful for the maturation of the immune system and, therefore, in strengthening the defence mechanisms against infections, or even preventing the development of immune-mediated diseases, such as asthma [4].

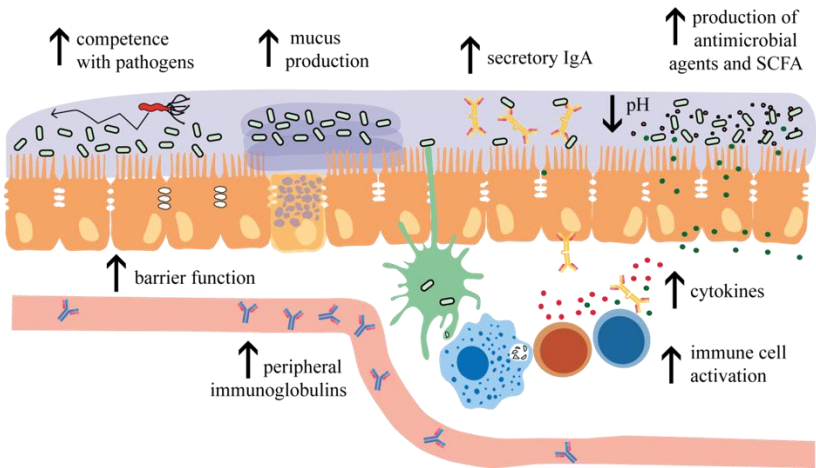


Figure 1. Main mechanisms of probiotics to potentiate the anti-infective capacity and modulate the immune system of the organism.

Not all bacteria induce the same effects in an organism and these effects could be different depending on age. In this case, when the target is the infant, it would be of interest to assess those types of bacteria obtained from a source related to early life, such as probiotics from breast milk or baby faces.

Rotavirus (RV) is the leading cause of severe diarrhoea among infants and young children and, although more standardized studies are needed, nowadays there is enough evidence to show that probiotics can help to fight against RV and other infectious and intestinal conditions.

Despite all the efforts made to evaluate the influence of these probiotic bacteria on infants' immune response, it is difficult to reach a conclusion due to the variability of the physiological or disease status studied, the numerous varieties of the probiotic strains, as well as the limitations in the number of participants. These are the reasons why most currently available data describing the effects of these compounds on immune response are derived from preclinical and *in vitro* studies.

On the basis of this background, the hypothesis that supports the current book chapter is that the immune response as well as the anti-infective capacity of the organism in early life can be enhanced by some probiotic bacteria derived from a neonatal source. Therefore, considering this

hypothesis, the main objective of this work is to show, with three particular representative studies, the beneficial effect of probiotic bacteria of importance in early life on the immune development and prevention against RV infections. The potential effect of these particular strains associated with early life, either isolated from breast milk or from baby faeces, on the immune system should be evaluated by *in vitro* and *in vivo* models before their introduction to babies, for example, in infant formulas.

1. *In vitro* immunomodulatory actions of breast milk probiotics

Breast milk has been traditionally considered to be sterile; however, current scientific studies have shown that it contains cultivable strains of at least 19 species of bacteria belonging to at least ten different genera (Table 1). Most of the bacteria isolated belong to the genera *Staphylococcus*, *Streptococcus*, *Lactobacillus* and *Bifidobacterium*, and some of them have already been used in human nutrition for their probiotic activity [7]. Therefore, breast milk constitutes a continuous source of commensal and potentially probiotic bacteria, since an infant that consumes approximately 800 mL of milk /day would ingest between 10^5 and 10^7 bacteria daily [8]. These findings would suggest that breastfeeding helps to shape the immune system's development early in life in order to achieve a competent function of the gut and a balanced immune homeostasis.

Despite all the advances made in probiotic research there is still a lack of a systematic analysis of the immunomodulatory potential of these bacterial strains in human cells and relatively little information is available regarding their mechanisms of action. For this reason, in the study by Pérez Cano *et al.* [9], the effects of two lactobacillus strains isolated from human milk on the modulation of the activation and cytokine profile of peripheral blood mononuclear cell (PBMC) subsets *in vitro* were evaluated. Briefly, *Lactobacillus salivarius* CECT5713 and *Lactobacillus fermentum* CECT5716 at 10^6 bacteria/mL were co-cultured with PBMC (10^6 /mL) from eight healthy donors for 24 h. The activation status (CD69 expression) of natural killer (NK) cells (CD56⁺), total T cells (CD3⁺), cytotoxic T cells (CD8⁺) and helper T cells (CD4⁺) was determined by flow cytometry. Regulatory T cells (Treg) were also quantified by intracellular Foxp3 evaluation [9].

Table 1. Bacteria isolated from human breast milk. Adapted from Fernández *et al.* [8].

Genera	Species	References
<i>Bifidobacterium</i>	<i>adolescentis, bifidum, breve, longum</i>	[10–12]
<i>Enterococcus</i>	<i>faecium, faecalis, durans, hirae, mundtii</i>	[13–16]
<i>Kocuria</i>	<i>rhizophila</i>	
<i>Lactobacillus</i>	<i>acidophilus, fermentum, plantarum, gasseri, crispatus, rhamnosus, salivarius, reuteri, casei, gastricus, vaginalis, animalis, brevis, helveticus,</i>	[13–20]
<i>Lactococcus</i>	<i>lactis</i>	[14, 15]
<i>Leuconostoc</i>	<i>mesenteroides</i>	[14, 15]
<i>Pediococcus</i>	<i>pentosaceus</i>	[11, 12]
<i>Rothia</i>	<i>mucilaginoso</i>	[14, 15]
<i>Staphylococcus</i>	<i>epidermidis, aureus, capitis, hominis</i>	[14, 15, 17]
<i>Streptococcus</i>	<i>mitis, salivarius, oris, parasanguis, lactarius, australis, gallolyticus, vestibularis</i>	[11, 12, 14–17]

To our knowledge this is the first time that the effects of these breast milk probiotics on specific lymphocyte subsets, including Treg cells, were reported. The results obtained in such a study demonstrated that *L. fermentum* CECT5716 and *L. salivarius* CECT5713 – derived from breast milk – were potent activators of NK cells by highly increasing their proportion through the expression of the activation marker CD69. Moreover, both strains were moderate activators of either CD4⁺ or CD8⁺ T cells – even though the increase of CD69 expression was not as evident as the one above. Finally, there was no impact of the breast milk probiotic bacteria on NK-T cell activation status. Thus, both strains have an influence on both innate and acquired immunity (Fig. 2).

Both milk strains *L. fermentum* CECT5716 and *L. salivarius* CECT5713, significantly induced a twofold rise in the Treg proportion with respect to resting cells ($p < 0.05$), although the percentage of Treg did not exceed 1% of the CD4⁺ T-cell population.

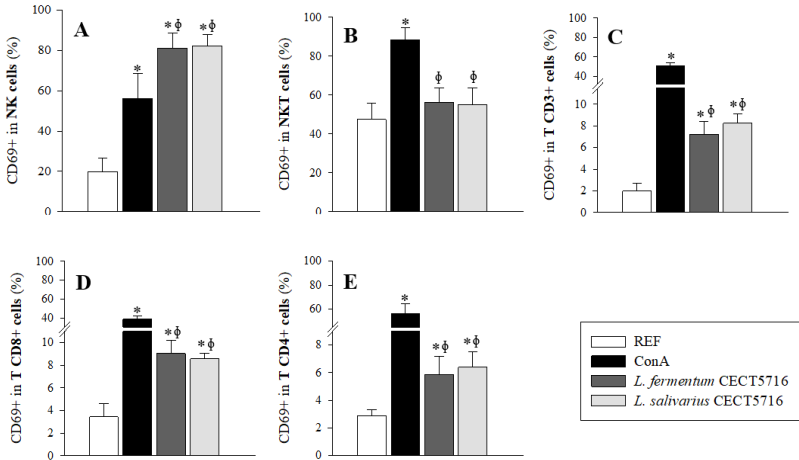


Figure 2. Effect of *L. fermentum* CECT5716 and *L. salivarius* CECT5713 on the expression marker CD69+ of specific lymphocyte subsets from Pérez-Cano *et al.* [9]. Activated **A.** NK cells, **B.** NKT cells, **C.** CD3+ T cells, **D.** CD8+ T cells and **E.** CD4+ T cells. Concanavalin A (ConA) was used as positive control. Data are expressed as mean \pm SEM values of 3–8 healthy donors. Differences between control, ConA and bacterial species were tested by one-way ANOVA. Significance: * $P < 0.05$ vs. control; $\phi P < 0.05$ vs. ConA.

On the other hand, in order to evaluate the induction ability of a wide range of pro- and anti-inflammatory cytokines and chemokines a semi-quantitative method to simultaneously profile the relative levels of 32 selected cytokines and chemokines was used. The Proteome Profiler TM Array with human cytokine array panel A (R&D Systems Europe Ltd., Abingdon, UK) used in the study included C5a, CD40L, G-CSF, GM-CSF, GXCL1,8 and 10–12, CCL1–CCL5, sICAM-1, IFN γ , IL-1a, IL-1b, IL-1ra, IL-2, IL-4, IL-5, IL-6, IL-10, IL-12p70, IL-13, IL-16, IL-17, IL-17E, IL-23, IL-27, IL-32a, MIF, Serpin E-1 and TNF α . Furthermore quantification of IFN γ , IL-1b, IL-2, IL-4, IL-5, IL-6, IL-8, IL-10, IL-12p70, TNF α , TNF β , MIP-1a and MIP-1b was performed using the human Th1/Th2 plex kit from Bender Medsystems GmbH (Vienna, Austria) and GM-CSF and TGF- β 1/- β 2 by ELISA [21].

The results showed that human PBMC, either in resting conditions, stimulated with LPS or co-cultured with live probiotic bacteria for 24 h displayed different patterns of cytokine secretion (Fig. 3). Unstimulated cells

did not evidence the expression of most of the molecules studied; however, LPS-stimulated cells secreted most of the cytokines and chemokines included in the panel, specifically CCL2, CCL5, MIP-1 α , MIP-1 β , TNF α , Il-1 β , IL-6, IL-18, GRO α and sICAM-. *L. fermentum* CECT5716 and *L. salivarius* CECT5713 promoted the secretion of CCL2, CCL5, GRO α and sICAM-1; the amounts obtained were similar to those induced by LPS (Fig. 3).

In addition, the probiotic bacteria were better inducers of TNF α , MIP-1 β , Il-1 β and IL-18 than LPS and also activated IL-1 α and C5a production in the PBMC, which were not induced by LPS. Overall, two strain-specific effects were found: on the one hand, the *L. fermentum* CECT5716 seem to induce IFN γ , and on the other, *L. salivarius* CECT5713 seem to induce GM-CSF, both in a strong way [21].

Further quantification of most of the cytokines and chemokines assayed above were later confirmed by the human Th1/Th2 plex kit from Bender Medsystems GmbH (Vienna, Austria) and by ELISA [21] (Fig. 4).

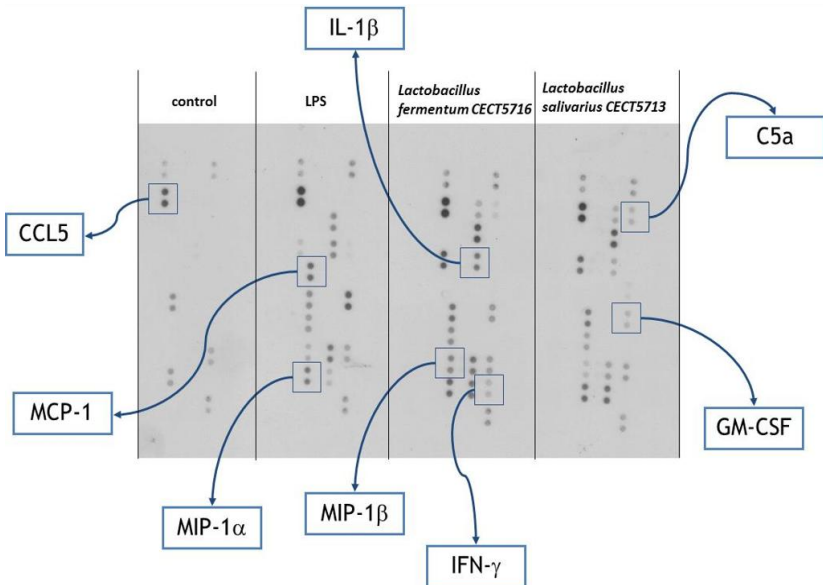


Figure 3. Semi-quantitative determination of relative levels of 32 selected cytokines and chemokines in the presence of *L. fermentum* CECT5716 and *L. salivarius* CECT5713. Results derived from Pérez-Cano *et al.* [9].

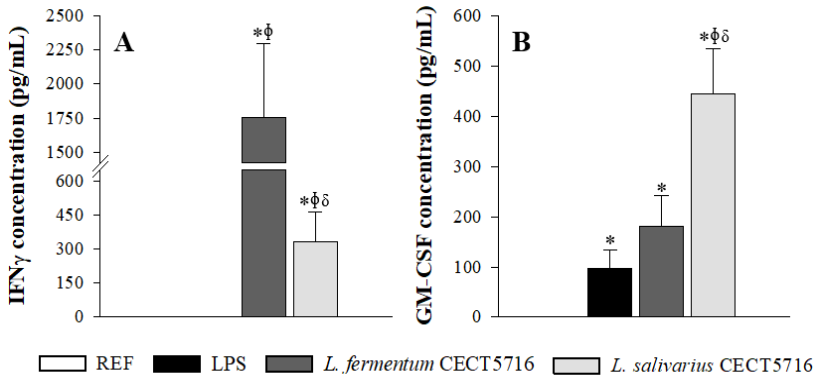


Figure 4. IFN- γ and GM-CSF concentration in PBMC co-cultured with *L. fermentum* CECT5716 and *L. salivarius* CECT5713 media from Pérez-Cano *et al.* [9]. LPS was used as positive control. Data are expressed as mean \pm SEM values of 3–8 healthy donors. Differences between control, LPS and bacterial species were tested by one-way ANOVA. Significance: *P<0.05 vs. control; ϕ P<0.05 vs. LPS; δ vs. *L. fermentum* CETC15716.

In conclusion, this study demonstrates that *L. salivarius* CECT5713 and *L. fermentum* CECT5716 enhanced the activation of NK and T-cell subsets and the expansion of Treg cells, suggesting their ability to strengthen both innate and adaptive immune responses. Moreover, both strains are able to induce a broad array of cytokines in a strain-specific manner. It should be stated that *L. fermentum* and *L. salivarius* from non-breast milk sources also induce the production of a broad array of cytokines [21], and their immunomodulatory importance in early life should also be further studied.

2. *In vivo* effect of probiotics in health: Immune development

The next step after investigating the immunomodulatory potential of early life probiotics *in vitro* consisted of investigating the *in vivo* effect of the supplementation with these types of bacteria on the maturation of the intestinal and systemic immune system during the first stages of development. Very few studies have addressed this issue; in one example, Rigo-Adrover *et al.*, [22] investigated the impact of *Bifidobacterium breve* M-16V supplementation on some aspects of the immune system

development using a neonatal rat as a model. The neonatal rat has been considered as a suitable model for immunonutrition studies, because it allows the characterization of immune changes during suckling in several lymphoid compartments [1].

In the case of *B. breve* M-16V, although not a breast milk-derived probiotic bacteria, it is naturally present in infants' microbiota and has already shown immunomodulatory properties [23–27]. In Rigo Adrover *et al.*'s study, neonatal Lewis rats were supplemented with the probiotic strain or with vehicle during a 13-day period and on day 18 of life, splenocytes, mesenteric lymph node (MLN) cells and intraepithelial lymphocytes (IEL) were isolated as in previous studies adapted to neonatal rats [28, 29]. They were later purified, counted, and stained using immunofluorescence techniques. Main cell subsets were evaluated as well as intestinal aspects such as faecal consistency and immunoglobulin-A (IgA) levels.

Briefly, the study evidenced that *B. breve* M-16V administration during the rat suckling period influences the intestinal and systemic lymphocyte composition, modulates the percentage of cells expressing molecules involved in the interaction with intestinal bacteria such as TLR4, and also potentiates the intestinal IgA production. Regarding the changes in lymphocyte composition, very few changes were observed. Although this nutritional intervention did not seem to potentiate the systemic immune maturation, it increased the proportion of CD8+ NK cells in MLN and reduced that of CD4+ IEL and CD8 $\alpha\beta$ + TCR $\gamma\delta$ + IEL [22].

TLR4 presence in splenocytes was not affected by the nutritional intervention with the probiotic bacteria. On the contrary, it was increased in the MLN cells but not in IEL (Fig. 5A and B). However, the CD4+ T cell subset in the IEL increased the TLR4+ proportion due to the *B. breve* M-16V supplementation, suggesting that this increased bacteria–host interaction may have a role in the preparation of the intestinal immune system for a stronger response against infections. These results are in agreement with other studies conducted in adult animals [30–34]. The $\alpha E\beta 7$ integrin on the lymphocyte surface allows IEL retention in the intestine [35, 36]. For this reason, it was determined in the three compartments and although no changes were found in SPL, the percentage of MLN cells and IEL expressing $\alpha E\beta 7$ integrin was higher in animals fed with the probiotic ($p < 0.05$) (Fig. 5C and D). This result was evidenced in CD4+CD8, CD4–CD8+ and CD4–CD8 cells in both compartments.

Finally, the administration of the *B. breve* M-16V strain for 13 days during the suckling period enhanced the intestinal IgA production (Fig. 6), which is a typical feature of immuno-enhancing probiotic bacteria [22].

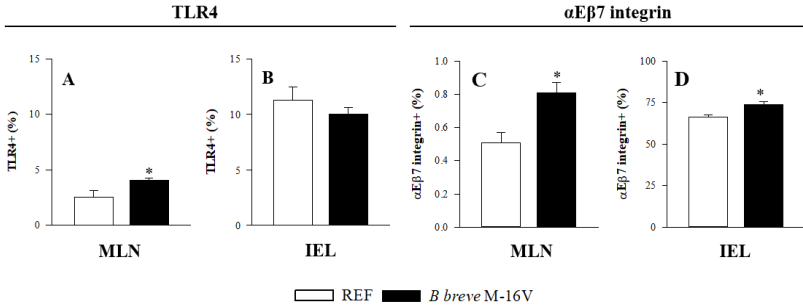


Figure 5. Surface TLR4 and $\alpha E\beta 7$ integrin expression in MLN and IEL lymphocyte in reference and *B. breve* M-16V supplemented rats from Rigo-Adrover *et al.* [22]. Data are expressed as mean \pm SEM (n = 8 animals/group). Significance: *P<0.05 vs. ref. [22].

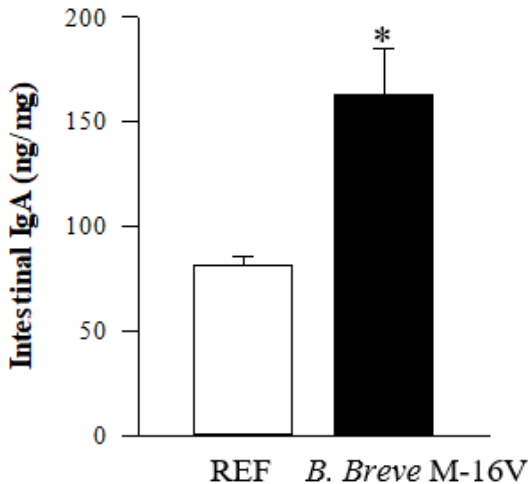


Figure 6. IgA concentration in intestinal washes of 19-day-old rats. Results are expressed as ng of IgA/mg of tissue (mean \pm SEM, n=8 animals/group) from Rigo-Adrover *et al.* [22]. Statistical differences: *p<0.05 vs. ref. [22].

3. *In vivo* effect of probiotics under infection: Rotavirus gastroenteritis

Rotavirus is the leading cause of severe diarrhoea among infants and young children and, although more standardized studies are needed, there is evidence that probiotics can help to fight against RV and other infectious and intestinal pathologies. In this context, due to its immunomodulatory potential, *B. breve* M-16V strain was also tested as a protective agent in such infective processes [22].

Briefly, the neonatal rats received the intervention with the *B. breve* M 16V from the 3rd to the 21st day of life (almost the entire suckling period) by oral gavage. On day 7, RV was orally administered as in previous studies [37]. Clinical variables were evaluated by means of scoring stools from 1 to 4 (diarrhoea index [DI]) based on colour, texture and amount. These scores allow the obtained results to be expressed as incidence and severity, as well as the maximum value of the above variables as indicators.

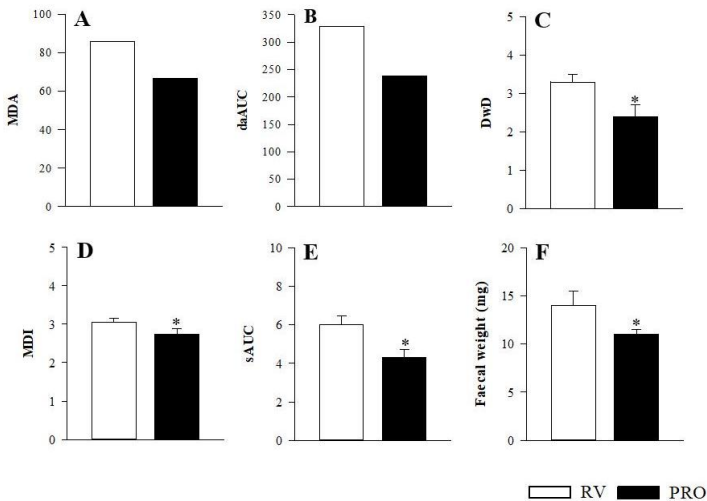


Figure 7. Effect of the supplementation with *Bifidobacterium breve* M-16V in RV-induced diarrhoea animals from Rigo-Adrover *et al.* [22]. Diarrhoea production was studied by different parameters: **A.** proportion of animals with diarrhoea (MDA); **B.** diarrhoeic animals (DA); **C.** duration of the process, **D.** maximum diarrhoea index (MDI); **E.** severity; and **F.** weight of the faecal specimens. Data are expressed as mean \pm SEM (n = 8 animals/group). Significance: *P<0.05 vs. RV.

RV inoculated to 7-day-old animals induced diarrhoea in most of the animals for about 3–4 days (Fig. 7). The supplementation with the probiotic was able to significantly reduce the maximum proportion of animals with diarrhoea (MDA, Fig. 7A) but also the overall course of the diarrhoeic animals (DA, Fig. 7B). The *B. breve* M-16V also reduced the duration of the process (Fig. 7C) as well as its severity, as is observed in the lower values of the maximum diarrhoea index (MDI, Fig. 7D) and the overall severity throughout the process (Fig. 7E). The intervention also reduced the weight of the faecal specimens, which were increased due to the RV infection (Fig. 7F). The study also shows how the probiotic modulates the humoral immune response against the virus as well as the pattern of faecal short-chain fatty acids (SCFA) and the results derived after its use in a synbiotic combination [22].

4. Probiotics in infant formulas

There are several international organizations that are responsible for making recommendations and standards that must be accomplished when preparing formula types 1 and 2, such as the American Academy Committee on Pediatrics Nutrition (AAPCON) and the Committee on Nutrition of the European Society of Paediatric Gastroenterology, Hepatology and Nutrition (ESPGHAN). A summary of the guidance adapted in Spain can be found in Table 2. It summarizes the main components, including, for example, the proportion of oligosaccharides.

Infant formulas type 1 (0–6 months, 650 kcal/day) and infant formulas type 2 (6–12 months, 850 kcal/day) are quite different in composition with respect to infant formulas type 3 (12–36 months), which do not follow any specific guidance for its formulation.

The probiotics can be optionally added to these formulations in order to better mimic breast milk composition; however, no compilation of data showing a list of probiotics present in these types of products is available. Due to this fact, a pilot evaluation was performed with a total of 40 samples from Spanish stores (10 samples for each type of infant formula 1, 2 and 3 sold in pharmacies and 10 in supermarkets). The study was performed in September–December 2015 (Table 3). Overall, independently of the source providing the formula (pharmacy or supermarket) it can be observed that only a low proportion of them include probiotics (25%, 10/40); a proportion that increases if the synbiotic formulation is considered (30%, 12/40). It must be highlighted that depending on the origin of the product (pharmacy or supermarket) we can observe a high difference: 33.3 % (10/30) of

Table 2. Infant's formula composition. From BOE number. 64. Real Decreto 165/2014 which modifies BOE number. 131. Real Decreto 867/2008, 23 May [38, 39].

Nutrients	Infant formula type 1 (per 100 kcal)	Infant formula type 2 (per 100 kcal)
Energy (Kcal)	60–70/100 mL	60–70/100 mL
Carbohydrates (g)	9–14	9–14
Lactose (g)	>4.5	>4.5
Proteins (g)	1.8–3	1.8–3.5
Whey protein/casein	60/40	20/80
Fat (g)	4.4–6.0	4.0–6.0
Linoleic acid (mg)	300–1200	300–1200
Sodium (mg)	20–60	20–60
Potassium (mg)	60–160	60–160
Calcium (mg)	50–140	50–140
Phosphorus (mg)	25–90	25–90
Iron (mg)	0.3–1.3	0.6–2
Oligosaccharides (g)	<0.8	<0.8
Probiotic bacteria	not mentioned	not mentioned

formulas provided in pharmacies have probiotics (40%, 12/30 if synbiotics are included) whereas none of those found in the supermarkets (0%, 0/10) have probiotics in their composition. Regarding the influence of the type of formula, types 1, 2 and 3 contain probiotics in similar proportions, which comprises between 30 and 40%.

In all cases, the proportion of formulas with probiotics are lower than those with oligosaccharides (prebiotics), which are always higher than 40%, with the exception of the type 3 formulas sold in pharmacies which have only a 20% presence of prebiotics. This pilot study just highlights the low incorporation of probiotics into these types of products.

Table 3. Study of presence of probiotics and prebiotics in infant's formula on the Spanish market (2016). Total samples analysed: 40.

Content	Pharmacy				Supermarket
	Total N=30 (%)	Type 1 N=10 (%)	Type 2 N=10 (%)	Type 3 N=10 (%)	Total N=10 (%)
None	N=6 (20%)	N=2 (20%)	N=0 (0%)	N=4 (40%)	N=6 (60%)
Oligosaccharides	N=12 (40%)	N=5 (50%)	N=5 (50%)	N=2 (20%)	N=4 (40%)
Probiotics	N=10 (33.3%)	N=3 (30%)	N=4 (40%)	N=3 (30%)	N=0 (0%)
Synbiotics	N=2 (6.7%)	N=0 (0%)	N=1 (10%)	N=1 (10%)	N=0 (0%)

5. Conclusions

Overall, early life probiotics have not only demonstrated their immunomodulatory potential *in vitro* and their beneficial effects on immune development but also in the context of infection, as is the case of the rotavirus-induced gastroenteritis in the neonatal rat model. Further studies are needed in order to provide a better understanding of their mechanisms of action and whether they can be considered for inclusion in infant formulas or supplements, to be used as strategies for promoting the maturation of the neonatal immune system or even for protecting against human rotavirus-induced diarrhoea in children. Regardless of their presence in breast milk and the positive effects of this type of probiotic bacteria, they are poorly included in infant formulas.

Acknowledgements

The authors are grateful to Karen Knipping from Nutricia Research and Monica Olivares from Biosearch S.L. for providing the probiotics used in these studies. We also thank Prof. Parveen Yaqoob from the University of Reading where the *in vitro* studies were performed, as well as the Animal Experimental Unit in the Faculty of Pharmacy and Food Science where the animal work was developed. We also thank Prof. Laura Baldomà from the University of Barcelona for her critical revision of the manuscript.

References

1. Pérez-Cano, F. J., Franch, À., Castellote, C., Castell, M., Franch, À., Castellote, C., Castell, M. 2012, *Clin. Dev. Immunol.*, 2012, 537310.
2. Hill, C., Guarner, F., Reid, G., Gibson, G. R., Merenstein, D. J., Pot, B., Sanders, M. E. 2014, *Nat. Rev. Gastroenterol. Hepatol.*, 11, 506.
3. Food safety and quality: Probiotics [Internet]. [cited 2017 Jan 17]. Available from: <http://www.fao.org/food/food-safety-quality/a-z-index/probiotics/en/>
4. Ashraf, R., Shah, N. P. 2014, *Crit. Rev. Food Sci. Nutr.*, 54, 938.
5. Folligne, B., Nutten, S., Grangette, C., Dennin, V., Goudercourt, D., Poiret, S., Pot, B. 2007, *World J. Gastroenterol.*, 13, 236.
6. Shida, K., Nanno, M. 2008, *Trends Immunol.*, 29, 565.
7. Gomez-Gallego, C., Garcia-Mantrana, I., Salminen, S., Collado, M. C. 2016, *Semin. Fetal Neonatal Med.*, 21, 400.
8. Fernández, L., Langa, S., Martín, V., Maldonado, A., Jiménez, E., Martín, R., Rodríguez, J. M. 2013, *Pharmacol. Res.*, 69, 1.
9. Pérez-Cano, F. J., Dong, H., Yaqoob, P. 2010, *Immunobiology*, 215, 996.
10. Martín, R., Jiménez, E., Heilig, H., Fernández, L., Marín, M. L., Zoetendal, E. G., Rodríguez, J. M. 2009, *Appl. Environ. Microbiol.*, 75, 965.
11. Martín, V., Mañes-Lázaro, R., Rodríguez, J. M., Maldonado-Barragán, A. 2011, *Int. J. Syst. Evol. Microbiol.*, 61, 1048.
12. Martín, V., Maldonado-Barragán, A., Moles, L., Rodríguez-Baños, M., Campo, R. Del, Fernández, L., Jiménez, E. 2012, *J. Hum. Lact.*, 28, 36.
13. Martín, R., Langa, S., Reviriego, C., Jiménez, E., Marín, M. L., Xaus, J., Rodríguez, J. M. 2003, *J. Pediatr.*, 143, 754.
14. Heikkilä, M. P., Saris, P. E. J. E. J., Heikkilä, M. P., Saris, P. E. J. E. J. 2003, *J. Appl. Microbiol.*, 95, 471.
15. Beasley, S. S., Saris, P. E. J. 2004, *Appl. Environ. Microbiol.*, 70, 5051.
16. Albesharat, R., Ehrmann, M. A., Korakli, M., Yazaji, S., Vogel, R. F. 2011, *Syst. Appl. Microbiol.*, 34, 148.
17. Gavin, A., Ostovar, K. 1977, *J. Food Prot.*, 40, 614.
18. West, P. A., Hewitt, J. H., Murphy, O. M. 1979, *J. Appl. Bacteriol.*, 46, 269.
19. Martín, R., Jiménez, E., Olivares, M., Marín, M. L., Fernández, L., Xaus, J., Rodríguez, J. M. 2006, *Int. J. Food Microbiol.*, 112, 35.
20. Oncel, M. Y., Sari, F. N., Arayici, S., Guzoglu, N., Erdeve, O., Uras, N., Dilmen, U. 2014, *Arch. Dis. Child. Fetal Neonatal Ed.*, 99, F110.
21. Pérez-Cano, F. J., Dong, H., Yaqoob, P. 2010, *Immunobiology*, 215, 996.
22. Rigo-Adrover, M. del M., Franch, À., Castell, M., Pérez-Cano, F. J. 2016, *PLoS One*, 11, e0166082.
23. Pärty, A., Kalliomäki, M., Wacklin, P., Salminen, S., Isolauri, E. 2015, *Pediatr. Res.*, 77, 823.
24. Hashemi, A., Villa, C. R., Comelli, E. M., Hill, C., Guarner, F., Reid, G., Michalowicz, B. S. 2016, *Food Funct.*, 7, 1752.

25. Hougee, S., Vriesema, A. J. M., Wijering, S. C., Knippels, L. M. J., Folkerts, G., Nijkamp, F. P., Garssen, J. 2010, *Int. Arch. Allergy Immunol.*, 151, 107.
26. Van De Pol, M. A., Lutter, R., Smids, B. S., Weersink, E. J. M., Van Der Zee, J. S. 2011, *Allergy*, 66, 39.
27. Kivit, S., Saeland, E., Kraneveld, A. D., Kant, H. J. G., Schouten, B., Esch, B. C. A. M., Willemsen, L. E. M. 2012, *Allergy*, 67, 343.
28. Pérez-Cano, F. J., Castellote, C., González-Castro, A. M., Pelegrí, C., Castell, M., Franch, A. 2005, *Pediatr. Res.*, 58, 885.
29. Ramos-Romero, S., Pérez-Cano, F. J., Castellote, C., Castell, M., Franch, À. 2012, *Br. J. Nutr.*, 107, 378.
30. Borruel, N., Carol, M., Casellas, F., Antolín, M., de Lara, F., Espín, E., Malagelada, J. R. 2002, *Gut*, 51, 659.
31. Carol, M., Borruel, N., Antolin, M., Llopis, M., Casellas, F., Guarner, F., Malagelada, J.R. 2006, *J. Leukoc. Biol.*, 79, 917.
32. Hu, G., Yang, S., Hu, W., Wen, Z., He, D., Zeng, L., Zhu, Q. 2015, *Exp. Ther. Med.*, 11, 33.
33. Amit-Romach, E., Uni, Z., Reifen, R. 2010, *Mol. Nutr. Food Res.*, 54, 277.
34. Castillo, N. A., Perdigon, G., de Moreno de Leblanc, A. 2011, *BMC Microbiol*, 11, 177.
35. Cepek, K. L., Shaw, S. K., Parker, C. M., Russell, G. J., Morrow, J. S., Rimm, D. L., Brenner, M. B. 1994, *Nature*, 372, 190.
36. Kilshaw, P. J. 1999, *Mol. Pathol.*, 52, 203.
37. Pérez-Cano, F. J., Castell, M., Castellote, C., Franch, À. 2007, *Pediatr. Res.*, 62, 658.
38. BOE 2008, *BOE 131, 30 mayo 2008*, 25121-25137.
39. BOE 2014, *BOE 64, 15 marzo 2014*, 23266-23269.



Research Signpost
Trivandrum
Kerala, India

Recent Advances in Pharmaceutical Sciences VII, 2017: 35-49 ISBN: 978-81-308-0573-3
Editors: Diego Muñoz-Torrero, Montserrat Riu and Carles Feliu

3. Dietary exposure biomarkers in nutritional intervention and observational studies to discover biomarkers of intake and disease risk through an HPLC-QToF-MS metabolomics approach

Mar Garcia-Aloy^{1,2}, Rafael Llorach^{1,2}, Mireia Urpi-Sarda^{1,2},
Rosa Vázquez-Fresno¹, Olga Jáuregui^{2,3} and Cristina Andres-Lacueva^{1,2}
¹*Biomarkers and Nutrimental Laboratory, Department of Nutrition, Food Sciences and Gastronomy, Campus Torribera, Faculty of Pharmacy and Food Sciences, University of Barcelona, Barcelona, Spain;* ²*CIBER de Fragilidad y Envejecimiento Saludable (CIBERFES), Instituto de Salud Carlos III, Barcelona, Spain;* ³*Scientific and Technological Centres of the University of Barcelona (CCIT-UB), 08028 Barcelona, Spain*

Abstract. Health is highly influenced by food intake. Nutrimental metabolomics has been proposed as a tool for assessing the changes in metabolome associated with food consumption and/or the effects of a dietary intervention. In this chapter, we have summarized the most relevant results of our recent research on the identification of biomarkers related to food ingestion (biomarkers of intake), as well as their potential association with health (biomarkers of effect), through the application of an untargeted HPLC-QToF-MS metabolomics approach in nutritional studies

Correspondence/Reprint request: Dr. Mar Garcia-Aloy and Prof. Cristina Andres-Lacueva. Biomarkers and Nutrimental Laboratory, Department of Nutrition, Food Sciences and Gastronomy, Faculty of Pharmacy and Food Sciences, University of Barcelona, Avda. Joan XXIII, 27-31, 08028 Barcelona, Spain.
E-mail: margarcia@ub.edu and candres@ub.edu

with different designs. The results have shown that diet-related differences in urinary metabolome are associated with food digestion, microbiota metabolism and endogenous metabolism; and the predictive capacity of dietary exposition can be improved using multimetabolite combined models compared with the use of single compounds

Introduction

Evaluation of the effects of food on health requires results to be obtained in studies that allow conclusions to be reached with the maximum degree of scientific evidence and, based on this information, solid and reliable recommendations to be elaborated for consumers. For this reason, precise measurement of dietary intake is a crucial factor in studies that analyse the relationships between diet and health. Traditionally, dietary intake data have been obtained from food surveys. The most commonly used methods are food frequency questionnaires, 24-hour recalls and dietary records. However, in spite of being the most frequently used methods, they present a series of methodological limitations due to systematic and random errors [1, 2]. These drawbacks may attenuate the relative risk estimates and decrease the statistical power of the studies [3, 4] and it has been pointed out that they are one of the causes of some of the reported inconsistencies between food and health in the scientific literature, since the effects of diet on risk factors may be distorted due to errors in the assessment of intake (in the case of observational studies) or due to a lack of compliance with the assigned nutritional intervention (in the case of intervention studies) [5].

Faced with this situation, and given the need to obtain a more precise intake assessment, nutritional biomarkers have emerged as a precise and objective tool for the determination of dietary exposure that could complement the data obtained from food surveys [6]. Biomarkers have been defined as “a characteristic that is objectively measured and evaluated as an indicator of normal biological processes, pathogenic processes, or pharmacologic responses to a therapeutic intervention” [7]. Biomarkers can be divided into three categories: i) exposure biomarkers, defined as those exogenous compounds, or some of their metabolites, that can be measured in a biological sample of the organism; ii) effect biomarkers, defined as those measurable elements related to a biochemical or physiological alteration in the organism that, depending on the magnitude, may be associated with a possible deterioration in health or disease; and (iii) susceptibility biomarkers, defined as those substances that indicate the body’s ability to respond to a particular exposure [8, 9].

Within the field of food sciences, a nutritional biomarker is any biochemical, functional or clinical indicator measured in a biological sample

that reflects the nutritional status with respect to the intake or metabolism of dietary components, as well as the biological consequences of food intake [10]. An ideal dietary biomarker should accurately indicate the level of intake and should be specific, sensitive and applicable to a large number of populations [6]. In this respect, the most important criteria to take into account when using dietary biomarkers are summarized in Table 1.

Table 1. Biological and analytical considerations for biomarkers of dietary exposure. Adaptation of Andersen 2014 [11], from Spencer *et al.* 2008 [12], Jenab *et al.* 2009 [6] and Manach *et al.* 2009 [13].

Analytical methods	Sample	It is necessary to define the type of sample, the time of its collection, and the conditions of storage and preparation.
	Methodology	The marker should be quantifiable by a defined method and the analytical error should be known.
Biological considerations	Relation to the exposure	The association between food intake and the exposure marker should be causal. That is, the marker should be a known compound (or a metabolite) present in the food.
	Sensitivity and specificity	The biomarker should be as particular of the evaluated food as possible, so that the percentage of true positive values for exposure (sensitivity), and true negative values for non-exposure (specificity), should be as high as possible.
	Dose-response	There should be a positive association between the level of exposure and the measured level of the biomarker.
	Time of exposure	It should be determined whether it is a short-term (reflects recent consumption of food) or long-term (reflects habitual intake) exposure marker.
	Population	The population in which the exposure marker can be applied should be known.
	Interindividual variation	The main potential sources of interindividual variation (such as genotypes, gender, age, smoking, microbiota, etc.) should be investigated.

In the investigation of new biological markers related to diet, metabolomics has emerged as a powerful tool for the discovery of new nutritional biomarkers of intake and effect [14]. Metabolomics is the science that studies the metabolome, i.e. the set of metabolites (defined as those intermediate molecules and products of metabolism with a molecular weight less than 1500 Da) present in a biological system (cell, tissue or fluid) [15–17]. The diet influences two fractions of the human metabolome: i) the food metabolome, which includes all external metabolites derived from dietary exposure; and (ii) the endogenous metabolome, which includes all the metabolites produced by the organism [18]. In recent years, there has been a significant increase in the number of publications in this field (Fig. 1). This demonstrates the growing interest that is being devoted to this discipline, as well as the potential it offers in research.

With the introduction of metabolomics in the field of nutritional research, the concept of nutritional metabolomics, or nutrimetabolomics, has emerged. It has been defined as the omics discipline that studies how the diet affects the whole metabolome [19].

Feeding induces changes in the metabolism of the organism, which can be evaluated by the analysis of the endogenous and exogenous metabolites in biofluids. These metabolites can be used as objective and accurate biomarkers of food consumption and/or the effects of a dietary intervention. The food metabolome includes all metabolites derived from food intake, their

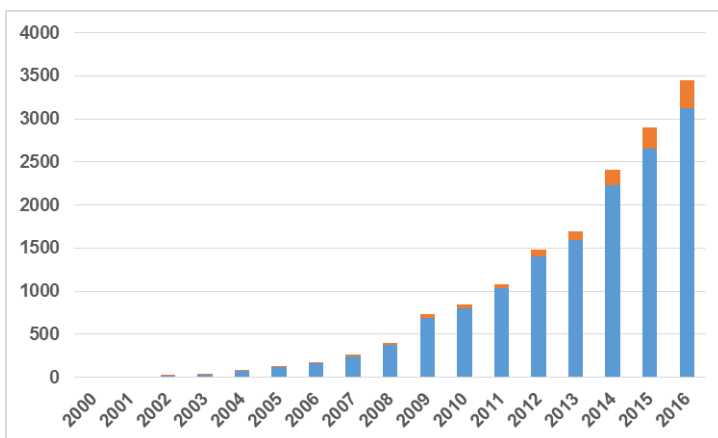


Figure 1. Number of publications per year appearing in PubMed using the search “metabolomics” (the number of publications resulting from the search “metabolomics & nutrition” in the same database is indicated in orange).

absorption and their biotransformation in the tissues or organs or by the microbiota [20]. In light of this, the application of metabolomics in nutritional studies has become a new strategy in obtaining new biomarkers related to the evaluation of the nutritional status of an individual, food consumption, biological consequences produced after a nutritional intervention, or the study of metabolic mechanisms in response to diet according to a specific metabolic phenotype [13, 17, 21]. The food metabolome has a high complexity and variability, since it is estimated that food contains > 25,000 different compounds, the great majority of which will undergo various metabolic processes in the organism [18]. This particular characteristic makes the food metabolome a very important source of information about the diet of individuals, and its characterization would enable eating habits to be monitored in an objective and precise way, and the influence food has on the risk of developing diseases could be studied [18].

Herein we will summarize the main results of our recent research on the discovery of new biomarkers of dietary exposure in a population from the Mediterranean region at high risk of cardiovascular disease through the application of an untargeted HPLC-QToF-MS metabolomics approach in nutritional studies with different designs. Different foods habitually consumed within the dietary pattern of the studied populations were selected. Specifically, the metabolic fingerprint of white and whole-grain bread [22], nuts [23, 24] and cocoa [25, 26] was analysed.

1. HPLC-QToF-MS untargeted metabolomics analyses

1.1. Identification of biomarkers of bread consumption in a free-living population

The objective of this work was to identify biomarkers of bread consumption by applying a nutrimetabolomics strategy [22]. Using an untargeted HPLC-QToF-MS approach together with multivariate analysis, the urine of 155 free-living individuals stratified into three groups according to their usual bread consumption was analysed (56 non-bread consumers, 48 consumers of white bread and 51 consumers of whole-grain bread).

The most differentiated metabolites ($VIP \geq 1.5$; Table 2) included plant phytochemical compounds, such as benzoxazinoid and alkylresorcinol metabolites, and compounds produced by gut microbiota (such as enterolactones, hydroxybenzoic and dihydroferulic acid metabolites). Pyrrolidine, 3-indolecarboxylic acid glucuronide, riboflavin, 2,8-dihydroxyquinoline glucuronide and N- α -acetylcitrulline were also tentatively identified.

Table 2. Metabolites identified with different bread consumption levels.

RT (min)	Detected mass (m/z)	Assignment	Identification	NBC	NBC	WHB
				vs WHB	vs WGB	vs WGB
<i>Benzoxazinoid-related compounds</i>						
0.88	188.0049	[M-H]-	2-Aminophenol sulphate	↑	↑	-
1.48	328.1036	[M+H]+	HPAA glucuronide	↑	↑	-
	326.0651	[M-H]-		-	↑	-
2.07	168.0609	[M+H]+	HHPAA	-	↑	↑
3.40	372.0925	[M+H]+	HMBOA glucuronide	↑	-	-
	370.0772	[M-H]-		↑	↑	-
3.68	326.0922	[M-H]-	HBOA glycoside	-	↑	↑
3.72	152.0671	[M+H]+	HPPA	-	↑	-
4.78	196.0596	[M+H]+	HMBOA	↑	↑	-
	194.0410	[M-H]-		↑	↑	-
<i>Alkylresorcinol metabolites</i>						
2.85	357.0791	[M-H]-	DHPPA glucuronide	↑	↑	↑
3.12	233.0118	[M-H]-	3,5-Dihydroxyphenylethanol sulphate	-	↑	-
5.75	289.0412	[M-H]-	DHPPTA sulphate	-	↑	↑
<i>Microbial-derived metabolites</i>						
3.67	313.0558	[M-H]-	Hydroxybenzoic acid GlcA	↑	↑	-
4.72	275.0219	[M-H]-	Dihydroferulic acid sulphate	-	↑	↑
6.32	299.1278	[M+H-GlcA]+	Enterolactone glucuronide	-	↑	↑
	473.1447	[M-H]-		-	↑	↑
<i>Markers of heat-treated food products</i>						
2.73	255.1345	[M+H]+	Pyrraline	-	↑	-
	253.1172	[M-H]-		-	↑	↑
<i>Other exogenous metabolites</i>						
3.25	338.0871	[M+H]+	3-Indolecarboxylic acid	-	↑	↑
	336.0697	[M-H]-	glucuronide	-	↑	↑
4.65	377.1475	[M+H]+	Riboflavine	↑	↑	↑
<i>Endogenous metabolites</i>						
0.63	218.1140	[M+H]+	N- α -Acetylcitrulline	-	↓	-
4.20	338.0882	[M+H]+	2,8-Dihydroxyquinoline	-	↑	↑
	160.0382	[M-H-GlcA]-	glucuronide	-	↑	↑

DHPPA, 3-(3,5-dihydroxyphenyl) propanoic acid; DHPPTA, 5-(3,5-dihydroxyphenyl) pentanoic acid; GlcA, glucuronide; HBOA, 2-hydroxy-1,4-benzoxazin-3-one; HHPAA, 2-hydroxy-N-(2-hydroxyphenyl) acetamide; HMBOA, 2-hydroxy-7-methoxy-2H-1,4-benzoxazin-3-one; HPAA, N-(2-hydroxyphenyl) acetamide; HPPA, 2-hydroxy-N-(2-hydroxyphenyl) acetamide; NCB, non-consumers of bread; RT, retention time; WGB, whole-grain bread consumers; WHB, white-bread consumers.

↑ indicates significantly higher levels in the second group of the comparison; ↓ indicates significantly lower levels in the second group of the comparison.

A stepwise logistic regression analysis was used to combine several metabolites in a multimetabolite model to predict bread consumption. ROC curves were constructed to assess the predictive capacity of both the individual metabolites and their combination (multimetabolite models). The values of the area under the curve [AUC (95% CI)] of the combined models ranged from 77.8% (69.1% – 86.4%) to 93.7% (89.4% – 98.1%), whereas the AUCs for the metabolites included in the prediction models had weaker values when they were evaluated individually. The AUCs ranged from 58.1% (46.6% – 69.7%) to 78.4% (69.8% – 87.1%).

The results of this study demonstrated that a daily bread intake has a significant impact on the urinary metabolome, although this is evaluated in free-living conditions. It was also shown that the predictive ability of a combination of various biomarkers of dietary exposure is better than using single biomarkers.

1.2. Nutritional biomarkers of regular nut consumption in intervention and observational studies

Healthy effects of nuts have been attributed to their particular chemical composition. Monitoring metabolites present in biological samples after nut consumption could help to unveil the pathways involved in the effects of this food on the human organism. Therefore, changes in the urinary metabolome of patients with metabolic syndrome undergoing a 12-week nutritional intervention with a daily intake of 30 grams of nuts were determined through an untargeted metabolomics approach [23]. In line with this study, the urinary metabolome of habitual consumers of walnuts in free-living conditions was characterized using the same methodology [24].

This strategy revealed several markers associated with nut intake in both studies. They included markers of fatty acid metabolism, phase II and microbial-derived metabolites of nut polyphenols, and intermediate metabolites of the tryptophan/serotonin metabolic pathway. The increased excretion of serotonin metabolites was associated with nut consumption for the first time in the intervention study [23] and some of them were replicated in the observational study [24].

In the observational study, subjects were divided into two groups (training and validation sets) and a stepwise logistic regression analysis was used to select a multimetabolite prediction model for walnut exposure in the training set [24]. The predictive model of exposure to walnuts included at least one component of each class. The AUC (95% CI) for the combined biomarker model was 93.5% (90.1% – 96.8%) in the training set and 90.2% (85.9% – 94.6%) in the validation set. In contrast, the AUC values for individual metabolites were $\leq 85\%$ in all cases (Fig. 2).

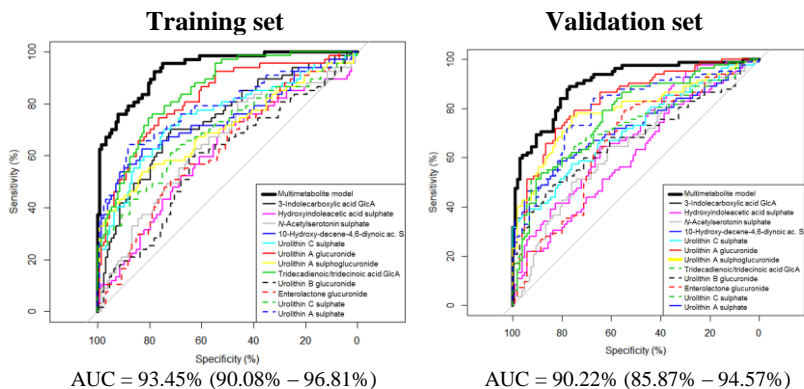


Figure 2. ROC curves of multimetabolite prediction biomarker model (black line) and of included individual metabolites (coloured lines) in the training and validation sets.

1.3. Analysis of the metabolic footprint of cocoa product exposure in studies with different designs

An interventional and an observational study were developed for the study of biomarkers of habitual consumption of cocoa. The design of intervention study was a randomized, crossover and controlled 4-week clinical trial involving 22 participants [27], whereas in the observational, the urinary metabolome of 32 consumers of cocoa products and 32 matched subjects not consuming cocoa was profiled [28]. In the nutritional intervention study, subjects received 40 g/day of cocoa powder in 500 mL of skimmed milk or 500 mL/day of skimmed milk as control. Twenty-four-hour urine samples were collected at the beginning of the study and after each intervention period. An untargeted metabolomics strategy using HPLC-QToF-MS followed by multivariate data analysis was applied to all urine samples.

Most compounds identified as being discriminant for cocoa consumption were related to theobromine and polyphenol metabolism, as well as to compounds produced during cocoa processing. In the case of the endogenous metabolites, the identifications suggested a reduction in the urinary levels of acylcarnitines and sulphation of tyrosine. These metabolites may be related to cardiovascular disease, although specific studies are needed to evaluate whether changes in these markers are a consequence of some metabolic alterations associated with cocoa intake, or are caused by decreased or increased regulation of some metabolic pathways that are affected by the consumption of this food product.

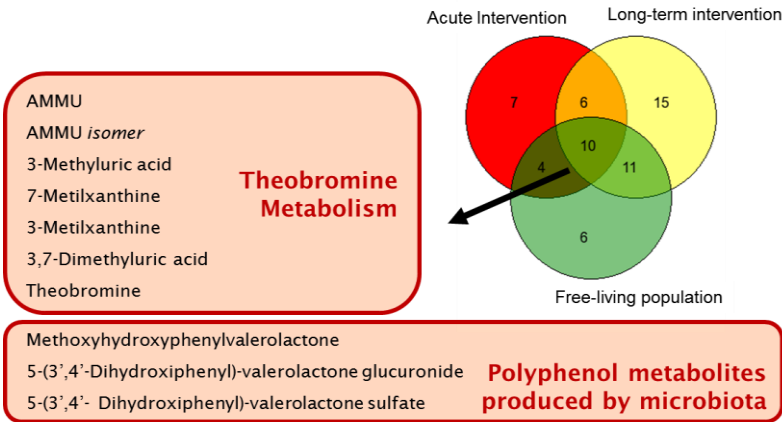


Figure 3. Venn diagram showing overlapping and unique metabolites associated with cocoa consumption for the three types of study.

A Venn diagram was produced to display how many metabolites were characteristic of cocoa exposure in both studies [27, 28], together with those in another previous acute study that also used cocoa [29]. Fig. 3 shows that 10 metabolites were discriminant for cocoa consumption independently of the study design. These metabolites belong to the metabolic pathway of theobromine and to the microbial metabolism of cocoa polyphenols. These 10 metabolites were considered for the development of the multimetabolite biomarker model. The AUC values (95% CI) for the model were 95.7% (89.8–100 %) and 92.6% (81.9–100 %) in training and validation sets, respectively, whereas the AUCs for individual metabolites were <90%.

2. Replication of biomarkers of dietary exposure in nutritional studies with differentiated designs

There are practically no studies aimed at the replication of biomarkers of dietary exposure in populations in free-living conditions [30]. In this context, the replication of markers allows the level of evidence of observed associations to be increased, as previously suggested for genomic studies [31].

Diet control is a very important factor in the study of biomarkers of dietary exposure. It may have a high influence on the results, since the foods to which individuals are exposed during a clinical trial depend on dietary interventions or restrictions, or on the eating habits of individuals in the case

of observational studies [18]. This aspect has an important repercussion on the specificity and sensitivity of the candidate biomarkers. On the one hand, the markers identified in controlled intervention studies may not have sufficient specificity when attempting to apply them in observational studies because habitual diets may include other foods that also contain the same markers and that have been restricted during a nutritional intervention. On the other hand, when observational studies are being developed it should be taken into account that many foods are usually consumed together, following certain patterns of intake, which can lead to the identification of biased low-sensitivity markers [18]. Thus, the replication of a marker in studies with differentiated designs (in this case, controlled interventions and observational studies) is an indication that it is a metabolite with high specificity and sensitivity [11].

The studies summarized in this chapter have evidenced the replication of the discriminant metabolites of the metabolic footprint associated with the consumption of certain foods. Initially, markers of nut and cocoa consumption were characterized in controlled nutritional intervention studies [23, 25], most of which were also discriminant in a population analysed using an observational study design and taking into consideration their usual diet under free-living conditions [24, 26].

Another aspect to consider in the study of biomarkers is the type of biological sample used. Urine, along with plasma and serum, is one of the biological fluids most frequently used in nutrimental studies, and it has been shown to reflect a higher concentration of metabolites derived from food than plasma [18]. Twenty-four-hour urine samples have been described as a more robust method for monitoring daily dietary intake than the use of spot urine samples [12, 32]. The clinical trials with dietary interventions included in this chapter used 24-hour urine samples [23, 25]. However, collecting 24-hour urine samples is a difficult and cumbersome task, especially in large-scale epidemiological studies [32, 33]. Therefore, the replication of the exposure markers (initially characterized in 24-hour urine samples) in spot urine samples reinforces their discriminatory power independently of the type of sample used [24, 26].

Finally, the time course of excretion will define whether the compound is a short-, medium- or long-term marker. For example, in the study of urinary metabolome associated with habitual cocoa consumption, it was observed that metabolites that remained discriminant independently of the study design were those with an excretion pattern of at least 24-hours after ingesting the food, such as theobromine and polyphenol metabolites derived

from microbial metabolism [34, 35]. Therefore, these observations reinforce the concept that in observational studies, where subjects are evaluated under free-living conditions, biomarkers that are excreted later or during a wide time frame may be better predictors of food intake than those that are rapidly excreted [36, 37]. In contrast, short-term biomarkers will only be useful in those populations that consume the corresponding dietary source with some regularity and frequency [38].

3. Design of multimetabolite biomarker models to improve the prediction of dietary exposure

Given that most food constituents are widely distributed in several foods, very few compounds can be considered biomarkers of a particular food or food group. This would be the case of proline betaine for citrus intake [39] and resveratrol for wine consumption [40]. Additionally, it must also be taken into account that in some cases differentiated compounds, after undergoing various metabolic processes in the organism, may converge with common metabolites, as is the case for several groups of polyphenols in wine, which, after their absorption and metabolism, are usually transformed into common phenolic acids [41], or the different classes of ellagitannins that are found in walnuts, pomegranates and strawberries, which microbiota metabolize to common urolithins [42, 43].

In order to solve this issue, it has been proposed that by combining more than one compound in a multimetabolite model, a more precise measurement of consumption could be achieved. It was shown that generating models of biomarkers formed by more than one metabolite provided better results than with the measurements obtained for each individual compound [22, 24, 26]. These results reinforce the hypothesis that an improved discriminate dietary exposure ability is achieved through the use of biomarker models made of more than one metabolite. It is important to emphasize that these models are constructed of metabolites of different classes, most probably because each of these metabolites gives complementary information on dietary intake, whereas those that are left out of the model probably do not contribute any additional biological information to that which has already been part of the corresponding model.

To date, there have been very few cases in the scientific literature that have tried to work with combinations of nutritional biomarkers to improve the predictive capacity of dietary exposure measures [18]. One of the few examples that have been proposed so far is the ratio between two

alkylresorcinols for the consumption of whole grains [44]. However, in studies reported in this chapter a new proposal has been made that allows the consideration of ≥ 2 metabolites. This represents an important novelty in the field of nutrimetabolomics by opening an alternative route for the discovery of new biomarkers of dietary exposure.

4. Future perspectives

The application of metabolomics to the study of biomarkers of dietary exposure is still far from being exploited in depth. For example, most of the available untargeted nutrimetabolomics studies have been exploratory. Thus, for some markers there are very few studies with which to compare the results. For this reason, it is very important to continue replicating the markers in different populations and in studies with different designs.

Targeted studies on dose-response behaviours and interindividual differences are also needed before biomarkers can routinely be applied in nutritional studies. In fact, the maximum utilization of the data obtained through untargeted metabolomic studies is obtained when qualitative and quantitative analyses are combined, since the quantitative measurements of the markers using a targeted approach and in a controlled study improve its applicability and interpretation. Additionally, it will provide information that can be very useful in interpreting the metabolic pathways affected [45].

Some untargeted metabolomic studies have been performed to identify markers of the usual dietary patterns [46, 47], but the studies are too different in design and in the analytical approaches used. The results of these studies showed that dietary patterns are reflected in urine and plasma, although it is necessary to propose new studies focused on the determination of the inherent footprint of this food consumption to reinforce its predictive power.

The most recently proposed challenge includes the integration of different omic technologies (genomics, proteomics, transcriptomics and metabolomics) to obtain a more complete picture of health status and, thus, to unravel the links between disease prevention and dietary intake. Therefore, in future studies, the comprehensive understanding of dietary effects needs the approaches of systems biology, including genomics, proteomics, transcriptomics and metabolomics, combined with a suitable experimental design and a sufficient number of included subjects to be able to find the variables associated with the effects associated with the diet. These studies will require multidisciplinary working teams.

At the same time, it would also be interesting to analyse the relationships between classical health markers and biomarkers measured by untargeted metabolomics, with the aim of deciphering the biological connection between traditional clinical parameters and metabolic markers.

5. Conclusions

The main conclusion drawn from this work is that the application of an untargeted metabolomics strategy in the study of nutritional biomarkers enables the main differences in the urinary metabolome associated with dietary intake to be characterized. They are associated with food digestion, microbial metabolism and endogenous metabolism. Most of the biomarkers characterized in clinical trials of nutritional intervention have been replicated in individuals evaluated observationally in free-living conditions. The biomarkers that are usually replicated as discriminatory in studies with different designs (i.e. nutritional interventions and observational studies) are those that usually present a medium- and/or long-term urinary excretion with respect to the moment of ingestion of the corresponding food. The predictive ability of dietary exposure through multimetabolite biomarker models is greater than the ability of single metabolites when they are evaluated individually. The combined models could be extremely useful in improving accuracy during the evaluation of dietary intake

Acknowledgements

This work was supported by the Spanish National Grant AGL2009-13906-C02-01 from the Spanish Ministry of Economy and Competitiveness (MINECO) and co-founded by FEDER (Fondo Europeo de Desarrollo Regional); the MINECO and the Joint Programming Initiative “A Healthy Diet for a Healthy Life” (JPI HDHL, website: <http://www.healthydietforhealthylife.eu>) grant FOOTBALL-PCIN-2014-133; and the European Cooperation in Science and Technology (COST) grant COST Action FA 1403 POSITIVE (Interindividual variation in response to the consumption of plant food bioactives and determinants involved). We are also grateful for the grant 2014-SGR-1566 from the Generalitat de Catalunya’s Agency AGAUR, and the “CIBER de Fragilidad y Envejecimiento Saludable (CIBERFES)” (Instituto de Salud Carlos III). MG-A thanks the AGAUR for the predoctoral FI-DGR 2011 fellowship. M.U.-S. thanks the Ramon y Cajal program from the MINECO and Fondo Social Europeo.

References

1. Bingham SA. 2002, *Public Health Nutr*, 5, 821.
2. Livingstone MBE., Black AE. 2003, *J Nutr*, 133, 895S.
3. Bingham SA., Luben R., Welch A., Wareham N., Khaw KT., Day N. 2003, *Lancet*, 362, 212.
4. Kaaks R., Ferrari P. 2006, *Ann Epidemiol*, 16, 377.
5. Kristal AR., Peters U., Potter JD. 2005, *Cancer Epidemiol Biomarkers Prev*, 14, 2826.
6. Jenab M., Slimani N., Bictash M., Ferrari P., Bingham SA. 2009, *Hum Genet*, 125, 507.
7. Biomarkers Definitions Working Group. 2001, *Clin Pharmacol Ther*, 69, 89.
8. WHO. 1993, Geneva: World Health Organization.
9. Schulte PA. 2005, *Mutat Res*, 592, 155.
10. Potischman N., Freudenheim JL. 2003, *J Nutr*, 873S.
11. Andersen M-BS. Dissertation, University of Copenhagen, 2014.
12. Spencer JPE., Abd El Mohsen MM., Minihane A-M., Mathers JC. 2008, *Br J Nutr*, 99, 12.
13. Manach C., Hubert J., Llorach R., Scalbert A. 2009, *Mol Nutr Food Res*, 53, 1303.
14. Rezzi S., Ramadan Z., Fay LB., Kochhar S. 2007, *J Proteome Res*, 6, 513.
15. Oliver SG., Winson MK., Kell DB., Baganz F. 1998, *Trends Biotechnol*, 16, 373.
16. Fiehn O. 2002, *Plant Mol Biol*, 48, 155.
17. Wishart DS. 2008, *Trends Food Sci Technol*, 19, 482.
18. Scalbert A., Brennan L., Manach C., Andres-Lacueva C., Dragsted LO., Draper J., Rappaport SM., van der Hooft JJJ., Wishart DS. 2014, *Am J Clin Nutr*, 99, 1286.
19. Zhang X., Yap Y., Wei D., Chen G., Chen F. 2008, *Biotechnol Adv*, 26, 169.
20. Fardet A., Llorach R., Orsoni A., Martin J-F., Pujos-Guillot E., Lapiere C., Scalbert A. 2008, *J Nutr*, 138, 1282.
21. Oresic M. 2009, *Nutr Metab Cardiovasc Dis*, 19, 816.
22. Garcia-Aloy M., Llorach R., Urpi-Sarda M., Tulipani S., Salas-Salvadó J., Martínez-González MA., Corella D., Fitó M., Estruch R., Serra-Majem L., Andres-Lacueva C. 2015, *Metabolomics*, 11, 155.
23. Tulipani S., Llorach R., Jáuregui O., López-Uriarte P., Garcia-Aloy M., Bullo M., Salas-Salvadó J., Andrés-Lacueva C. 2011, *J Proteome Res*, 10, 5047.
24. Garcia-Aloy M., Llorach R., Urpi-Sarda M., Tulipani S., Estruch R., Martínez-González MA., Corella D., Fitó M., Ros E., Salas-Salvadó J., Andres-Lacueva C. 2014, *J Proteome Res*, 13, 3476.
25. Llorach R., Urpi-Sarda M., Tulipani S., Garcia-Aloy M., Monagas M., Andres-Lacueva C. 2013, *Mol Nutr Food Res*, 57, 962.
26. Garcia-Aloy M., Llorach R., Urpi-Sarda M., Jáuregui O., Corella D., Ruiz-Canela M., Salas-Salvadó J., Fitó M., Ros E., Estruch R., Andres-Lacueva C. 2015, *Mol Nutr Food Res*, 59, 212.

27. Llorach R., Urpi-Sarda M., Tulipani S., Garcia-Aloy M., Monagas M., Andres-Lacueva C. 2013, *Mol Nutr Food Res*, 57, 962.
28. Garcia-Aloy M., Llorach R., Urpi-Sarda M., Jáuregui O., Corella D., Ruiz-Canela M., Salas-Salvadó J., Fitó M., Ros E., Estruch R., Andres-Lacueva C. 2015, *Mol Nutr Food Res*, 59, 212.
29. Llorach R., Urpi-Sarda M., Jauregui O., Monagas M., Andres-Lacueva C. 2009, *J Proteome Res*, 8, 5060. American Chemical Society.
30. Llorach R., Garcia-Aloy M., Tulipani S., Vazquez-Fresno R., Andres-Lacueva C. 2012, *J Agric Food Chem*, 60, 8797.
31. Chanock SJ., Manolio T., Boehnke M., Boerwinkle E., Hunter DJ., Thomas G., Hirschhorn JN., Abecasis G., Altshuler D., Bailey-Wilson JE., Brooks LD., Cardon LR., Daly M., Donnelly P., Fraumeni JF., Freimer NB., Gerhard DS., Gunter C., Guttmacher AE., Guyer MS., Harris EL., Hoh J., Hoover R., Kong CA., Merikangas KR., Morton CC., Palmer LJ., Phimister EG., Rice JP., Roberts J., Rotimi C., Tucker MA., Vogan KJ., Wacholder S., Wijsman EM., Winn DM., Collins FS. 2007, *Nature*, 447, 655.
32. Zamora-Ros R., Rabassa M., Cherubini A., Urpi-Sarda M., Llorach R., Bandinelli S., Ferrucci L., Andres-Lacueva C. 2011, *Anal Chim Acta*, 704, 110.
33. Potischman N. 2003, *J Nutr*, 875S.
34. Rodopoulos N., Höjvall L., Norman A. 1996, *Scand J Clin Lab Invest*, 56, 373.
35. Llorach R., Urpi-Sarda M., Jauregui O., Monagas M., Andres-Lacueva C. 2009, *J Proteome Res*, 8, 5060.
36. Pujos-Guillot E., Hubert J., Martin J-F., Lyan B., Quintana M., Claude S., Chabanas B., Rothwell JA., Bennetau-Pelissero C., Scalbert A., Comte B., Hercberg S., Morand C., Galan P., Manach C. 2013, *J Proteome Res*, 12, 1645.
37. Andersen M-BS., Kristensen M., Manach C., Pujos-Guillot E., Poulsen SK., Larsen TM., Astrup A., Dragsted LO. 2014, *Anal Bioanal Chem*, 406, 1829.
38. Lloyd AJ., Beckmann M., Haldar S., Seal C., Brandt K., Draper J. 2013, *Am J Clin Nutr*, 97, 377.
39. Heinzmann SS., Brown IJ., Chan Q., Bictash M., Dumas M-E., Kochhar S., Stamler J., Holmes E., Elliott P., Nicholson JK. 2010, *Am J Clin Nutr*, 92, 436.
40. Zamora-Ros R., Urpi-Sardà M., Lamuela-Raventós RM., Estruch R., Martínez-González MÁ., Bulló M., Arós F., Cherubini A., Andres-Lacueva C. 2009, *Free Radic Biol Med*, 46, 1562.
41. Boto-Ordóñez M., Rothwell JA., Andres-Lacueva C., Manach C., Scalbert A., Urpi-Sarda M. 2014, *Mol Nutr Food Res*, 58, 466.
42. Espín JC., Larrosa M., García-Conesa MT., Tomás-Barberán F. 2013, *Evid Based Complement Alternat Med*, 2013, 270418.
43. Garcia-Muñoz C., Vaillant F. 2014, *Crit Rev Food Sci Nutr*, 54, 1584.
44. Chen Y., Ross AB., Aman P., Kamal-Eldin A. 2004, *J Agric Food Chem*, 52, 8242.
45. Dettmer K., Aronov PA., Hammock BD. 2007, *Mass Spectrom Rev*, 26, 51.
46. O'Sullivan A., Gibney MJ., Brennan L. 2011, *Am J Clin Nutr*, 93, 314.
47. Andersen M-BS., Rinnan Å., Manach C., Poulsen SK., Pujos-Guillot E., Larsen TM., Astrup A., Dragsted LO. 2014, *J Proteome Res*, 13, 1405.



Research Signpost
Trivandrum
Kerala, India

Recent Advances in Pharmaceutical Sciences VII, 2017: 51-68 ISBN: 978-81-308-0573-3
Editors: Diego Muñoz-Torrero, Montserrat Riu and Carles Feliu

4. Polypurine Reverse Hoogsteen Hairpins as a tool for gene repair and editing

Carles Ciudad, Anna Solé, Alex J. Félix and Véronique Noé
Department of Biochemistry and Physiology, School of Pharmacy and Food Sciences
University of Barcelona, Barcelona, Spain

Abstract. We describe the design and use of repair-PPRHs and editing-PPRHs as a new methodology either to correct a point mutation or to edit a genomic fragment of the *dihydrofolate reductase* gene in Chinese Hamster Ovary (CHO) cells. Repair-PPRHs are formed by a PPRH core, following the Reverse Hoogsteen bonds rules, covalently connected to a repair tail, which is homologous to the mutated region of the dsDNA except for the repaired nucleotide. Several point mutations in the endogenous *dhfr* gene have been successfully repaired in mammalian cells using repair-PPRHs, including a deletion, an insertion, and single and double substitutions in different regions of the gene. All repaired colonies showed high levels of DHFR protein and activity, and the corrected nucleotide was confirmed in all DNA sequences. Editing-PPRHs are formed by a PPRH core, covalently connected to a sequence tail homologous to the upstream and downstream regions of the DNA fragment to be edited. All edited colonies showed high levels of DHFR protein and activity, and the edition was confirmed in all DNA sequences.

Correspondence/Reprint request: Dr. Véronique Noé, Department of Biochemistry and Physiology, School of Pharmacy and Food Sciences, University of Barcelona, 08028 Barcelona, Spain. E-mail: vnoe@ub.edu

Introduction

Mutations are a natural process that alters the DNA and are constantly taking place in the genome. It is estimated that tens of thousands of changes happen daily in the DNA of a human cell [1]. Not all the mutations result in functional impairment, but in some cases, small changes in the DNA sequence can provoke an enormous impact on an entire living being. Therefore, these mutations need to be reversed by the DNA repair machinery that fixes DNA damage such as mismatched nucleotides, DNA cross-links, bulky adducts and splicing broken DNA strands back together.

Depending on the cells affected, mutations can be classified in two groups: inherited mutations, when they affect germ cells, and the alteration can often be passed on to offspring; and acquired mutations, that can spontaneously arise during the life of an organism in somatic cells. Mutations of the latter can result from normal metabolic activities including DNA replication errors, spontaneous lesions such as depurination and deamination of the DNA, and the generation of reactive oxygen species (ROS), but can also result from environmental factors such as physical or chemical mutagens [2–4] (Fig. 1).

Point mutations are a type of mutations that typically refer to an alteration of a single or a few adjacent base pairs in a DNA sequence. They usually take place during DNA replication, although other endogenous and

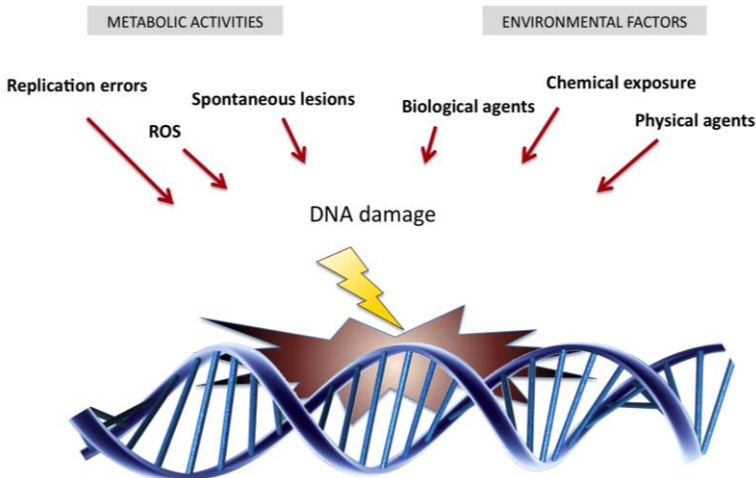


Figure 1. Causes of DNA damage.

exogenous agents can be implicated. Some point mutations are beneficial or have no effect. Polymorphisms for instance, are mutations that generally do not cause functional damage under basal conditions. Nonetheless, these alterations can also be detrimental for gene function at various levels. If the mutation occurs in the promoter region of a gene, the expression of this gene may be altered. If the alteration is caused in a coding region, the activity may change and in the case of insertions or deletions a frame shift can be produced, thus changing the whole peptide or provoking the appearance of a nonsense mutation originating a truncation of the protein. In addition, if the mutated base pair is found near or in the intron-exon junction, it can result in a splicing alteration of the mRNA.

DNA damage may lead towards a large variety of lesions, including mismatches, chemical adducts or single- and double-strand breaks (DSBs). Therefore, different repair pathways have evolved, each focused on a particular type of lesion.

If DNA damage affects terminally differentiated cells, DNA damage repair will ensure the integrity of the transcribed genome. However, if DNA damage occurs in dividing cells, “cell cycle checkpoints” will detect the damage by sensor proteins, and by means of different protein complexes, signal transducers and effector proteins. These effector proteins will lead to the repair of DNA or will temporarily stop the proliferating cells in their cell cycle progression to provide enough time to the DNA repair machinery to act. Some of these important cell cycle checkpoint proteins are ataxia telangiectasa mutated (ATM) and ATM and Rad3 related (ATR) that act as signal transducers. In response to DNA damage in G1, for example, these proteins will phosphorylate p53, which acts as a transcription factor for p21, leading to an inhibition of both cyclinE/Cdk2 and cyclinA/Cdk2 complexes, and therefore an inhibition of G1/S transition, thus preventing the synthesis of damaged DNA [5–8]. However, the specific pathway that will be activated is determined by the type of DNA damage. When repair processes fail and DNA damage cannot be repaired, cells may become senescent or can be conducted to programmed cell death or apoptosis. Apoptosis is conducted by different protein factors such as the anti-apoptotic protein Bcl-2, inhibited directly or indirectly by p53 [9]. If any of these processes do not work properly, there may be an unregulated cell division that can lead to the formation of a tumor, which could become cancerous.

DNA damage checkpoints can halt cell proliferation, but the repair machinery is required to prevent the transduction of mutations to daughter

cells. DNA-damage-signaling and DNA repair are believed to be linked and operate collectively [10,11]. As mentioned before, since there is a wide diversity of possible lesions, a large variety of DNA repair mechanisms have evolved, such as direct reversal repair, base excision repair (BER), nucleotide excision repair (NER), mismatch repair (MMR), and DSB repair (Fig. 2).

Gene augmentation therapy (GAT) is one of the most studied strategies to treat diseases caused by point mutations; it consists of introducing copies of the wild type gene in the affected cells to obtain the functional protein in sufficient amounts to restore the normal phenotype. This strategy is especially available for recessive diseases, since the mutated gene does not interfere with the normal product, and the amount of this product does not need a rigorous regulation to recover a normal phenotype. However, it presents some drawbacks, as random gene integration in the genome, and the loss of endogenous regulator elements of the gene. As an alternative, a different philosophy for gene repair was developed to correct point mutations in their endogenous loci using different types of oligonucleotides. These strategies consisted of targeting

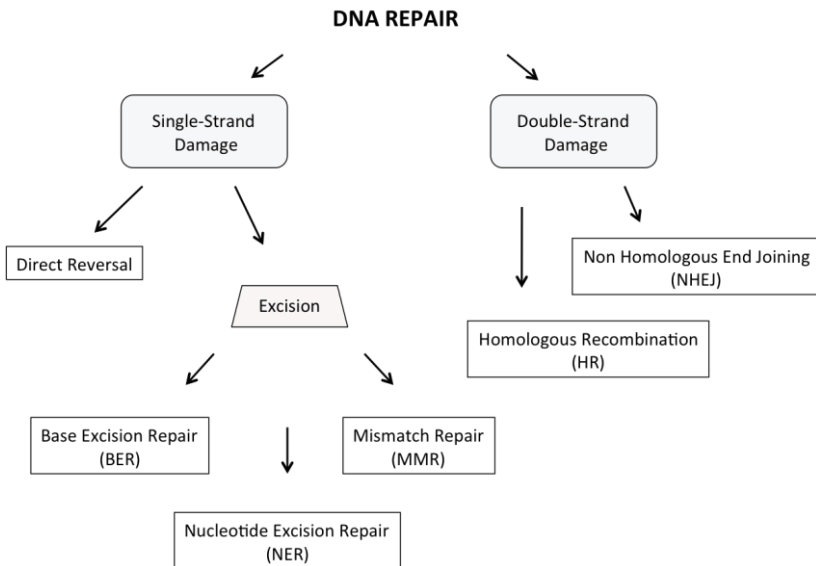


Figure 2. Scheme of DNA repair responses.

the genomic DNA with an oligonucleotide complementary to the DNA sequence, except for the corrected nucleotide. In the last years, different approaches have emerged in this direction, such as chimeric RNA-DNA oligonucleotides, single-stranded oligonucleotides (ssOs), bifunctional triple-helix-forming oligonucleotides (TFBO), or peptide nucleic acids (PNAs).

Programmable endonucleases such as zinc-finger nucleases (ZFN), transcription activator-like effector nucleases (TALENs) and Clustered Regulatory Interspaced Short Palindromic Repeats (CRISPR)/CRISPR-associated 9 (Cas9), are artificial proteins composed of a sequence specific DNA-binding domain fused to a nuclease, that are able to provoke double strand breaks (DSBs) in the genome, thus stimulating the cellular DNA repair-mechanisms, including error-prone non-homologous end joining (NHEJ), in the absence of a homologous DNA template, and homologous recombination (HR), in the presence of a synthetic repair template [12]. These site-specific nucleases have shown to edit DNA to disrupt, introduce, invert, or delete genes [13]. Although to a lesser extent, these tools are also being studied to correct point mutations [13,14].

1. Polypurine reverse Hoogsteen Hairpins

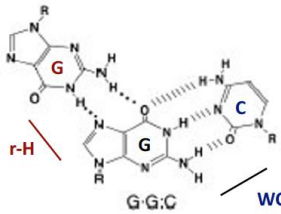
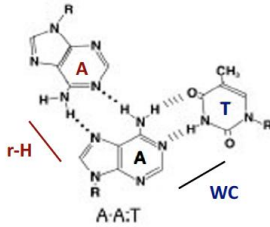
PPRHs are non-modified DNA molecules formed by two antiparallel polypurine strands linked by a pentathymidine loop that allows the formation of intramolecular reverse-Hoogsteen bonds between both strands. These hairpins bind to polypyrimidine stretches in the DNA via Watson-Crick bonds, while maintaining the hairpin structure (Fig. 3). It was demonstrated that PPRHs, upon binding their polypyrimidine target in a dsDNA, were able to displace the polypurine strand of the target duplex configuration [15,16].

Because the polypyrimidine domains can be found in both strands of the DNA, PPRHs can be designed to target either one of the strands of genomic DNA. PPRHs directed against the template strand of the DNA are called template-PPRHs, while the ones targeting the coding strand of the DNA are called coding-PPRHs, which are also able to bind transcribed mRNA, since it has the same sequence and orientation than the coding strand of the DNA. Therefore, PPRHs can act as antigene and antisense oligonucleotides depending on the strand they target (Fig. 4). PPRHs were first described for gene silencing [15–20].

PPRH hairpin = PolyPurine Reverse-Hoogsteen hairpin

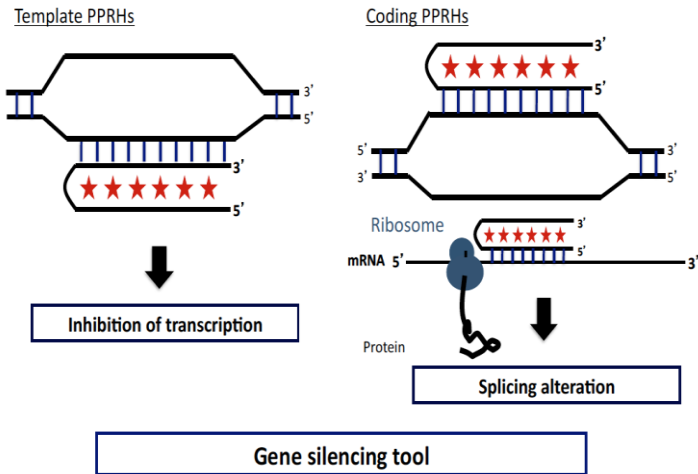
▪ Double-stranded DNA molecule:

- Linked by 5-T loop
- Reverse Hoogsteen bonds between antiparallel purine strands
- Watson-Crick with genomic DNA
- pH-independent, Salts required



Watson-Crick bond ★ Reverse-Hoogsteen bond

Figure 3. PPRH characteristics and structure.



Watson-Crick bond ★ Reverse-Hoogsteen bond

Figure 4. PPRHs for gene silencing.

2. Repair-PPRHs

Repair-PPRHs are Polypurine reverse Hoogsteen hairpins bearing an extension sequence at one end homologous to the DNA strand to be repaired but containing the wild type nucleotide instead of the mutation. We made a successful first attempt to correct a point mutation at the endogenous *locus* of the *dhfr* gene. Homologous recombination was found to play an important role in the mechanism for gene correction by repair-PPRHs [21].

Next we wanted to expand the use of repair-PPRHs and improve the methodology to correct a representative collection of different types of mutations (substitutions, double substitutions, deletions, and insertions) at an endogenous *locus* in a mammalian genome. To achieve this goal, we again used the *dhfr* gene as a model because it is a selectable marker that readily allows for the identification of repaired clones, and because of the availability of an extensive collection of endogenous mutants obtained by UV irradiation, and different chemicals such as *N*-hydroxy-aminofluorene [22–26].

To test the potential of repair-PPRHs in different types of point mutations, we used a collection of various *dhfr* mutant cells; all derived from the parental cell line UA21 [27], which carries only one copy of the *dhfr*

Table 1. Compendium of different mutant cell lines subjected to correction using Repair-PPRHs.

Cell line	Position	Alteration	Base change	Coding change (normal termination is at 562)
DA5	541 (exon 6)	Deletion (-G)	GAA > -AA	Opal at 584 in exon 6
DA7	235 (exon 3)	Substitution	GAG > TAG	Amber in place
DI33A	493 (exon6)	Insertion (+G)	GGG / GGGG	Opal at 505
DP12B	370 – 2 (intron 4)	Substitution	ag > tg	Exon 5 skipped Opal at 504
DU8	136 +1 (exon2/ intron2)	Double substitution	G/gt > A/at	Exon 2 skipped Opal at 139
DF42	541 (exon 6)	Substitution	GAA > TAA	Ochre in place

polypyrimidine regions near to the point mutations and proceeded according to the rules of PPRH construction [16,17]. When encountering purine interruptions in the polypyrimidine stretches, we chose the WT-PPRH strategy, which includes the base complementary to the target interruption in the PPRH core [28].

Table 2 shows the names and sequences of the repair-PPRHs as well as the cell line used. The corresponding corrected nucleotide in the repair-PPRHs is shown in bold and bigger size. Bulleted symbols represent reverse-Hoogsteen bonds.

In all of the experiments, DHFR mRNA levels, protein levels, enzyme activity levels and DNA sequences were determined as follows. Different numbers of cells, ranging from 1,000 to 150,000 were plated and the corresponding repair-PPRHs were transfected using 2 to 5 μg of DNA. Six random cell colonies surviving in -GHT medium from different experiments were expanded individually, and the targeted DNA region was PCR-amplified and sequenced. Cells were subsequently analyzed for DHFR mRNA, protein, and enzyme activity levels. DHFR protein levels in the repaired cells were measured by Western blot performed with 100 μg of total protein extracts and were normalized to tubulin levels. Protein levels in the repaired colonies were referred to those of the positive control UA21. DHFR activity was determined by the incorporation of 2 μCi of 6- ^3H deoxyuridine to the DNA. Cells were collected and lysed with SDS after 24 h. Radioactivity was counted in a scintillation counter. DHFR mRNA levels were measured using qRT-PCR and were normalized to APRT. DHFR mRNA levels of the repaired colonies were also referred to the positive control UA21.

3. Correction of single point mutations using Repair-PPRHs

The first cell line subjected to correction by repair-PPRHs was DA5, where the deletion of a guanine in exon 6 of the *dhfr* gene results in a frame shift that generates a premature opal stop codon (TGA). The repair-PPRH used (HpDE6rep) contained three pyrimidine interruptions, and its hairpin core was extended with 25nt at the 5' end including the missing guanine. We confirmed the presence of the corrected nucleotide in all repaired colonies analyzed. DHFR mRNA levels in the repaired cells were higher than in the mutant DA5 cell line. The protein was restored in all cases, and it showed high levels of DHFR activity (Fig. 5). The next step was to test whether repair-PPRHs were also able to correct substitutions. Thus, we chose DA7 cells that contain a substitution of a guanine by a thymine in exon 3, producing an amber stop codon (TAG) in situ. A 20nt

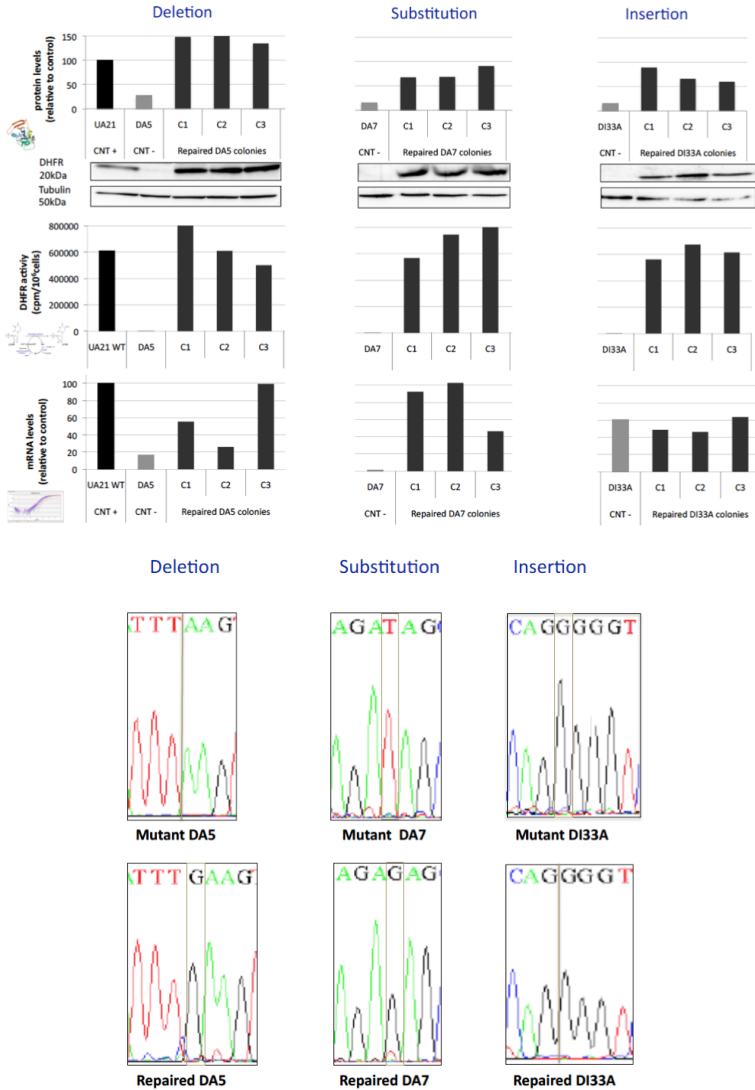


Figure 5. Correction of a deletion, a substitution and an insertion in *dhfr* mutant cell lines. DHFR protein levels, DHFR activity, DHFR mRNA levels and DNA sequences in repaired cells are shown. UA21 cells bearing a copy of the *dhfr* wild type gene are used as a positive control whereas the mutant cell line corresponds to the negative control.

polypyrimidine sequence in the template strand upstream of the point mutation was used to design HpDE3rep. The sequence tail was extended from the 3' end of the hairpin core, with the wild type guanine instead of the thymine present in the mutant. After the isolation of the surviving colonies, we confirmed the corrected guanine in the DNA sequence, high levels of mRNA, protein, and activity compared to DA7 cells (Fig. 5).

Insertions are another type of point mutation very detrimental due to the disruption of the reading frame of a sequence. We chose the DI33A cell line to test whether repair-PPRHs were able to correct an insertion of a guanine in dhfr exon 6. Two repair-PPRHs were designed.

HpDE6-4rep using a 14nt pyrimidine sequence found in the coding strand upstream of the mutation, and HpDE6-5rep using a 15nt sequence in the template strand downstream of the mutation. Both repair-PPRHs succeeded in correcting the mutation by introducing the missing guanine in the DNA sequence, and thus restoring DHFR protein and its activity [29]. The amount of DHFR mRNA of repaired cells was similar to those of the mutant cells (Fig. 5).

Substitutions can also be found in non-coding regions, without changes in the amino acid sequence. However, an alteration in an intron may affect splicing and lead to a frame shift in the subsequent downstream amino acid sequence. Hence, the DP12B mutant cell line was chosen to test the capacity of repair-PPRHs to correct a substitution of an adenine by a thymine at the penultimate position of intron 4 that causes the skipping of exon 5 and a subsequent opal premature stop codon in exon 6. We searched for polypyrimidine sequences in both DNA strands near the point mutation, finding different domains. HpDI4-2rep originated from a 13nt polypyrimidine sequence in the template strand, 18nt upstream of the mutation. The second repair-PPRH target was 22nt, contained one purine interruption and was found 41nt upstream of the mutation. In this case, it was not feasible to design a repair tail directly attached to the hairpin core, because the total repair-PPRH sequence would exceed a length of 100nt in the synthesis of oligonucleotides. Therefore, we attempted a different design in which the hairpin core and the repair tail were connected by 5 thymidines instead of the whole intervening sequence between them. This PPRH was called SDR-HpDI4-3rep, for Short-Distance-Repair hairpin, since it skipped 26 nucleotides of the intron. Upon transfection, surviving colonies were obtained in selective medium with HpDI4-2rep and SDR-HpDI4-3rep. These colonies were isolated and analyzed, and DHFR mRNA levels were comparable to the mutant cells. The DNA sequence was corrected and the protein was restored showing DHFR activity (Fig. 6) [29].

Our results showed that repair-PPRHs could correct different types of single nucleotide mutations. The next challenge would be to repair double point mutants. Thus, DU8 cells were selected to test the ability of repair-PPRHs to correct the tandem mutation of two nucleotides. DU8 cells contain a substitution of 2 nucleotides, Gg > Aa, involving the last nucleotide of exon 2, and the first nucleotide of intron 2. This change does not involve a nonsense mutation *in situ*, but provokes the skipping of exon 2, which disrupts the reading frame. As a consequence, an opal stop codon appears prematurely. Two different repair-PPRHs were designed for this approach: HpDE2-1rep, located 7nt upstream of the mutation, and HpDE2-2rep, 12nt downstream of the mutation. The structure of HpDE2-1rep is that of a hairpin core of 13nt, containing two pyrimidine interruptions, followed by a 24nt tail bearing the corrected nucleotides. In HpDE2-2rep the hairpin core contains 10nt, with one interruption, ending in a 25nt repair tail. Both repair-PPRHs succeeded in correcting the double point mutation at all levels (Fig. 6) [29].

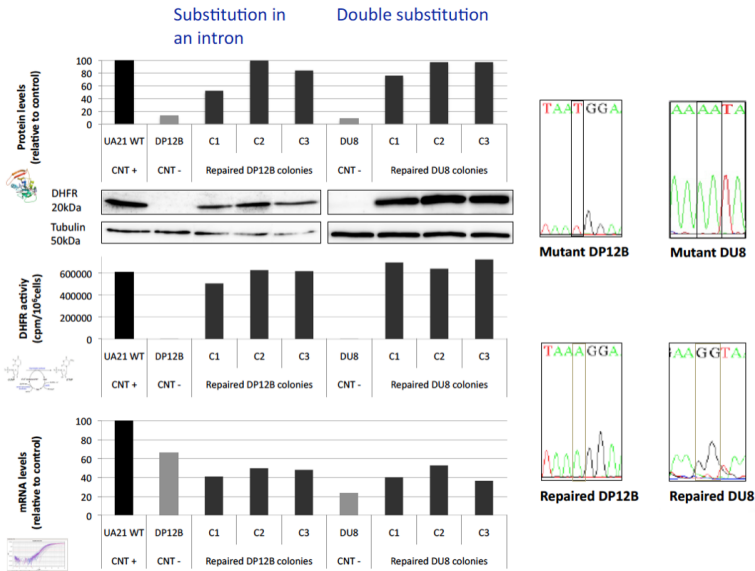


Figure 6. Correction of a substitution in an intron and a double substitution in *dhfr* mutant cell lines. DHFR protein levels, DHFR activity, DHFR mRNA levels and DNA sequences in repaired cells are shown. Experimental conditions are the same as described before. UA21 cells bearing a copy of the *dhfr* wild type gene are used as a positive control whereas the mutant cell line corresponds to the negative control.

One of the limitations of this methodology could reside in finding homopurine domains relatively close to the point mutation. To solve this, we designed a Long Distance Repair-PPRH (LDR-PPRH) which contains a hairpin core hundreds of nucleotides away from the location of the mutation, linked by 5 Ts to the repair tail. This approach was tested in DF42 cells, containing a substitution of a guanine by a thymine in exon 6 resulting in an ochre stop codon (TAA). We designed a repair tail at the location of the point mutation, and a hairpin core targeting a sequence located 662nt downstream. This repair-PPRH was called LDR-HpDE6-1rep, formed by a hairpin core of 22nt in each homopurine strand containing three pyrimidine interruptions, and a tail of 31nt. In parallel, we also tested HpDE6rep, a regular repair-PPRH, and we obtained similar results

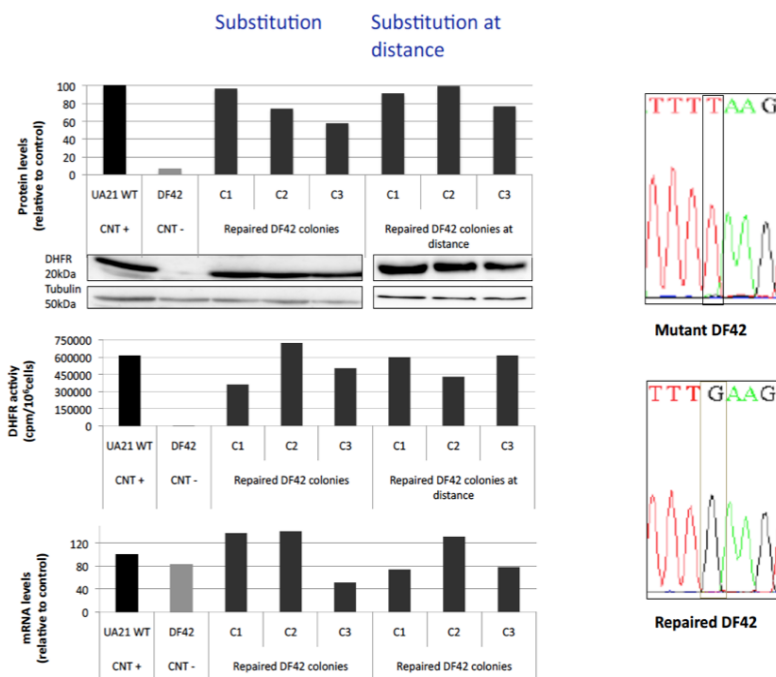


Figure 7. Correction of a G substitution in DF42 cell line. DHFR protein levels, DHFR activity, DHFR mRNA levels, and DNA sequences in repaired cells are shown. Experimental conditions are the same as described before. UA21 cells bearing a copy of the *dhfr* wild type gene are used as a positive control whereas the mutant cell line corresponds to the negative control.

for both approaches. The levels of mRNA in the repaired cells were similar to those of the mutant. However, repaired colonies recovered DHFR protein with high activity, and the nucleotide was corrected in the DNA sequence (Fig. 7) [29].

4. Editing-PPRHs

Duchenne muscular dystrophy (DMD) is a progressive and fatal degenerative muscle disease caused by mutations due to large deletions (approx. 65%) in the DMD gene encoding for the dystrophin protein. Accordingly, the resulting reading frame involves an aberrant dystrophin translation, causing the absence of the protein essential for the muscle. This leads to an irreversible damage of muscle fibers that are replaced by adipose tissue. A variant of the disease, the Becker muscular dystrophy (BMD), results in a much milder phenotype. This disease is also caused by mutations in the dystrophin gene, but they do not completely disrupt the reading frame of the protein, and thus allow the production of a reduced version of a partially functional protein. In DMD one or several exons are deleted, and this mutation interferes with the assembly of the full-length mRNA. This fact led to the development of a therapeutic strategy for DMD called "exon skipping strategy", in which antisense deoxyoligonucleotides (aODNs) are used to mediate the elimination of the mutated exon, alone or with additional adjacent exons, to restore the reading frame of the protein. In these conditions, the expression of a shorter but functional dystrophin protein is induced, simulating the BMD phenotype [30]. Theoretically, exon skipping could be used to treat approximately 90%, 80%, and 98% of DMD patients with deletion, duplication, and nonsense mutations, respectively [31]. Several aODNs developed using different chemical modifications such as 2'OMethyl (Prosensa Inc., Switzerland) and morpholinos (PMOs) (AVI Biopharma, UK) are currently in Phase II or Phase III trials to validate the effectiveness of this therapeutic approach.

In order to explore the capability of PPRHs to cause Exon-skipping at the DNA level to be applied to the DMD gene as a possible therapeutic tool, we probed the potential of PPRHs for this purpose using a gene with a clean metabolic selection. In this regard, the editing abilities of PPRHs were explored using a stably transfected DHFR mutant with duplication of Exon-2 of the *dhfr* gene that causes a frameshift abolishing DHFR activity. Chen and Chasin [32] developed this model generating NB6 cells, carrying that minigene with 2 Exons 2 of the *dhfr* gene (D22) (Fig. 8).

Those cells are auxotrophic for glycine, hypoxanthine and thymidine. However, strategies that induce Exon-skipping of that minigene within NB6 cells and recover prototrophy for one carbon metabolism. Therefore, Exon-skipping can be positively detected and selected by growing NB6 cells in $-GHT$ medium. This approach was used to test the capability of PPRHs to cause Exon-skipping at the DNA level.

The sequence corresponding to the pD22 minigene was analyzed for polypurine target regions and the corresponding editing-PPRHs were designed, by attaching to the end of one strand of the PPRH core, a sequence tail homologous to the upstream and downstream regions of the PstI restriction site in the original *dhfr* minigene pDCH1P (Fig. 9).

pD22

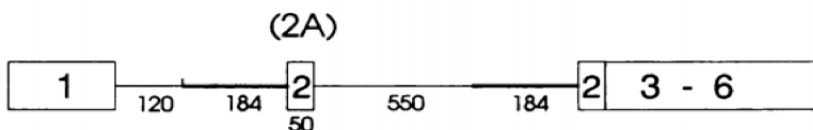


Figure 8. Structure of the pD22 *dhfr* minigene. The Chinese hamster *dhfr* minigene pDCH1P containing the six exons of the gene, intron 1, about 900 bp of the 5' flank, and the first of the two major polyadenylation sites in exon 6 was used to construct pD22 in which a 0.8-kb PstI-BstEII genomic DNA fragment containing exon 2 and flanks was cloned into the unique PstI site in intron 1 of pDCH1P.

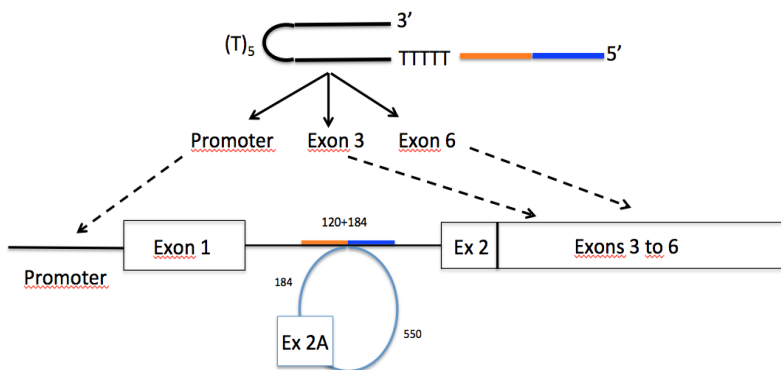


Figure 9. Structure of the different Editing-PPRH used to edit the extra exon 2 present in the *dhfr* minigene pD22 stably transfected in NB6 cells.

150,000 NB6 cells were plated and the corresponding editing-PPRHs were transfected using 2 to 5 μg of DNA. Random cell colonies surviving in $-\text{GHT}$ medium from different experiments were expanded individually, and the targeted DNA region was PCR-amplified and sequenced. Cells were subsequently analyzed for DHFR protein, and enzyme activity levels. As it can be seen in Fig. 10, in all the clones analyzed, DHFR protein was restored, and it showed high levels of DHFR activity. Furthermore, the DNA sequencing results proved that the *dhfr* sequence in all the surviving clones corresponded to the wild type *dhfr* minigene with just one copy of Exon 2 (data not shown).

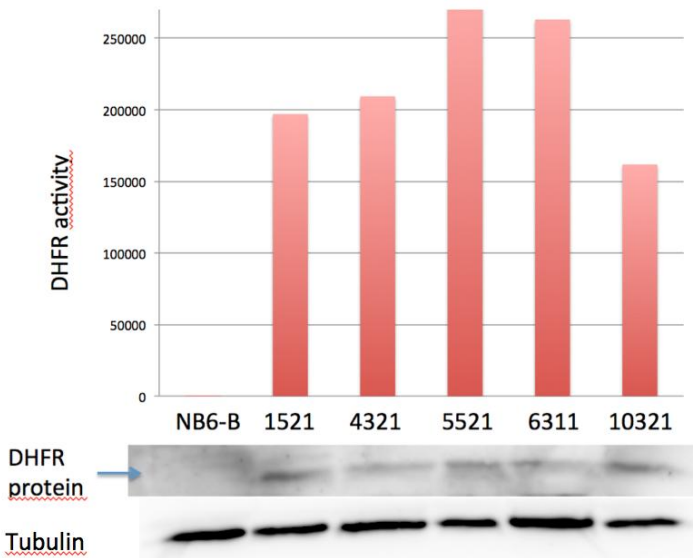


Figure 10. DHFR activity and protein levels. Experimental conditions as described. DHFR activity and protein levels in the edited colonies were compared to those of the control NB6-B cells.

5. Conclusion

We provide evidences that repair-PPRHs have the ability to correct different types of mutations in mammalian cells. Therefore, our method may offer an alternative, simple, and powerful tool for gene therapy to correct many disorders caused by point mutations. In addition, we show that

editing-PPRHs represent an alternative method to ZFN, TALEN and CRISPR/Cas9 site specific nucleases for efficient editing, without the difficulty in constructing and delivering exogenous enzymes, the off-target effect caused by the nucleases, and the non-homologous end joining effects stimulated after a DNA double strand break.

Acknowledgements

The work was supported by Grants SAF2011-23582 and SAF2014-51825-R from “Plan Nacional de Investigación Científica” (Spain). Our group holds the Quality Mention from the “Generalitat de Catalunya” 2014-SGR96. A.S. was recipient of a FI fellowship from the “Generalitat de Catalunya”. A.J. is recipient of a FPU fellowship from the “Ministerio de Educación”.

References

1. Jackson, S.P., Bartek, J. 2009, *Nature*, 461, 1071.
2. Lodish, H., Berk, A., Zipursky, L., Matsudaira, P., Baltimore, D., Darnell, J. 2004, *Molecular Cell Biology*, 4th Edition.
3. Luch, A. 2005, *Discov Med*, 5, 472.
4. Bernstein KA, Mimitou EP, Mihalevic MJ, Chen H, Sunjaveric I, Symington LS, Rothstein R. 2013, *Genetics*, 195,1241.
5. Canman, C.E., Lim, D.-S. 1999 *Oncogene*, 17, 3301.
6. Banin, S., Moyal, L., Shieh, S., Taya, Y., Anderson, C.W., Chessa, L., Smorodinsky, N.I., Prives, C., Reiss, Y., Shiloh, Y., Ziv, Y.1998, *Science*, 281,1674.
7. Tibbetts R.S., Brumbaugh, K.M., Williams, J.M., Sarkaria, J.N., Cliby, W.A., Shieh, S.Y., Taya, Y., Prives, C., Abraham, R.T.1999, *Genes Dev*, 13, 152.
8. Liu N, Bryant PE. 1994, *Int J Radiat Biol*, 66, S115.
9. Wiman KG. 2006, *Cell Death Differ*, 13, 921.
10. Martinho RG¹, Lindsay HD, Flaggs G, DeMaggio AJ, Hoekstra MF, Carr AM, Bentley N.J.1998, *EMBO J*, 17, 7239.
11. Latif, C., Harvey, S.H., O’Connell, S.J. 2001, *Sci World J*, 1, 684.
12. Wyman, C., Kanaar, R. 2006, *Annu Rev Genet*, 40, 363.
13. Carroll, D., Beumer, K.J. 2014, *Methods*, 69, 137.
14. Ochiai, H. 2015, *Int J Mol Sci*, 16, 21128.
15. Coma, S., Noe, V., Eritja, R., Ciudad, C. J. 2005, *Oligonucleotides*, 15, 269.
16. de Almagro, M. C., Coma, S., Noe, V., Ciudad, C. J. 2009, *J. Biol. Chem.*, 284, 11579.
17. de Almagro, M. C., Mencia, N., Noe, V., Ciudad, C. J. 2011 *Hum. Gene Ther.* 2011, 22, 451.

18. Rodriguez, L., Villalobos, X., Dakhel, S., Padilla, L., Hervas, R., Hernandez, J. L., Ciudad, C. J., Noe, V. 2013, *Biochem. Pharmacol.*, 86, 1541.
19. Villalobos, X., Rodriguez, L., Prevot, J., Oleaga, C.; Ciudad, C. J.; Noe, V. 2014, *Mol. Pharm.*, 11, 254.
20. Villalobos, X., Rodriguez, L., Sole, A., Lliberos, C., Mencia, N., Ciudad, C. J., Noe, V. 2015, *Nucleic Acid Ther.*, 25, 198.
21. Sole, A., Villalobos, X., Ciudad, C. J., Noe, V. 2014, *Hum. Gene Ther. Methods*, 25, 288.
22. Carothers, A. M., Urlaub, G., Steigerwalt, R. W., Chasin, L. A., Grunberger, D. 1986, *Proc Natl Acad Sci U S A*, 83, 6519.
23. Urlaub, G., Mitchell, P. J., Ciudad, C. J., Chasin, L. A. 1989, *Mol. Cell. Biol.*, 9, 2868.
24. Chasin, L. A., Urlaub, G., Mitchell, P., Ciudad, C., Barth, J., Carothers, A. M., Steigerwalt, R., Grunberger, D. 1990, *Prog. Clin. Biol. Res.*, 340A, 295.
25. Carothers, A. M., Urlaub, G., Grunberger, D., Chasin, L. A. 1993, *Mol. Cell. Biol.*, 13, 5085.
26. Carothers, A. M., Urlaub, G., Mucha, J., Yuan, W., Chasin, L. A., Grunberger, D. 1993, *Carcinogenesis*, 14, 2181.
27. Urlaub, G., Kas, E., Carothers, A. M., Chasin, L. A. 1983, *Cell*, 33, 405.
28. Rodriguez, L., Villalobos, X., Sole, A., Lliberos, C., Ciudad, C. J., Noe, V. 2015, *Mol. Pharm.*, 12, 867.
29. Solé, A., Ciudad, C.J., Chasin, L.A., Noé, V. 2016, *Biochem Pharmacol*, 110–111, 16.
30. Douglas, A.G.L., Wood, M.J.A. 2013, *Mol Cell Neurosci*, 56, 169.
31. Echigoya, Y., Yokota, T. 2014, *Nucleic Acid Ther*, 24, 57.
32. Chen, I.T., Chasin, L.A. 1993, *Mol Cell Biol*, 13, 289.



Research Signpost
Trivandrum
Kerala, India

Recent Advances in Pharmaceutical Sciences VII, 2017: 69-82 ISBN: 978-81-308-0573-3
Editors: Diego Muñoz-Torrero, Montserrat Riu and Carles Feliu

5. Research in natural products: Amaryllidaceae ornamental plants as sources of bioactive compounds

Laura Torras-Claveria, Luciana Tallini, Francesc Viladomat,
and Jaume Bastida

*Department of Biology, Healthcare and the Environment, Faculty of Pharmacy and Food Sciences,
University of Barcelona, 08028 Barcelona, Catalonia, Spain*

Abstract. Amaryllidaceae plants are known for their ornamental flowers all over the world, but they also have a medicinal value owing to their exclusive group of alkaloids. The Amaryllidaceae alkaloids have a wide range of important biological activities, notably anti-tumoral, anti-parasitic, and acetylcholinesterase inhibition. This review focuses on the chemical characteristics of Amaryllidaceae plants and alkaloids, as well as the different methodologies applied in their study, including promising new docking studies.

Introduction

Amaryllidaceae plants are known for their outstanding attractive flowers (Figure 1), and are widely used and cultivated for ornamental purposes. For example, *Narcissus* species are extensively cultivated and exported for

Correspondence/Reprint request: Dr. Jaume Bastida, Department of Biology, Healthcare and the Environment, Faculty of Pharmacy and Food Sciences, University of Barcelona, 08028 Barcelona, Catalonia, Spain
E-mail: jaumbastida@ub.edu

ornamental use in the UK and the Netherlands, as are *Lycoris* species in China and Japan, while *Crinum* species are appreciated for their lily-like flowers [1].



Figure 1. *Hymenocallis* spp. (Amaryllidaceae) from Venezuela

Amaryllidaceae plants also have a long history of use for medicinal purposes. The specific type of alkaloids they contain, named Amaryllidaceae alkaloids, display a wide range of biological activities such as antiviral, antimalarial, anticancer and anticholinesterasic [2].

1. Amaryllidaceae family characteristics

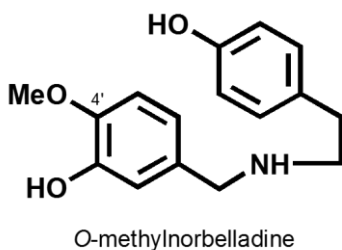
The Amaryllidaceae family, of the order Asparagales, consists of bulbous flowering plants, and is divided in three subfamilies (Agapanthoideae, Allioideae and Amaryllidoideae) previously considered as three separate families. The term “Amaryllidaceae”, whether referring to plants or alkaloids, is ubiquitous in the phytochemical and pharmaceutical literature on the subfamily Amaryllidoideae [1, 3]. The monocotyledonous Amaryllidoideae subfamily comprises around 1000 species in 60 genera with a pantropical distribution, above all in three geographic locations: Andean South America, Southern Africa and the Mediterranean coast. Amaryllidoideae plants have a high capacity for adaptation. Those of the genera *Leptochiton* and *Paramongaia* survive in areas with a very arid

climate, since bulbs can remain latent for long periods, while *Hippeastrum* and *Hymenocallis* thrive in humid woods [4].

The medicinal use of Amaryllidaceae plants goes back to the Classical period, when Hippocrates and Dioscorides were already using *Narcissus* oil to treat illnesses thought to be linked to uterine tumours. References to *Narcissus* usage against cancer are also found in Pliny the Elder and the Bible. Today Amaryllidaceae plants are still extensively used in traditional medicine in several countries. For example, *Ammocharis* is cooked and used as an enema for blood cleansing or to cure open wounds; bulbs of *Brunsvigia* are applied as antiseptic dressing on fresh wounds and their decoctions treat coughs, colds, and liver diseases; *Clivia* species are used to treat snakebites and wounds, and to facilitate birth; *Crinum* species are applied as a powerful emetic, to treat tumours (Asia and America) and colds, wash wounds and haemorrhoids, as a gynecological remedy (South Africa) and a rubefacient in the treatment of rheumatism (India) [5].

2. Amaryllidaceae alkaloids

Virtually exclusive to the Amaryllidoideae subfamily, the Amaryllidaceae alkaloids have anti-viral, anti-parasitic, anti-cancer and anti- cholinesterasic



<i>ortho-para'</i>	<i>para-para'</i>	<i>para-ortho'</i>
<u>types</u>	<u>types</u>	<u>types</u>
lycorine homolycorine	crinine haemanthamine tazettine narciclasine montanine	galanthamine

Figure 2. Three options of cyclization of the precursor *O*-methylnorbelladine and the resulting alkaloid types.

activities, which are probably the origin of many of the traditional medicinal uses of Amaryllidaceae plants. Although structurally diverse, Amaryllidaceae alkaloids are biogenetically related and can be classified into nine basic skeleton groups: norbelladine-, lycorine-, homolycorine-, crinine-, haemanthamine-, narciclasine-, tazettine-, montanine-, and galanthamine-types. However, there are exceptions like graciline or plicamine, which cannot be classified in any of these classical groups, and a new plicamine-type alkaloid was recently identified in *Narcissus broussonetii* [6].

All Amaryllidaceae alkaloids derive from the amino acids L-phenylalanine and L-tyrosine, from which the common precursor *O*-methylnorbellamine is synthesized. A final cyclisation step with different phenol oxidative couplings leads to a diversification of structures (Figure 2) [7].

3. Study of the genus *Narcissus*

The genus *Narcissus* comprises more than one hundred wild species and is mainly distributed around the Mediterranean Sea, including south-western Europe, North Africa, Italy and the Balkans. This genus has an ornamental value, and its easy hybridization has allowed numerous cultivars to be developed.

The traditional medicinal uses of this genus are well documented. The Bible mentions the treatment of symptoms that could now be defined as cancer with *Narcissus poeticus*. Chinese, North African and Arabian medicine continues using this treatment. Today, it is known that *N. poeticus* contains 0.012% of the antineoplastic agent narciclasine [8].

The first isolated Amaryllidaceae alkaloid was lycorine, from *Narcissus pseudonarcissus* by Gerrard in 1877 [9]. Since then, numerous Amaryllidaceae alkaloids have been isolated in more than 40 wild species and over 100 cultivars. The most common alkaloids in *Narcissus* species are lycorine- and homolycorine-types; notably, they do not contain crinine-type alkaloids, as they synthesise alkaloids with the 5,10b-ethano bridge in an α , not β position [8].

Amaryllidaceae alkaloids isolated in the genus *Narcissus* were reviewed by Bastida *et al.* (2006) [8], and others have been identified by the same group since then [6, 7, 10, 11, 12, 13, 14].

4. Amaryllidaceae plants in traditional medicine in South Africa

Folk medicine still plays a crucial role in the healthcare of a great part of the population in South Africa. It has been estimated that around 27 million South Africans consult traditional healers. Contrary to popular belief, this practice is not restricted to poor and uneducated people, whose access to western medicine is limited by cost or distance, but extends to all sectors of the society [15, 16].

The use of Amaryllidaceae plants in traditional South African medicine by indigenous people has a long history, and some applications were also adopted by early European colonists. Today several concoctions, decoctions, extracts and herbal preparations of Amaryllidaceae species can be found in local traditional medicinal markets. For example, *Apodolirion buchananii* is taken for stomach disorders and *Brunsvigia* species are used against infertility in [16]. Since the application of Amaryllidaceae plants to wounds is widespread, it was suspected that they had antibacterial properties. Indeed, several Amaryllidaceae alkaloids have been isolated and identified in these plants and their antibacterial [17], antifungal [18] antiviral [19], anti-inflammatory and antiparasitic [18] activities have been determined.

5. Amaryllidaceae alkaloids from Amaryllidaceae plants in Ibero-America

Ibero-America, together with South Africa, is a centre of diversification of the Amarylloideae subfamily. While many species remain unexplored, knowledge of Ibero-American Amaryllidaceae plants has advanced considerably in recent years. For example, the novel alkaloid phaedranamine was identified together with 7 known alkaloids in *Phaedranassa dubia* (Colombia) [20]. *Zephyranthes concolor* (Mexico) was studied for the first time in 2011 and 6 Amaryllidaceae alkaloids were identified [21]. Wild Amaryllidaceae species (*Habranthus jamesonii*, *Phycella herbertiana*, *Rhodophiala mendocina*, and *Zephyranthes filifolia*) from the Argentinian Andes were analysed for their alkaloid composition for the first time in 2011, revealing the presence of galanthamine and good acetylcholinesterase activity [22]. The alkaloid composition of the Colombian endemic species *Caliphruria subedentata*, one of only four species of the infrequent genus *Caliphruria*, was analysed by GC-MS and 18 alkaloids were identified, in addition to six others isolated with classical phytochemical methods [23]. The new alkaloid 1-epidemethylbowdensine

was reported for the first time in *Crinum erubescens* collected in Costa Rica [24].

Hippeastrum is a well-known ornamental genus from South America with around 70 species, 34 of them found in Brazil, which according to nrDNA ITS sequences is the area of origin of the genus [25]. In a review focusing on the chemistry and biological activity of Amaryllidaceae alkaloids in the genus *Hippeastrum*, de Andrade *et al.* (2012) [25] include several new Amaryllidaceae alkaloids they identified for the first time, notably 2 α ,7-dimethoxyhomolycorine and candimine in *Hippeastrum morelianum* [26], and 11 β -hydroxygalanthamine in *Hippeastrum papilio* [27]. Other new alkaloids have been identified for the first time in the Brazilian species *Hippeastrum aulicum* and *H. calypratrum* (aulicine, 3-*O*-methylepipimacowine, 11-oxohaemanthamine and 7-methoxy-*O*-methyllycorenine) [28], and *H. breviflorum* (9-*O*-demethyllycosinine B) [29]. Recently, more new Amaryllidaceae alkaloids have been identified in *H. papilio* (hippabiline, papiline, 3-*O*-demethyl-3-*O*-(3-hydroxybutanoyl)-haemanthamine) [30].

In Argentina, the genus *Hippeastrum* comprises nine widely distributed and poorly studied species, some of them used in traditional medicine by the Toba indigenous community. *H. argentinum* has recently been studied in terms of alkaloid composition and biological activity and two new alkaloids were identified (4-*O*-methylangustine and 7-hydroxyclyvonine). Furthermore, promising docking studies activities are being carried out [31].

6. Study of galanthamine-producing species

Galanthamine is an Amaryllidaceae alkaloid sold as a drug under the commercial name of Reminyl[®] in Europe and Razadine[®] in the USA for the palliative treatment of mild to moderate stages of Alzheimer's disease. Galanthamine can be obtained by chemical synthesis, but the yield is too low to be economically feasible. Instead, it is obtained from natural sources such as *Galanthus nivalis*, *Leucojum aestivum*, *Lycoris radiata* and different species of *Narcissus*. However, several problems, including unsuccessful cultivation or slow regeneration, make it difficult to meet the increasing pharmaceutical demands for this drug [14]. Another issue is the great chemodiversity in one of the main industrial sources of galanthamine, *Leucojum aestivum*. Balearic populations of this species have an alkaloid profile dominated by crinine-type

compounds, while in those close to the Danube River homolycorine-type alkaloids are dominant. In populations from east Bulgaria the main alkaloid is lycorine, and only populations in south Bulgaria were found to predominantly contain galanthamine-type compounds. Thus, the content of galanthamine in *Leucojum aestivum* can range from 0.2 to 95% of total alkaloids [32].

More than 27,000 names of *Narcissus* ornamental cultivars have been registered in the International Daffodil Register and some intersectional cultivars have also been reported as potential sources of galanthamine. These cultivars present some advantages for alkaloid production, as they are less affected by planting depth and density, and large-scale cultivation has already been established for the ornamental plant industry [14]. In this context, 105 ornamental varieties of *Narcissus* were analysed by GC-MS for

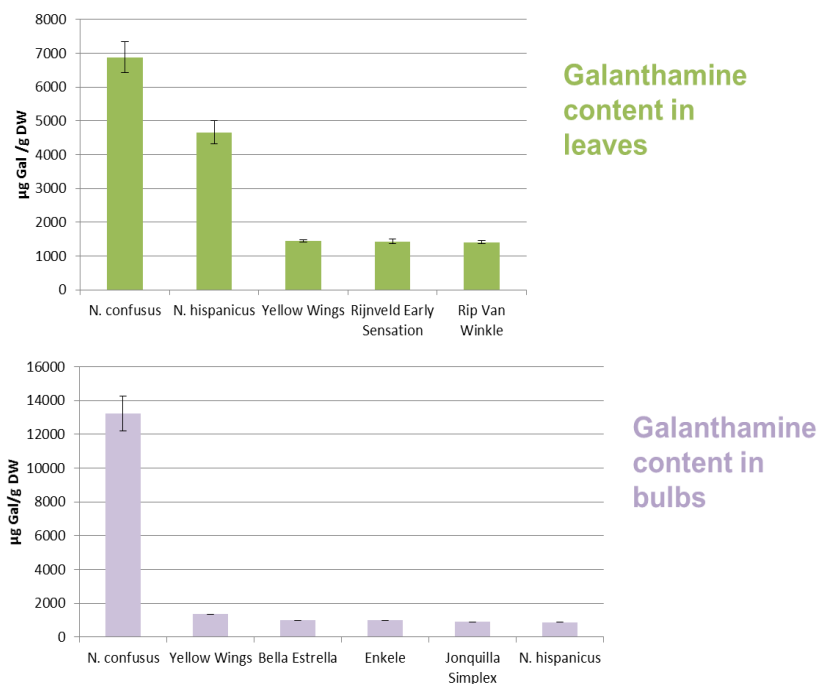


Figure 3. *Narcissus* varieties with highest galanthamine content

their galanthamine content and acetylcholinesterase inhibitory activity, distinguishing between bulbs and leaf tissues. The highest content of galanthamine was found in leaves from *N. hispanicus*, followed by the cultivars 'Rijnveld Early Sensation' and 'Rip van Winkle', and the bulbs of the cultivars 'Yellow Wings' and 'Bella Estrella', which could constitute promising new sources of this valuable metabolite (Figure 3) [14].

The total alkaloid composition of these varieties was also determined by GC-MS, comparing alkaloid mass spectra and the Kovats Retention Index with those of authentic standards previously isolated and identified by spectroscopic methods by our group in other Amaryllidaceae plants. Also, a k-means cluster analysis was performed with ornamental varieties according to the alkaloid composition of leaves and bulbs separately, obtaining 5 clusters of cultivars in each tissue. A correspondence analysis was performed to detect a possible relationship between those clusters according to the alkaloid composition and horticultural divisions of *Narcissus* ornamental varieties [7].

7. Pharmacological activity

7.1. Antitumoral

Antitumoral activity was one of the first biological effects attributed to Amaryllidaceae plants. In the early 1980s, several reports on cytotoxic and antineoplastic activities of certain Amaryllidaceae alkaloids appeared, but it was in 1995 when a significant number of Amaryllidaceae alkaloids with different skeleton types were evaluated for their cytotoxicity against a panel of human and murine cell lines. While almost all Amaryllidaceae alkaloids tested were active against fibroblastic LMTK murine cells, pretazettine was the most active against human tumoral Molt4 lymphoid cells, but with no activity against human tumoral hepatoma cells, HepG2. Conversely, lycorenine was the most active against HepG2 cells, and almost inactive against Molt4 cells [33]. Since then, other Amaryllidaceae alkaloids have proved active against other cell lines [34, 35, 36]. Selective apoptosis-inducing effects have been observed in Amaryllidaceae alkaloids of different structural types, leading to structure-activity studies (SAR). For example, an α -ethanobridge and a free hydroxyl at the C-11 position are required for the potent apoptosis induced by crinane- and lycorine-type Amaryllidaceae alkaloids in tumor cells [37, 38, 39]. The

phenanthridinones, exemplified by narciclasine and pancratistatine, have recently attracted considerable interest owing to their potent cell line-specific anticancer activities and minimal effect on normal cells, and a clinical candidate is earmarked for commercialisation in the next decade. Their mechanism is thought to be based on the initiation of cell death via the apoptotic pathway [40].

7.2. Antiparasitic

Antiparasitic properties have been found in some Amaryllidaceae alkaloids. For example, lycorine, augustine and crinamine are the principal antimalarial constituents of *Crinum amabile*, especially augustine, which inhibited both chloroquine-sensitive and chloroquine-resistant strains of *Plasmodium falciparum*. Haemanthamine, haemanthidine, 3-epihydroxybulbispermine, galanthine and pancracine are also particularly active against these parasites, some even more so than the standards currently used for treatment [41].

In relation to Chagas disease and Sleeping Sickness, haemanthidine, pancracine, 3-*O*-acetylsanguinine and 1,2-*O*-diacetylycorine showed biological activity against *Trypanosoma cruzi* and *Trypanosoma brucei-rhodesiense* [20]. The activity of alkaloids isolated in *Phaedranassa dubia* was evaluated against a range of parasitic protozoa, and ungeremine showed the best activity against *T. brucei-rhodesiense*, *T. cruzi* and *P. falciparum* [20]. Compounds from *Galanthus trojanus* also demonstrated antiparasitic properties, protopine being especially promising for its high selectivity and potency against *T. brucei-rhodesiense* and *P. falciparum* K1, which is a drug-resistant strain [42]. Also, the ethanolic extract of *Narcissus broussonetii* demonstrated significant activity against *T. cruzi* [6].

7.3. Acetylcholinesterase inhibition

Inhibition of the acetylcholinesterase enzyme is one of the most important biological activities of certain Amaryllidaceae alkaloids. Galanthamine is currently the only Amaryllidaceae alkaloid commercially sold for the treatment of mild-to-moderate stages of Alzheimer's disease, owing to its capacity to inhibit the enzyme acetylcholinesterase in the brain and, at same time, interact with nicotinic receptors. Thus, the levels of acetylcholine in the brain, which decline in people with Alzheimer's disease, can be maintained [1, 43]. Inhibition of acetylcholinesterase activity has

been reported in other Amaryllidaceae alkaloids, including sanguinine, montanine, 11-hydroxygalanthamine, epinorgalanthamine, and assoanine [44, 45, 46], and some of them, such as sanguinine, are even more potent than galanthamine. However, the extra hydroxyl group of sanguinine, available for the interaction with acetylcholinesterase, makes the molecule more hydrophilic, thus reducing its ability to cross the blood-brain barrier [47]. Also, natural *N*-alkylated galanthamine derivatives such as *N*-allylnorgalanthamine and *N*-(14-methylallyl)norgalanthamine demonstrate a higher inhibition of acetylcholinesterase than galanthamine [48].

7.4. Docking studies

Docking is the use of computational methods to predict the preferred conformation of one molecule to another when they form a stable complex [49]. Docking studies performed with several Amaryllidaceae alkaloids and acetylcholinesterase and butyrylcholinesterase enzymes have revealed, for example, that not only galanthamine-type alkaloids could be useful for the treatment of Alzheimer's disease. Tazettine-type alkaloids should also be considered owing to the high selectivity of 3-epimacronine derivatives for binding the enzyme locus [50]. Docking and molecular dynamics simulation studies have recently shown butyrylcholinesterase inhibitory

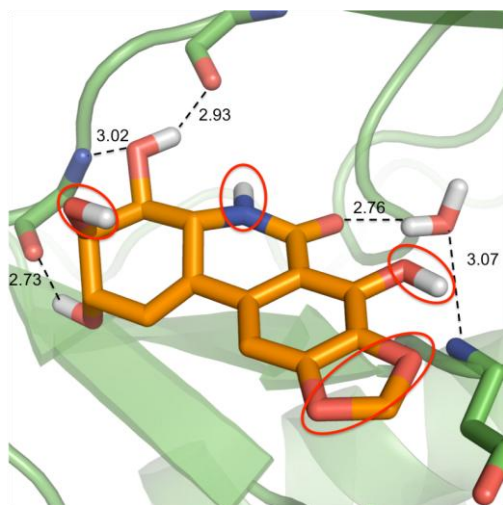


Figure 4. Putative binding mode of narciclasine in GSK-3 β enzyme.

activity in 7-hydroxyclyvonine, which interacts at the same binding site of the enzyme as galanthamine with very similar amino acids (Ortiz et al., 2016). Perspectives for the future include research into glycogen synthase kinase 3 β (GSK3 β) as a new therapeutic target for Amaryllidaceae alkaloids. This enzyme is involved in several cellular processes, including some proteins involved in Alzheimer's disease. Furthermore, there is a growing interest in GSK3 β from unicellular parasites, due to their prominent role in the regulation of circadian rhythms of parasites, which are responsible, for example, for the circadian fever caused by *P. falciparum*, (Figure 4) [51].

8. Conclusion

Amaryllidaceae plants are outstanding, economically important plants, not only for their ornamental value, but also as medicinal plants and sources of drugs and new therapeutic targets. Due to their considerable biodiversification, they are found in almost all the continents: Europe, Asia, Africa and America. Their use in traditional medicine remains important in certain areas, and is supported by numerous scientific studies that have demonstrated the bioactivity of these plants, caused by their content of a particular and exclusive type of alkaloids, named Amaryllidaceae alkaloids.

Acknowledgements

The authors, members of the group 2014 SGR920, are grateful to Dr. A. Marín, Dr. M. A. Molins, Dr. A. Linares, Dr. M. Feliz and Dr. O. Jáuregui from the Scientific and Technological Services of the University of Barcelona.

References

1. Takos, A. M., Rook, F. 2013, *Int. J. Mol. Sci.*, 14, 11713.
2. Bastida, J., Berkov, S., Torras-Claveria, L., Pigni, N. B., de Andrade, J. P., Martínez, V., Codina, C., Viladomat, F. 2011, *Recent Advances in Pharmaceutical Science*, Muñoz-Torrero, D. (Eds.), Transworld Research Network, Kerala, 65.
3. Chase, M. W., Reveal, J. L., Fay, M. F. 2009, *Bot. J. Linn. Soc.*, 161, 132.

4. Meerow, A. W., Snijman, D. A. 1998, The Families and Genera of Vascular Plants, Kubitzki, K. (Eds.), Springer, Berlin, Vol 3, 83.
5. Kornienko, A., Evidente, A. 2008, *Chem. Rev.*, 108, 1982.
6. de Andrade, J. P., Pigni, N. B., Torras-Claveria, L., Berkov, S., Codina, C., Viladomat, F., Bastida, J. 2012, *J. Pharm. Biomed. Anal.*, 70, 13.
7. Torras-Claveria, L., Berkov, S., Codina, C., Viladomat, F., Bastida, J. 2014, *Ind. Crop. Prod.*, 56, 211.
8. Bastida, J., Lavilla, R., Viladomat, F. 2006, The Alkaloids, Cordell, G. A. (Eds.), Elsevier, San Diego, 63, 87
9. Bastida, J., Viladomat, F., Codina, C. 1998, Studies in Natural Products Chemistry, Atta-ur-Rahman (Eds.), Elsevier, Amsterdam, 20, 323.
10. Berkov, S., Martinez-Frances, V., Bastida, J., Codina, C., Rios, S. 2014, *Phytochemistry*, 99, 95.
11. Pigni, N. B., Berkov, S., Elamrani, A., Benaissa, M., Viladomat, F., Codina, C., Bastida, J. 2010, *Molecules*, 15, 7083.
12. Pigni, N. B., Ríos-Ruiz, S., Martínez-Francés, V., Nair, J. J., Viladomat, F., Codina, C., Bastida, J. 2012, *J. Nat. Prod.*, 75, 1643.
13. Pigni, N. B., Ríos-Ruiz, S., Luque, F. J., Viladomat, F., Codina, C., Bastida, J. 2013, *Phytochemistry*, 95, 384.
14. Torras-Claveria, L., Berkov, S., Codina, C., Viladomat, F., Bastida, J. 2013, *Ind. Crop. Prod.*, 43, 237.
15. Mander, M., Ntuli, L., Diederichs, N., Mavunla K. 2007, *South African Health Review*, 13, 189.
16. Nair, J. J., van Staden, J. 2013, *Food Chem. Toxicol.*, 62, 262.
17. Cheesman, L., Nair, J. J., van Staden, J. 2012, *J. Ethnopharmacol.*, 140, 405.
18. Viladomat, F., Bastida, J., Codina, C., Nair, J. J., Campbell, W. E. 1997, Recent Research Developments in Phytochemistry, Pandalai, S. G. (Eds.), Research Signpost Publishers, Trivandrum, 131.
19. Nair, J. J., Bastida, J., Codina, C., Viladomat, F., van Staden, J. 2013, *Nat. Prod. Commun.*, 8, 1335.
20. Osorio, E. J., Berkov, S., Brun, R., Codina, C., Viladomat, F. 2010, *Phytochem. Lett.*, 3, 161.
21. Reyes-Chilpa, R., Berkov, S., Hernández-Ortega, S., Jankowski C. K., Arseneau, S., Clotet-Codina, I., Esté, J. A., Codina, C., Viladomat, F., Bastida, J. 2011., *Molecules*, 16, 9520.
22. Ortiz, J. E., Berkov, S., Pigni, N. B., Theoduloz, C., Roitman, G., Tapia, A., Bastida, J., Ferensin, G. E. 2012, *Molecules*, 17, 13473.
23. Cabezas, F., Pigni, N., Bastida, J., Codina, C., Viladomat, F. 2013, *Rev. Latinoamer. Quím.*, 41, 68.
24. Guerrieri, C. G., Pigni, N. B., de Andrade, J. P., dos Santos, V. D., Binns, F., Borges, W., Viladomat, F., Bastida, J. 2016. *Arab J Chem*, 9,688.
25. de Andrade, J. P., Pigni, N. B., Torras-Claveria, L., Guo, Y., Berkov, S., Reyes-Chilpa, R., El Amrani, A., Zuanazzi, J. A. S., Codina, C., Viladomat, F., Bastida, J. 2012, *Rev. Latinoamer. Quím.*, 40, 83.

26. Giordani, R. B., de Andrade, J. P., Verli, H., Dutilh, J. H., Henriques, A. T., Berkov, S., Bastida, J., Zuanazzi, J. A. 2011, *Magn. Reson. Chem.*, 49, 668.
27. de Andrade, J. P., Berkov, S., Viladomat, F., Codina, C., Zuanazzi, J. A. S., Bastida, J. 2011, *Molecules*, 16, 7097.
28. de Andrade, J. P., Guo, Y., Font-Bardia, M., Calvet, T., Dutilh, J., Viladomat, F., Codina, C., Nair, J. J., Zuanazzi, J. A. S., Bastida, J. 2014, *Phytochemistry*, 103, 188.
29. Sebben, C., Giordani, R. B., de Andrade, J. P., Berkov, S., Osorio, E. J., Sobral, M., de Almeida, M. V., Henriques, A. T., Bastida, J., Zuanazzi, J. A. S. 2015, *Rev. Bras. Farmacogn.-Braz. J. Pharmacogn.*, 25, 353.
30. Guo, Y., de Andrade, J. P., Pigni, N. B., Torras-Claveria, L., Tallini, L. R., Borges, W. S., Viladomat, F., Nair, J. J., Zuanazzi, J. A. S., Bastida, J. 2016, *Helv. Chim. Acta*, 99, 143.
31. Ortíz, J. E., Pigni, N. B., Andujar, S. A., Roitman, G., Suvire, F. D., Enriz, R. D., Tapia, A., Bastida, J., Ferensin, G. E. 2016, *J. Nat. Prod.*, 79, 1241.
32. Berkov, S., Georgieva, L., Kondakova, V., Viladomat, F., Bastida, J., Atanassov, A., Codina, C. 2013, *Biochem. Syst. Ecol.*, 46, 152.
33. Weniger, B., Italiano, L., Beck, J. P., Bastida, J., Bergoñón, S., Codina, C., Lobstein, A., Anton, R. 1995, *Planta Med.*, 61, 77.
34. Campbell, W. E., Nair, J. J., Gammon, D. W., Bastida, J., Codina, C., Viladomat, F., Smith, P. J., Albrecht, C. F. 1998, *Planta Med.*, 64, 91.
35. Berkov, S., Romani, S., Herrera, M., Viladomat, F., Codina, C., Momekov, G., Ionkova, I., Bastida, J. 2011, *Phytoter. Res.* 25, 1986.
36. Nair, J. J., Rárová, L., Strnad, M., Bastida, J., van Staden, J. 2012, *Bioorg. Med. Chem. Lett.*, 22, 6195.
37. McNulty, J., Nair, J. J., Codina, C., Bastida, J., Pandey, S., Gerasimoff, J., Griffin, C. 2007, *Phytochemistry*, 68, 1068.
38. McNulty, J., Nair, J. J., Bastida, J., Pandey, S., Griffin, C. 2009, *Nat. Prod. Commun.* 4, 483.
39. McNulty, J., Nair, J. J., Bastida, J., Pandey, S., Griffin, C. 2009, *Phytochemistry*, 70, 913.
40. Nair, J. J., Bastida, J., Viladomat, F., van Staden, J. 2012, *Nat. Prod. Commun.* 7, 1677.
41. Osorio, E. J., Robledo, S. M., Bastida, J. 2008, *The Alkaloids, Chemistry and Biology*, Cordell, G. A. (Eds.), Elsevier, San Diego, 66, 113.
42. Kaya, G. I., Sarikaya, B., Onur, M. A., Somer, N. U., Viladomat, F., Codina, C., Bastida, J., Lauinger, I. L., Kaiser, M., Tasdemir, D. 2011, *Phytochem. Lett.*, 4, 301.
43. Maelicke, A., Samochocki, M., Jostock, R., Fehrenbacher, A., Ludwig, J., Albuquerque, E. X., Zerlin, M. 2001, *Biol. Psychiatry*, 49, 2479.
44. López, S., Bastida, J., Viladomat, F., Codina, C. 2002, *Life Sci.*, 71, 2521.
45. Pagliosa, L. B., Monteiro, S. C., Silva, K. B., de Andrade, J. P., Dutilh, J., Bastida, J., Cammarota, M., Zuanazzi, J. A. S. 2010, *Phytomedicine*, 17, 698.
46. de Andrade, J. P., Giordani, R. B., Torras-Claveria, L., Pigni, N. B., Berkov, S., Font-Bardia, M., Calvet, T., Konrath, E., Bueno, K., Sachett, L. G., Dutilh, J. H.,

- Borges, W. S., Viladomat, F., Henriques, A. T., Nair, J. J., Zuanazzi, J. A. S., Bastida, J. 2016, *Phytochem. Rev.*, 15, 147.
47. Bores G.M., Huger, F.P., Petko, W., Mutlib, A.E., Camacho, F., Rush, D.K., Selk, D.E., Wolf, V., Kosley, R.W., Davis, L., Vargas, H.M. 1996, *J. Pharmacol. Exp. Ther.*, 277, 728.
48. Berkov, S., Codina, C., Viladomat, F., Bastida, J. 2008, *Bioorg. Med. Chem. Lett.*, 18, 2263.
49. Meng, X., Zhang, H., Mezei, M., Cui, M. 2011, *Curr. Comput. Aided Drug Des.*, 7, 146.
50. Cortes, N., Alvarez, R., Osorio, E. H., Alzate, F., Berkov, S., Osorio, E. 2015, *J. Pharm. Biomed. Anal.*, 102, 222.
51. García, I., Fall, Y., Gómez, G. 2010, *Curr. Pharm. Design*, 16, 2666.



Research Signpost
Trivandrum
Kerala, India

Recent Advances in Pharmaceutical Sciences VII, 2017: 83-100 ISBN: 978-81-308-0573-3
Editors: Diego Muñoz-Torrero, Montserrat Riu and Carles Felu

6. Deciphering the stack, a novel bacterial structure, by (cryo-) transmission electron microscopy and (cryo-) electron tomography

Lidia Delgado¹, Carmen López-Iglesias² and Elena Mercadé³

¹*Cryo-Electron Microscopy Unit, Scientific and Technological Centers, University of Barcelona, Barcelona, Spain;* ²*The Institute of Nanoscopy, Maastricht University, 6211 LK, Maastricht, The Netherlands* ³*Department of Biology, Health and Environment, Faculty of Pharmacy and Food Sciences, University of Barcelona, Barcelona, Spain*

Abstract. The recent development of cryo-electron microscopy and cryo-electron tomography has allowed prokaryotic cells to be studied in a close-to-native state, refining our knowledge of already known structures and enabling new ones to be discovered. Their application to the Antarctic cold-adapted bacterium *Pseudomonas deceptionensis* M1^T revealed the existence of a novel cytoplasmic structure called a “stack”, which to date has been visualized mainly in slow-growing cultures of *P. deceptionensis* M1^T. The stack appears as a set of stacked oval discs, variable in number, surrounded by a lipid bilayer. Found in the bacterial cytoplasm in varying amounts, stacks are located close to the cell membrane and to DNA fibers. Stacks were also visualized in slow-growing cultures of other bacteria and may play a role in the chromosome dynamics.

Correspondence/Reprint request: Dr. Elena Mercadé, Laboratory of Microbiology, Faculty of Pharmacy and Food Sciences, University of Barcelona, Barcelona, Spain. E-mail: mmercade@ub.edu

Introduction

For many years, the prokaryote cytoplasm was thought to be a homogeneous compartment containing macromolecules and few structures of interest compared to eukaryotic cells. In most prokaryotes, when the cytoplasm was visualized by conventional transmission electron microscopy (TEM), it was only possible to observe irregular areas of fibrous appearance corresponding to the nucleoid, and numerous small granules scattered throughout the rest of the cytoplasm, which are the ribosomes [1]. In some prokaryotes, inclusions and vesicles involved in several physiological processes were also observed [2], [3], [4], [5], [6], [7], [8].

Recent improvements in TEM have enhanced our knowledge of bacterial ultrastructure, and prokaryotes have been reappraised as organized assemblies of macromolecular machines [9] optimized to travel through and interact with complex and dynamic environments [10]. The task of deciphering the structure, function and spatial organization of molecular machines inside the fluid architecture of bacterial cells has emerged as a new challenge [10], [11], [12].

Cryo-electron microscopy (Cryo-EM) combined with electron tomography (ET) provides the highest available resolution for the imaging of biological specimens. These “pure” cryo-techniques have revealed cellular organelles and macromolecular assemblies in frozen-hydrated close-to-native samples. Importantly, they avoid the traditional preparation methods for TEM that involve treating samples with chemical fixatives, organic solvents, contrast-enhancing staining solutions, and resins, which can denature structures and introduce misleading artifacts [13], [14]. This is achieved by very high cooling rates that turn the intrinsic water of cells into vitreous ice, avoiding crystal formation and phase segregation between water and solutes [15]. One way to obtain the cooling rates required for water vitrification is the plunge-freezing method, in which ‘whole-mount’ plunge-frozen specimens are embedded in a thin film of vitreous ice, preserving their native cellular structures. The specimens can be imaged directly when their thickness is below 0.5 μm , a range that includes many bacteria and archaea [16], [17], [18], [19], [20], [21], [22], [23], [24], [25], [26], [27]. However, the Cryo-EM resolution of plunge-frozen whole bacteria is conditioned by the width of the sample, which in the worst of cases can limit the observation of macromolecular details.

Cryo-electron microscopy of vitreous sections (CEMOVIS) is an alternative technique to study frozen-hydrated bacteria and offers better resolution than the observation of whole-mount bacteria by plunge-freezing. It starts with high-pressure freezing (HPF), which can vitrify samples up to 200 μm by increasing the pressure to 2,048 bars during a cooling process of a few milliseconds. These conditions allow the water to become denser than liquid water (vitreous ice), and prevent ice crystal formation [15]. Ultrathin vitreous sections can be obtained directly from high-pressure frozen bacteria and imaged in the microscope, revealing macromolecular details such as the lipid bilayer membrane [28], [29]. However, it is important to bear in mind that the mechanical action of cutting can add conspicuous artifacts to the sample, so a correct interpretation is crucial [30].

Frozen-hydrated specimens can be processed by cryo-electron tomography (CET), which consists in producing a three-dimensional image of a solid object, allowing sectioning of the reconstructed volume and imaging of its internal structures. Tomography is performed by incrementally tilting the sample in the Cryo-EM through a range up to $\pm 70^\circ$ and it is imaged at each step. Afterwards, the tilt series of images is aligned and processed to generate a 3D reconstruction or tomogram of the specimen at a macromolecular resolution (around 4 nm). The limited tilt range in electron tomography results in a region empty of information in the Fourier space of the 3D reconstruction, referred to as the missing wedge. The resulting artifacts include blurring of the spatial features in the beam direction, which can result in 22% loss of information [31].

CET has been applied to previously characterized frozen-hydrated assemblies, providing new information and a greater understanding of the complex ultrastructure of prokaryotic cells in their natural context. This has given new insights into various aspects of prokaryotic physiology, including metabolism, interspecies cooperation and pathogenesis [10]. Furthermore, the use of Cryo-EM and CET has opened up fresh opportunities for discovering novel bacterial features, partly because new bacterial species are being analyzed, but also thanks to the improvements in sample preparation and gains in resolution [32], [33].

1. The stack, a novel bacterial structure

The stack was first visualized in the Antarctic bacterium *Pseudomonas deceptionensis* M1^T. The strain was isolated from marine sediment collected

on Deception Island and was described as rod-shaped (cell length: 1.5-2 μm ; cell diameter: 0.5 μm), catalase- and oxidase-positive, motile by means of a polar flagellum and psychrotolerant (able to grow at temperatures ranging from -4 to 34°C) [34]. With the aim of characterizing its ultrastructure, the strain was grown on different media, varying the time and temperature. Afterwards, cells were cryo-immobilized by HPF and processed by freeze-substitution (FS), Epon embedding and sectioning. The TEM analysis of the 60-nm Epon sections revealed a highly organized stacked structure located in the bacterial cytoplasm, which was unlike any cytoplasmic inclusion or structure reported to date. Interestingly, stacks have only been frequently observed in *P. deceptionensis* M1^T cells grown under specific slow-growth conditions, such as low incubation temperatures: on trypton soy agar (TSA) plates, for 12 days at 0°C. Under these growth conditions, 23.23% of the cells analyzed by TEM showed stacks in their cytoplasm. The frequent observation of stacks at 0°C may be associated with the slow growth of the strain at this temperature, which may prolong dynamic processes and make it easier to capture the temporary structures involved. In that case, stacks might be dynamic cytoplasmic structures required to localize certain molecules or enzymes in a particular place and cellular moment for a particular cellular function. Consequently, stacks may be quickly assembled where their function is required, to be then dismantled once their function is fulfilled [35], [1].

Semithin Epon sections of 250 nm of *P. deceptionensis* M1^T cells grown on TSA at 0°C for 12 days and processed by HPF-FS and Epon embedding were further explored three-dimensionally by ET. Dual-axis tilt series from the 250 nm Epon sections were acquired in the TEM at 200 kV, each tilt series being reconstructed using Tomo3D software. Tomograms corresponding to each series were combined with the IMOD software and the final dual-axis tomogram was obtained. Figure 1 shows the XY, ZY and XZ tomogram slices from the same point (marked by an asterisk in the different views) of the double-axis tomogram, and two views of its segmentation (B and C). The XY view in Figure 1A (top left image) clearly shows two contiguous stacks at an angle of 130° to each other. Both are located near the boundaries of the cell plasma membrane (PM) and the one on the left is perpendicular to the PM. In the YZ view, the stack appears as a pile of flat structures oriented perpendicularly to the surface (top right image). The XZ view (bottom left image) shows two oval structures, which correspond to the frontal views of two flat discs. The tomogram segmentation from the dual-axis tomogram observed in Figures 1B and 1C confirm the presence of two contiguous stacks, one on the right and the other on the left, formed by parallel oval discs [1].

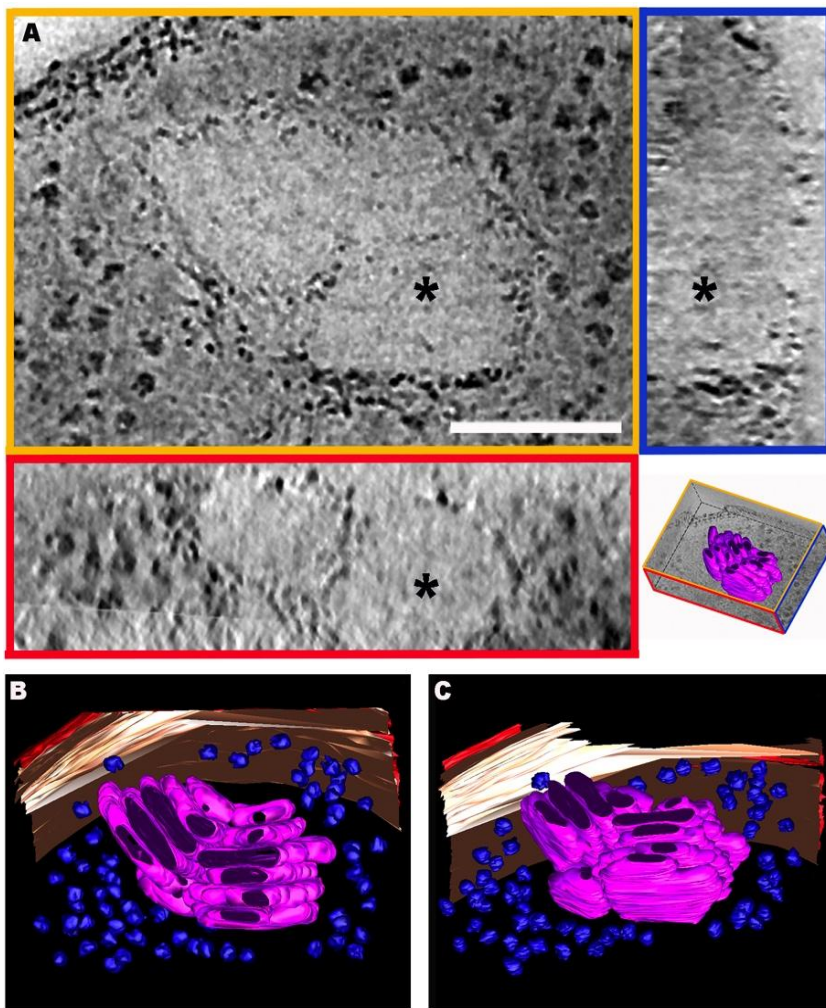


Figure 1. 3D visualization of stacks observed in *P. deceptionensis* M1^T cells after HPF-FS [1]. (A) 2 nm tomogram slices from the XYZ views of a tomogram reconstructed from a 250 nm Epon section. The asterisks correspond to the same point through the different views. Scale bar = 100 nm. The bottom right picture depicts the view distribution in the tomogram. (B-C) Two different views from the segmentation of the tomogram observed in (A). In red, the outer membrane; in cream-color, the PM; in blue, the ribosomes; and in pink, the discs.

Based on the data obtained, the stack was defined as a pile of oval-disc-shaped subunits surrounded by a membrane structure (from 1 to 14 discs per stack) localized in the bacterial cytoplasm. They were frequently found very near the PM, mostly very close to DNA fibers, and in variable number within each cell (1 to 4 stacks per cell, simultaneously). When more than one stack was observed simultaneously in the cytoplasm, they appeared isolated or grouped/contiguous [1]. Three-dimensionally, each subunit appeared as a flat oval disc, while in 2D views, the stack had either an oval structure or appeared as a pile of sticks (Fig. 2).

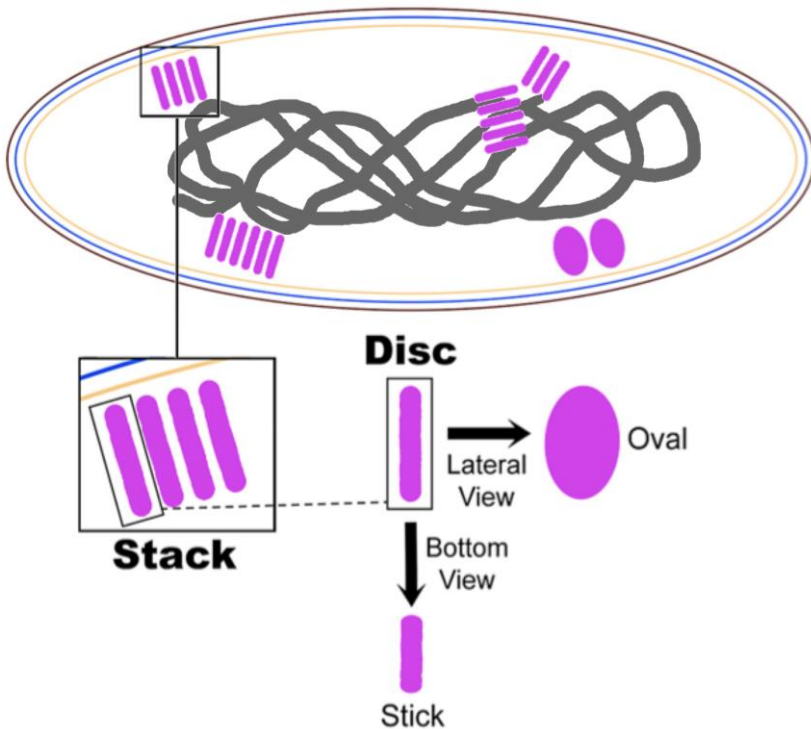


Figure 2. Model of a *Pseudomonas deceptionensis* M1^T cell showing stacks in the cytoplasm (adapted from [36]). Lateral and front views of the squared subunit are shown. In 2D views, the disc-shaped subunit of the stack can be observed as an oval structure or as a stick. Pink: stacks; grey: nucleoid; red: outer membrane; blue: peptidoglycan layer; cream-color: plasma membrane.

2. Stacks in the whole-cell context

With the aim of increasing knowledge of the architecture and spatial organization of stacks inside the cytoplasm, plunge-frozen whole

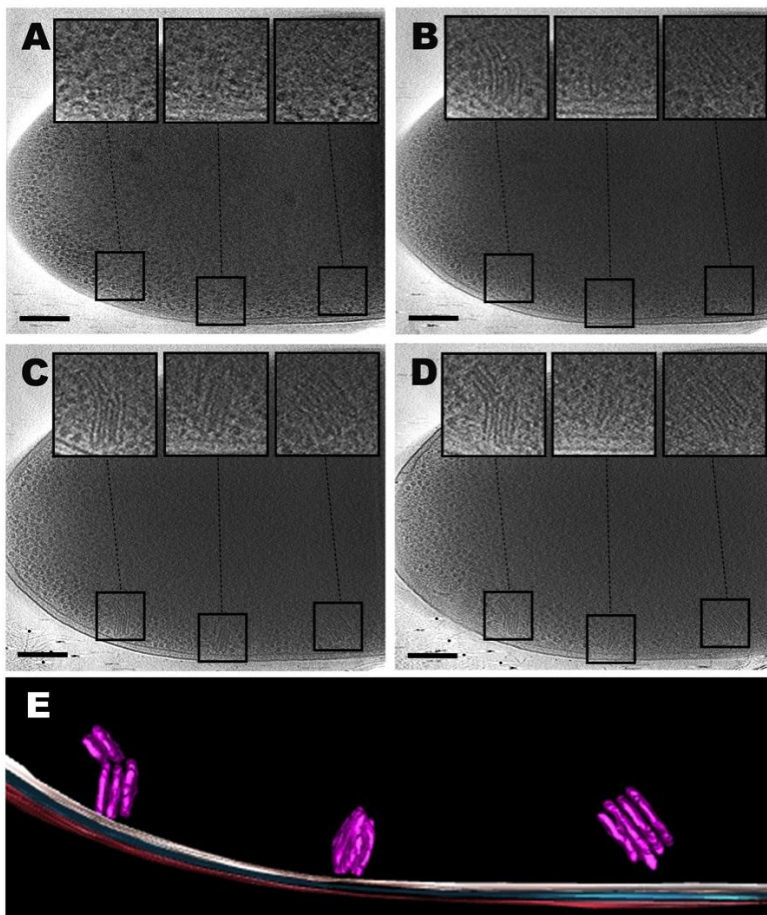


Figure 3. Stacks analyzed by CET of plunge-frozen whole bacteria. (A-D) 2-nm slices of a tomogram reconstructed from a plunge-frozen *P. deceptionensis* M1^T cell. Objective lens defocus: -6 μm . Pixel size: 0.85 nm. (E) Partial segmentation of the tomogram observed in (A-D). Pink: stacks; Red: outer membrane; Blue: peptidoglycan layer; Cream-color: PM. Scale bars = 200 nm.

P. deceptionensis M1^T cells were imaged by Cryo-TEM. Stacks were revealed in the peripheral regions of the bacteria, verifying that they were not artifacts derived from the previous preparation methods (Fig. 3A-D). They were only visible in areas thin enough to allow an electron beam to pass through, namely the peripheral areas of the cell. Measurements of the length and width of stack subunits in images with a pixel size of 0.81 nm provided the mean values of 90.7 ± 25 nm and 13.3 ± 1.7 nm, respectively. While the length of the discs was distinctly variable, the width was practically constant. It should be noted that the discs were separated by an apparently constant distance (5.2 ± 1.3 nm), although no spacing features were observed between them. Cryo-tomograms showed the stacks located at the inner perimeter of the *P. deceptionensis* M1^T cells and angled at 35 to 90° with respect to the PM. Figure 3E depicts the stack segmentation observed in the tomogram slices in Figures 3A-D [36].

Analysis of plunge-frozen bacteria also showed that each stack subunit was clearly delimited by an electron-dense layer resembling a lipid membrane, but no continuity between this layer and the PM was observed in the whole tomograms. Measurements of the width of the membrane-like layers surrounding these subunits and the width of the PM provided the mean values 4.2 ± 0.8 nm and 6 ± 1.1 nm, respectively. Analysis of the measurements by the one-factor ANOVA test gave a p-value < 0.0001 , and revealed significant differences between the widths of the two membrane types, suggesting differing composition or structure. Taken as a whole, these data indicate that stacks are not invaginations of the PM [36].

3. Nature of the membrane surrounding the stack subunits

To shed more light on the composition of the membrane surrounding the stack discs, 50-nm vitreous sections (VIS) of high-pressure frozen *P. deceptionensis* M1^T cells were analyzed by cryo-TEM, a technique that provides a better resolution than the study of plunge-frozen whole specimens (Fig. 4A and 4B). Depending on the orientation of the VIS with respect to the cells, the lipid bilayer pattern of the PM was observed, as well as a typical two-peak density profile (Fig. 4B, see squared area). The layer delimiting each stack subunit presented a similar electron density to the PM, although no bilayer pattern was discernible (Fig. 4A and 4B) [36].

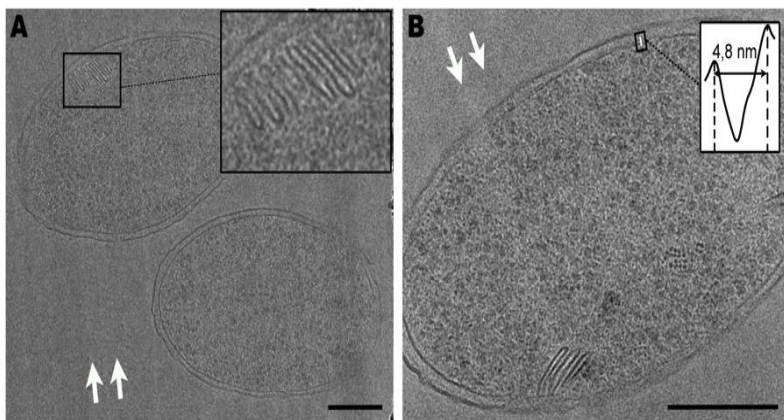


Figure 4. Cryo-TEM visualization of stacks in *P. deceptionensis* M1^T [36]. (A-B) 50-nm VIS. (B) The density profile of a section of the PM is observed in the squared area confirming the lipid bilayer pattern. White arrows indicate the cutting directions. Scale bars = 200 nm.

Cryo-electron tomography of vitreous sections (CETOVIS) was then carried out, recording tilt series of images from -60° to $+60^\circ$. The subsequent 4-nm resolution tomograms revealed that through the z-axis the stacks were composed of discs clearly delimited by membrane-like structures (Fig. 5A and 5C). Additionally, analysis of tomograms obtained from VIS revealed a lipid bilayer membrane pattern in the layer surrounding each disc (Fig. 5A see magnified area), which was confirmed by the density profile (Fig. 5A). It was notable that when stacks were observed in VIS tomograms, the PM lipid bilayer was frequently not resolved. As stacks are localized in the peripheral regions of the bacterial cytoplasm, the section cutting may occur away from the central plane. Consequently, the membrane is not cut perpendicularly and the overlapping head group regions obliterate the gap of the bilayer structure, thus obscuring visualization of the membrane bilayer pattern. Since the stacks appeared clearly delimited throughout the z-axis, more reliable segmentations of the structures were obtained (Fig. 5B and 5D) [36].

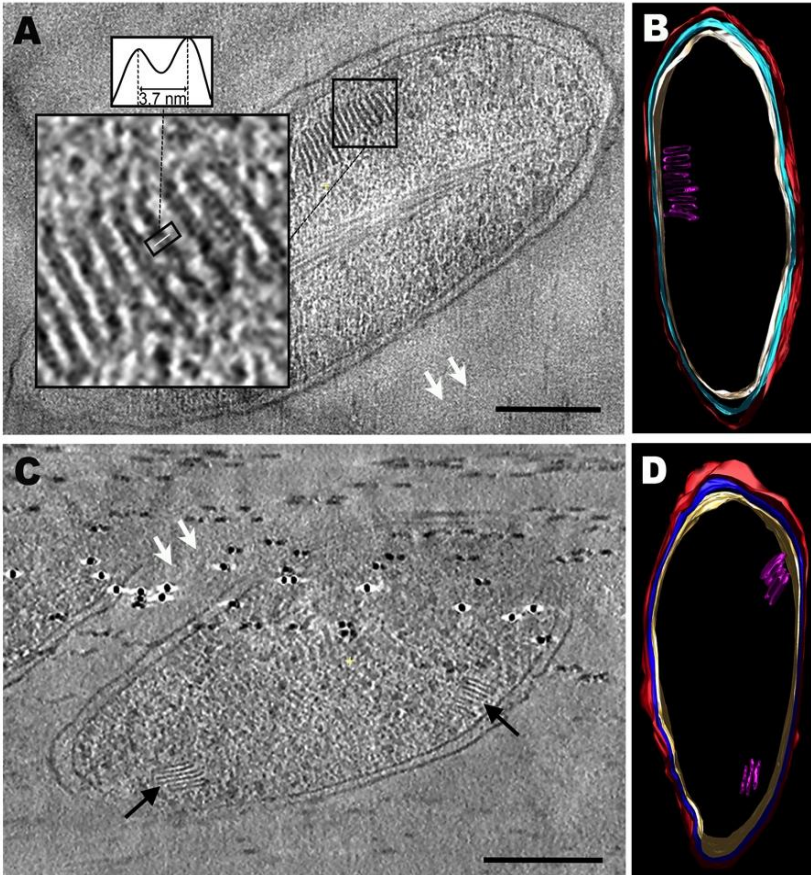


Figure 5. Stacks analyzed by CETOVIS [36]. (A and C) 1-nm slices of tomograms reconstructed from 50 nm vitreous sections of *P. deceptionensis* M1^T. Objective lens defocus: -6 μm . Pixel size: 0.71 nm. (A) The magnified square shows a fragment of one stack with subunits surrounded by a membrane-like structure exhibiting the typical pattern of a lipid bilayer membrane. The density profile of a section of the membrane-like structure surrounding the discs is observed in the upper squared area, revealing the typical two peaks of a lipid bilayer membrane. (C) Two stacks are observed isolated in different positions within the cytoplasm of the bacterial cell. (B and D) Segmentations of the tomograms observed in (A) and (C), respectively. Pink: stacks; red: outer membrane; Blue: peptidoglycan layer; Cream-color: PM. White arrows indicate the cutting direction. Scale bars = 200 nm.

4. Stack localization and the bacterial nucleoid

Interestingly, stacks observed near the periphery of HPF-FS Epon-embedded cells grown at 0°C for 12 days frequently appeared very close to DNA microfibrils from the nucleoid (Fig. 6A), in some cases

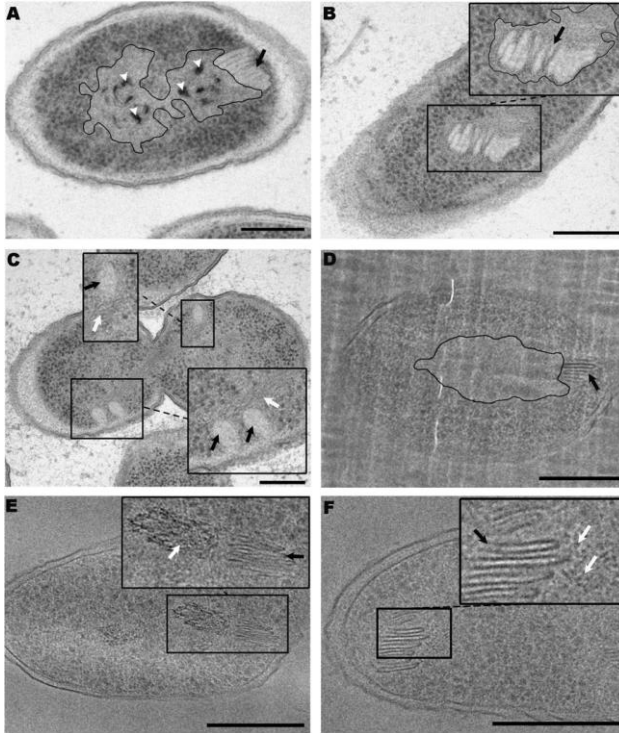


Figure 6. Stacks and DNA location in *P. deceptionensis* M1^T cells [1]. (A-C) TEM micrographs of 60 nm Epon sections of samples processed by HPF-FS. (A) Stack (black arrow) perpendicular to the plasma membrane and very close to the bacterial nucleoid (outlined area). The bacterial nucleoid shows poly P granules (white arrow heads). (B) Stack (black arrow) embedded in the nucleoid area (outlined area). (C) Dividing cell distributing its DNA among its daughter cells; stacks very close to the DNA microfibrils (white arrows). (D-F) CEMOVIS micrographs. (D) Stack (black arrow) very close to a RFA or nucleoid area (outlined area). (E) Stack (black arrow) in the vicinities of a locally ordered arrangement of DNA microfibrils (white arrow). (F) Stack (black arrow) very close to DNA microfibrils (white arrows). Scale bars = 250 nm.

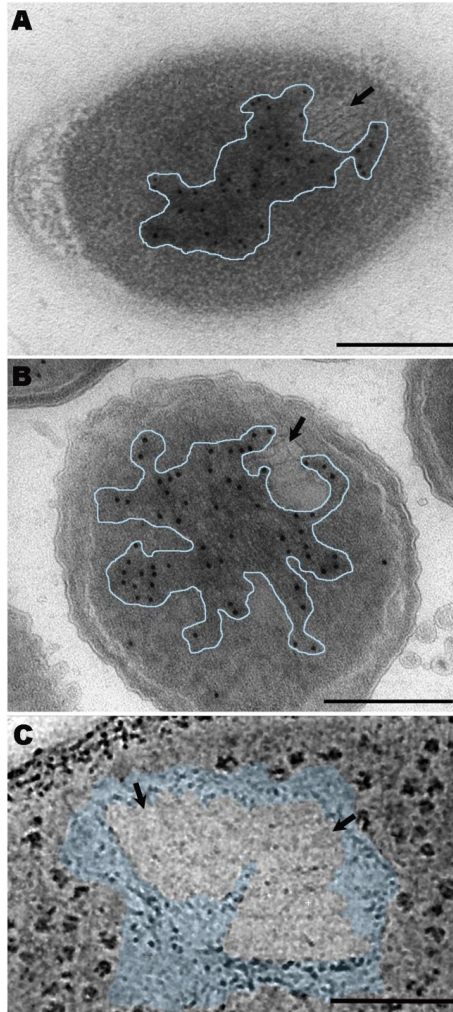


Figure 7. TEM studies analyzing the proximity between stacks and DNA *P. deceptionensis* M1^T [1]. (A) DNA immunolabeling on 60-nm HM23 Lowicryl sections from HPF-FS-processed samples. (B) DNA immunolabeling on a 60 nm section obtained by Tokuyasu's method. (A-B) Black arrows indicate stacks and outlined areas correspond to the nucleoid. (C) 2-nm tomogram slice of a tomogram reconstructed from a 250 nm Epon section of a HPF-FS-processed sample. Black arrows indicate stacks and the colored area corresponds to the nucleoid. Scale bars = 250 nm.

being completely embedded (Fig. 6B). Cells dividing and distributing their DNA among daughter cells also showed stacks very close to the DNA fibers (Fig. 6C). Additionally, inorganic polyphosphate (Poly P) granules, commonly observed in nucleoid areas, were frequently located very near to stacks (Fig. 6A, white arrow heads) [1].

The same proximity between DNA and stacks described in Epon sections was also observed in VIS. Stacks were localized next to ribosome-free areas (RFA) corresponding to the bacterial nucleoid (Fig. 6D). Locally ordered arrangements of DNA and DNA microfibers were also visualized very close to stacks (Fig. 6E and Fig. 6F) [1].

DNA immunolabeling and tomographic studies performed on samples of *P. deceptionensis* M1^T TSA-grown at 0°C for 12 days confirmed the co-localization of stacks and DNA. Immunolabeling experiments were performed in HM23 and Tokuyasu sections using a specific antibody for labeling double-stranded DNA. In the HM23 sections, we also amplified the signal obtained with a DNA staining method using potassium permanganate, which allows the chromatin distribution within the bacterial cytoplasm to be visualized. The micrographs again revealed stacks at the periphery of the bacterial cytoplasm, contiguous with or partially embedded in DNA microfibers (Fig. 7A and Fig. 7B). ET of Epon sections of *P. deceptionensis* M1^T cells showed stacks completely embedded in the bacterial nucleoid along the whole Z-axis (Fig. 7C) [1].

The frequent co-localization of the stacks and the bacterial nucleoid suggest a possible relationship between these new structures and certain processes involved in the bacterial chromosome dynamics. Further experiments are needed to explore this hypothesis [1].

5. Stacks in other bacterial species

The frequent presence of stacks very close to DNA microfibers suggests they could play a role in the bacterial chromosome dynamics, in which case their presence would not be limited to the *P. deceptionensis* M1^T strain. We therefore chose three bacterial species within the *Pseudomonas* genus, two of which, *P. psychrophila* DSM 17535^T and *P. fragi* DSM 3456^T, are closely related to *P. deceptionensis* M1^T, while the third, *P. fluorescens* ATCC 13430^T, is phylogenetically more distant. All the strains were grown on TSA plates for 12 days and the range of growth temperatures was determined for each species in order to reproduce slow-growing conditions. The samples

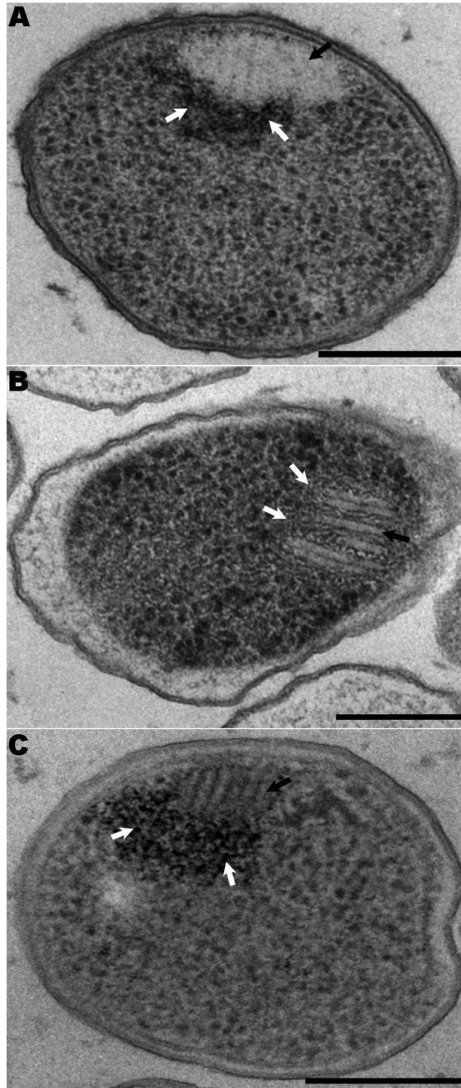


Figure 8. Stacks visualized in different *Pseudomonas* species from samples processed by HPF-FS [1]. (A-C) 60 nm Epon sections. (A) *P. psychrophila* DSM 17535^T TSA-grown culture. (B) *P. fragi* DSM 3456^T TSA-grown culture. (C) *P. fluorescens* ATCC 13430^T TSA-grown culture. (A-C) Black arrows indicate stacks and white arrows DNA microfibers. Scale bars = 250 nm.

were then processed by HPF-FS and Epon-embedding and imaged by TEM. Micrographs revealed that *P. psychrophila* DSM 17535^T and *P. fragi* DSM 3456^T incubated at 0°C, and *P. fluorescens* ATCC 13430^T incubated at 4°C all presented stacks in their cytoplasm. In these three strains, stacks were also found perpendicular to the PM, and close to DNA microfibers presenting inorganic polyphosphate, as described for *P. deceptionensis* M1^T (Fig. 8A, 8B and 8C) [1].

These results confirmed that stacks are not exclusive to the Antarctic bacterium *P. deceptionensis* M1^T, having been visualized in other species of the *Pseudomonas* genus, where they were structurally very similar and observed only in slow-growing cells, and close to DNA microfibers [1].

Other bacteria genera were studied to determine if the presence of this new bacterial feature was limited to species within the *Pseudomonas* genus. Two bacterial model species were selected: *Escherichia coli* W3310 and *Bacillus subtilis* ATCC6633. The presence of stacks in these species would help to determine their possible implication in the chromosome dynamics, thanks to the availability of molecular tools to study this process in these model species. Both strains were grown on TSA plates for 12 days and the range of growth temperatures was determined in order to reproduce slow-growing conditions (12°C). The samples were then processed by HPF-FS and Epon-embedding and imaged by TEM. Both strains revealed structures with a morphology, size and location indicative of stacks, but the subunits were not as clearly defined (Fig. 9). Although the data suggested that stacks might be present in other bacterial genera, further experiments are needed to determine the optimum growing conditions in the studied strains for an improved visualization before the hypothesis can be confirmed [35].

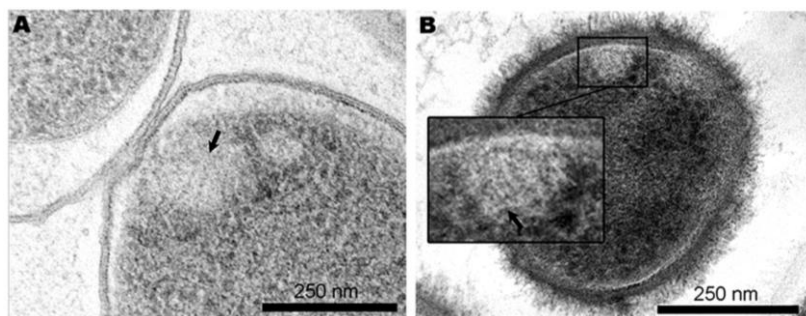


Figure 9. Stack-like structures visualized in *E. coli* W3310 (A) and *B. subtilis* ATCC6633 (B) processed by HPF-FS [35]. (A-B) 60 nm Epon sections. Black arrow and black squares highlight the stack-like structures.

6. Conclusion

Applying cryo-TEM techniques to study the Antarctic bacterium *P. deceptionensis* M1^T and other bacteria in slow-growing conditions has led to the discovery of a new cytoplasmic structure, termed a stack. This new bacterial feature can be described as a set of stacked discs surrounded by a lipid bilayer with a different composition from that of the PM. It is usually located at the boundaries of the cell cytoplasm, close to the PM and possibly not continuous with it, and frequently near the bacterial DNA microfibers, suggesting a possible role in the chromosome dynamics.

The combination of CET of plunge-frozen whole bacteria and CETOVIS has proved useful in providing reliable structural information about these new bacterial cytoplasmic structures at different resolutions and in a general cellular context.

Acknowledgements

The authors are grateful to Dr. Peter Peters and Dr. Jason Pierson (NKI-AVL) for their help to develop vitreous cryo-sectioning in our lab, to Dr. José Jesús Fernández (CNB) and to Dr. José María Seguí (COMAV) for their help to develop in tomography and 3D reconstructions in our lab, and Dr. Martin Rios (UB) for his statistical support. This work received funding from the following sources: grant CTQ2014-59632-R from the Ministerio de Economía y Competitividad, Spain; and grant 2014SGR1325 from the Departament d'Innovació, Universitats i Empresa from the Autonomous Government of Catalonia.

References

1. Delgado, L., Carrión, O., Martínez, G., López-Iglesias, C., Mercadé, E. 2013, *PLoS One*, Sep 9;8(9):e73297. doi:10.1371/journal.pone.0073297.
2. Walsby, A.E. 1994, *Microbiol. Rev.*, 58, 94.
3. Shively, J.M., Ball, F., Brown, D.H., Saunders, R.E. 1973, *Science*, 584.
4. Parsons, J.B., Dinesh, S.D., Deery, E., Leech, H.K., Brindley, A.A., Heldt, D., et al. 2008, *J. Biol. Chem.*, 283, 14366. doi:10.1074/jbc.M709214200.
5. O'Connell, J.D., Zhao, A., Ellington, A.D., Marcotte, E.M. 2012, *Annu. Rev. Cell Dev. Biol.* 28: 89. doi:10.1146/annurev-cellbio-101011-155841.
6. Shively, J.M. 1974, *Annu. Rev. Microbiol.*, 28, 167. doi:10.1146/annurev.mi.28.100174.001123.
7. Bazyliński, D.A., Frankel, R.B. 2004, *Nat. Rev. Microbiol.*, 2, 217. doi:10.1038/nrmicro842.

8. Niederman, R.A. in: Shively, J.M., editor 2006, *Springer Berlin Heidelberg*, 193–227. http://link.springer.com/chapter/10.1007/7171_025.
9. Alberts, B. 1998, *Cell*, 92, 291. doi:10.1016/S0092-8674(00)80922-8.
10. Oikonomou, C.M., Jensen, G.J. 2016, *Nat. Rev. Microbiol.*, 14, 205. doi:10.1038/nrmicro.2016.7.
11. Gitai, Z. 2005, *Cell*, 120, 577. doi:10.1016/j.cell.2005.02.026.
12. Milne, J.L.S., Subramaniam, S. 2009, *Nat. Rev. Microbiol.*, 7, 666. doi:10.1038/nrmicro2183.
13. Pilhofer, M., Ladinsky, M.S., McDowall, A.W., Jensen, G.J. 2010, *Methods Cell Biol.*, 96, 21. doi:10.1016/S0091-679X(10)96002-0.
14. Pilhofer, M., Aistleitner, K., Ladinsky, M.S., König, L., Horn, M., Jensen, G.J. 2014, *Environ. Microbiol.*, 16: 417–429. doi:10.1111/1462-2920.12299.
15. Studer, D., Humbel, B.M., Chiquet, M. 2008, *Histochem. Cell Biol.*, 130: 877. doi:10.1007/s00418-008-0500-1.
16. Beeby, M., Cho, M., Stubbe, J., Jensen, G.J. 2012, *J. Bacteriol.*, 194, 1092. doi:10.1128/JB.06125-11.
17. Toso, D.B., Henstra, A.M., Gunsalus, R.P., Zhou, Z.H. 2011, *Environ. Microbiol.*, 13, 2587. doi:10.1111/j.1462-2920.2011.02531.x.
18. Kudryashev, M., Cyrklaff, M., Wallich, R., Baumeister, W., Frischknecht, F. 2010, *J. Struct. Biol.*, 169, 54. doi:10.1016/j.jsb.2009.08.008.
19. Comolli, L.R., Baker, B.J., Downing, K.H., Siegerist, C.E., Banfield, J.F. 2008, *ISME J.*, 3, 159. doi:10.1038/ismej.2008.99.
20. Khursigara, C.M., Wu, X., Subramaniam, S. 2008, *J. Bacteriol.* 190, 6805. doi:10.1128/JB.00640-08.
21. Murphy, G.E., Matson, E.G., Leadbetter, J.R., Berg, H.C., Jensen, G.J. 2008, *Mol. Microbiol.*, 67, 1184. doi:10.1111/j.1365-2958.2008.06120.x.
22. Li, Z., Trimble, M.J., Brun, Y.V., Jensen, G.J. 2007, *EMBO J.*, 26, 4694. doi:10.1038/sj.emboj.7601895.
23. Zhang, P., Khursigara, C.M., Hartnell, L.M. 2007, *Proc. Natl. Acad. Sci. U.S.A.*, 104, 3777. doi:10.1073/pnas.0610106104.
24. Briegel, A., Dias, D.P., Li, Z., Jensen, R.B., Frangakis, A.S., Jensen, G.J. 2006, *Mol. Microbiol.*, 62, 5. doi:10.1111/j.1365-2958.2006.05355.x.
25. Comolli, L.R., Kundmann, M., Downing, K.H. 2006, *J. Microsc.*, 223, 40. doi:10.1111/j.1365-2818.2006.01597.x.
26. Komeili, A., Li, Z., Newman, D.K., Jensen, G.J. 2006, *Science*, 311, 242. doi:10.1126/science.1123231.
27. Scheffel, A., Gruska, M., Faivre, D., Linaroudis, A., Plitzko, J.M., Schüler, D. 2006, *Nature*, 44,; 110. doi:10.1038/nature04382.
28. Hoffmann, C., Leis, A., Niederweis, M., Plitzko, J.M., Engelhardt, H. 2008, *Proc. Natl. Acad. Sci.* 105, 3963. doi:10.1073/pnas.0709530105.
29. Zuber, B., Chami, M., Houssin, C., Dubochet, J., Griffiths, G., Daffé, M. 2008, *J. Bacteriol.*, 190, 5672. doi:10.1128/JB.01919-07.
30. Al-Amoudi, A., Studer, D., Dubochet, J. 2005, *J. Struct. Biol.*, 150, 109. doi:10.1016/j.jsb.2005.01.003.
31. Fernández, J.J. 2012, *Micron*, 43, 1010. doi:10.1016/j.micron.2012.05.003.

32. Moissl, C., Rachel, R., Briegel, A., Engelhardt, H., Huber, R. 2005, *Mol. Microbiol.*, 56, 361. doi:10.1111/j.1365-2958.2005.04294.x.
33. Shetty, A., Chen, S., Tocheva, E.I., Jensen, G.J., Hickey, W.J. 2011, *PLoS ONE*, 6: e20725. doi:10.1371/journal.pone.0020725.
34. Carrión, O., Miñana-Galbis, D., Montes, M.J., Mercadé, E. 2011, *Int. J. Syst. Evol. Microbiol.*, 61, 2401. doi:10.1099/ijs.0.024919-0.
35. Delgado, L. 2015, <http://diposit.ub.edu/dspace/handle/2445/63070>.
36. Delgado, L., Martínez, G., López-Iglesias, C., Mercadé, E. 2015, *J. Struct. Biol.* 189,220. doi:10.1016/j.jsb.2015.01.008.



Research Signpost
Trivandrum
Kerala, India

Recent Advances in Pharmaceutical Sciences VII, 2017: 101-114 ISBN: 978-81-308-0573-3

Editors: Diego Muñoz-Torrero, Montserrat Riu and Carles Feliu

7. Development of a strategy for the administration of praziquantel to the terrestrial edible snail *Cornu aspersum* parasitized by *Brachylaima* sp. metacercariae

Laia Gállego and Mercedes Gracenea

Laboratory of Parasitology, Department of Biology, Healthcare and the Environment, Faculty of Pharmacy and Food Sciences, University of Barcelona, Av. Joan XXIII s/n, 08028 Barcelona, Spain

Abstract. *Cornu aspersum* is a terrestrial edible snail, often parasitized by *Brachylaima* (Trematoda) metacercariae. Ingestion of undercooked snails by humans allows metacercariae to develop to adult in the intestine causing brachylaimiasis (expected mortality rate 5-10%). The treatment of these snails with praziquantel in the farms where they are reared would be a tool to control this food-borne disease. In the present work, a strategy has been proposed to administer the drug to the snails including quality control of the manufacturing of the feeding stuff supplemented with praziquantel and its acceptance by the snails.

Introduction

Cornu aspersum (= syn. *Helix aspersa*) (Müller, 1774) (Gastropoda: Helicidae) is a terrestrial edible snail of commercial interest. *Brachylaima*

Correspondence/Reprint request: Dra. Mercedes Gracenea, Department of Biology, Healthcare and the Environment, University of Barcelona, Av. Joan XXIII s/n, 08028 Barcelona, Spain. E-mail: gracenea@ub.edu

(Trematoda: Brachylaimidae) metacercariae often parasitize the kidney of the gastropod in nature and marketplaces [1, 2], where the prevalence of parasitization can reach 85.4%. Ingestion of undercooked snails by humans allows metacercariae to develop to adult in the intestine causing brachylaimiasis [3, 4]. The main presenting symptoms are diarrhoea (100%), abdominal pain (58%), anorexia (58%), and weight loss or poor weight gain (58%) due to the hematophagous nature of *Brachylaima* sp. intestinal adults [5, 6]. In Australia up to 13 human cases have been recorded [3, 4, 5]. Additionally, brachylaimiasis could reach a medical concern considering that in some trematode infection, eggs can enter the systemic circulation and reach other tissues, as cardiac one, and other organs producing pathological lesions [7, 8, 9]. In this sense, two of the human brachylaimid cases in Australia had cardiac conditions in which systemic trematode infection could not be entirely discarded [3]. Meerburg et al. [10] classified brachylaimiasis as pathology with an expected mortality rate in humans (without treatment) between 5 and 10% and claimed livestock and food products as one of the most important via to spreading this snail-borne disease to human. In Australia all recorded cases were produced due to accidental ingestion of snails. However, in countries such as China, France, Spain, Italy, Romania, etc., the consumption of snails is not accidental but usual, because snails are commonly consumed being part of the human diet [11, 12]. The Iberian Peninsula is the geographic area where the consumption of *C. aspersum* is of the most importance [13]. The countries which imported the greatest amount of snails in 2015 according to data retrieved from COMTRADE from United Nations [14] are: Spain (11,636,006 kg), France (2,793,846 kg), Portugal (1,896,886 kg), Greece (1,435,169 kg), Bosnia Herzegovina (1,067,479 kg), Romania (956,272 kg), Czech Republic (839,391 kg), Italy (807,872 kg), Turkey (674,197 kg), Hungary (387,782 kg), Malaysia (338,737 kg), Lithuania (278,841 kg), Hong Kong (276,153 kg), China (258,269 kg), and Serbia (241,844 kg).

This scenario implies a higher risk of human parasitization, and its consequent acquisition of brachylaimiasis, a disease which is actually underdiagnosed for several reasons. Firstly, the observation of eggs in human feces is difficult due to the small size of the eggs (25-30 μm length), secondly, the diagnosis is not under of the regular clinical practices in areas where the snail consumption is usual, and thirdly, the clinical signs are largely unspecific. Up to the date, snails are not subject to any parasitological control prior its distribution in public marketplaces. In this context, the development of a pharmacological treatment of farmed snails would be a potential tool to control brachylaimiasis.

1. *Cornu aspersum* and heliciculture farms facilities

C. aspersum presents a big cone-globulus shell with a high spiral, hard and opaque, being its height between 18-40mm and its maximum diameter 20-45 mm. Its color varies from brown to grey, including five darkened lines. Its shell aperture is wide, obliquus and rounded. The peristome is thick, reflected and whitish [15, 16].

Heliciculture farms (Fig. 1) are focused on the rearing of snails, the most under semi-intensive conditions (temperature is not controlled and humidity is managed through sprinklers). These farms are delimited by fences and covered by a net to protect snail from invaders such as small mammals or birds. The emplacement is divided through rails containing herbage, where snails are located. The snail food is placed on a plastic feeding located over a metallic frame supporting mesh pieces vertically disposed. (Fig. 2) [15].

A 100 m² snail farm could allow about 17,000 adults. According to Chevallier [15] the maximum density of *C. aspersum* adults (9g) would be 170 snails/m², and for young specimens the maximum density are 300 snails/m² (5g) and 750 snails/m² (2g).



Figure 1. Heliciculture farm in Spain. Detail of rails containing herbage where the snails are reared.



Figure 2. Heliculture farm in Spain. Detail of mesh pieces vertically disposed supported by a metallic frame where snails rest.

2. Strategies of the administration of Praziquantel in the veterinary field

Praziquantel (PZQ) is an anthelmintic drug extensively used in the laboratory, as well as in the field, mainly against nematodes and trematodes. In the laboratory, PZQ has been administrated as subcutaneous injection single dose in hamsters parasitized by *Schistosoma magrebowiei* [17], or by oral administration single dose through gastric tube or syringe in mice parasitized by *Schistosoma japonicum*, in hamsters parasitized by *Echinostoma paraensei*, and in albin rats parasitized by *Fibricola seoulensis* [18, 19, 20]. In farms or natural reserves, oral administration is the widest used, rarely as single dose through syringe assistance, for instance the case of goats parasitized by *Schistosoma bovis* [21], and mostly as medicated feeding stuff. This last way is the most common strategy not only intended for PZQ [22, 23], but as well for other drugs [24, 25, 26, 27, 28]. Notwithstanding, heliculture farms are distinguished from common farms or natural reserves, because of the extremely high number of specimens reared in (See section 1) [15]. Hereby, the only economically viable strategy to treat snails would be to administer it

through medicated feeding stuff in the usual feeding system of the heliculture farm.

The most recent works on gastropods treated with PZQ, involve species such as the aquatic snail *Lymnaea stagnalis* (Gastropoda: Lymnaeidae) parasitized by *Echinoparyphium aconatium*, treated with a bath of PZQ (10 mg/L) [29], and *Biomphalaria glabrata* infected with *Schistosoma mansoni* treated with PZQ over a 72 h period, in this case in the food (20-30 micrograms/g body weight including shell weight) [30].

3. Chemistry of Praziquantel

PZQ is a lipophilic compound with a molecular weight of 312.40, slightly soluble in water, and easily soluble in alcohols and chloroform. It is a white crystalline powder, not odorous, with a bitter taste (Fig. 3).

Nowadays, the mechanism of action of PZQ remains unknown. PZQ produces a disruption of Ca²⁺ homeostasis, initiating a cascade of events, such as a sustained contraction of the worm musculature, and vacuolization and disruption of the parasite tegument, which leads to the elimination of parasites from the host [31].

Despite of the unknown mechanism of action, PZQ remains being the drug of choice for the treatment of trematodosis. Its effectiveness has been

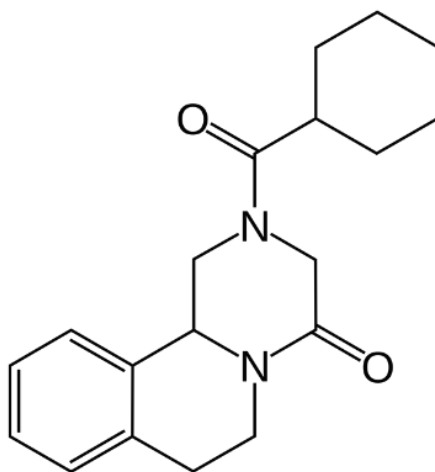


Figure 3. Chemical structure of praziquantel.

demonstrated in fish, goat and ovine species intended for human consumption [21, 22, 32]. In regards of trematodes, PZQ has been used against *Clonorchis sinensis* [33], *Echinostoma paraensei* [19] and *Schistosoma mansoni* [30, 34], *Schistosoma japonicum*, *Dicrocoelium dendriticum*, *Metagonimus yokogawai*, *Opisthorchis viverrini*, *Paragonimus westermani*, and *Neodiplostomum seoulense* [35].

4. Dosage design and snail food consumption by *C. aspersum*

Data on snail food consumption by *C. aspersum* were provided by heliculture professionals in farms: 150 g of snail food per 4.14 kg snails without shell each day.

It was decided to prepare an initial dosage form considering 400 PZQmg/snail kg, with the purpose of developing an optimal dosage form mixing PZQ with snail food. Being calculations as follow:

$$\frac{400 \text{ PZQmg}}{1 \text{ kg snails}} \times \frac{4.14 \text{ kg snails}}{150 \text{ g snail food}} = \frac{1656 \text{ PZQmg}}{150 \text{ g snail food}} = \frac{1.656 \text{ PZQg}}{0.150 \text{ kg snail food}} = \frac{11.04 \text{ PZQg}}{1 \text{ kg snail food}}$$

Taking into account that ulterior experiments could involve a design with boxes of 10 specimens each, it must be calculated as well the adequate amount of snail food to place in each box to cover the nutritional needs of the snails. An adult specimen in markets without shell is about 4-5 g. Thus, a 10 adult specimen group would have a total weight of 50 g without shell. Considering what stated in the previous paragraph it is possible to calculate the group consumption as follows:

$$0.050 \text{ kg snails} \times \frac{150 \text{ g snail food}}{4.14 \text{ kg snails}} = 1.81 \text{ g snail food}$$

5. Manufacturing the snail food supplemented with Praziquantel

According to the European Pharmacopoeia 9.2 [36] veterinary oral powders are preparations consisting of solid, loose, dry particles of varying degrees of fineness. They contain one or more active substances, with or without excipients. They are generally administered in or with water or another suitable liquid, as well as they may be swallowed directly. And premixes for medicated feeding stuffs for veterinary use are mixtures of one or more active substances, usually in suitable bases, that are prepared to facilitate feeding the active substances to animals. Premixes occur in granulated, powdered, semi-solid or liquid form. When used as powders or

granules, they are free-flowing and homogeneous; any aggregates break apart during normal handling. The particle size and other properties are such as to ensure uniform distribution of the active substance in the final feed. Unless otherwise justified and authorized, the instructions for use state that the concentration of a premix in granulated or powdered form is at least 0.5% in the medicated feeding stuff [36].

Taking into account the statements from the Pharmacopoeia 9.2, a first lot of 0.150 kg of snail food supplemented with PZQ was manufactured containing 11.04 PZQg/kg snail food. The amount of PZQ to be incorporated was calculated as follows:

$$\frac{11.04 \text{ PZQg}}{1 \text{ kg snail food}} \times 0.150 \text{ kg} = 1.656 \text{ g PZQ}$$

PZQ (Lot L11060258, 99.52% pure) amount was weighted (1.656 g) as well as the snail food (148.34 g) and manually mixed through mortar, firstly incorporating the total amount of PZQ and, adding small amounts of snail food in three times until adding the total amount. The total mixing time was controlled by a timer being it 20 minutes. A sample of 10 g of the mixture was taken to be analyzed through HPLC-MS/MS.

6. Quality control of the snail food supplemented with Praziquantel

Due to the characteristics of the mixture and the total amount of the lot, an uniformity of mass test was performed to assess homogeneity of the mixture, being the acceptance value of 15%. For this purpose, it was used a HPLC-MS/MS method to determine PZQ in the mixture: 50 mg of supplemented snail food (11.04 PZQmg/g snail food) were diluted in 10 ml of methanol (HPLC-grade), the supernatant was filtered through a Durapore PVDF 0.45 Mm Ø Millipore Millex-HV syringe driven unit and disposed in a vial and diluted 1:10 prior to injection in HPLC-MS/MS.

Theoretical concentration of the solution for injection was calculated as follows:

$$50 \text{ mg of PZQ supplemented snail food} \times \frac{11.04 \text{ PZQmg}}{1000 \text{ mg supplemented snail food}} \times \frac{1}{10 \text{ ml methanol}} \\ \times \frac{1000 \text{ PZQ } \mu\text{g}}{1 \text{ PZQ mg}} \times \frac{1}{10 \text{ ml methanol}} = 5.52 \text{ } \mu\text{gPZQ/ml}$$

The HPLC-MS/MS conditions comprehended an Acquity UPLC system, equipped with a binary pump and DAD detector (Waters, Milford MA, USA) and coupled to an API 3000 triple quadrupole mass spectrometer (Sciex, Concord, Ont., Canada). The reversed stationary phase employed was a Luna C18 column 50 x 2.0 mm id., 5 μ m; Phenomenex, Torrance, CA, USA). The mobile phase was acetonitrile as eluent A and 0.1% acetic acid in Milli-Q water as eluent B. The elution started at 25% of A and was increased linearly up to 65% of A in 2.5 min and kept isocratic for 0.5 min. It was returned to the initial conditions in 0.1 min and the reequilibration time was 1.9 min. The flow rate was 1.00 ml/min. All the samples were filtered through 0.22 μ m filters before the chromatographic analyses and the injection volume was 10 μ l.

Ionization was achieved with a TurboIonSpray interface (ESI) operating in positive mode and data were collected in multiple reaction monitoring mode (MRM). The ionization parameters were: capillary voltage 5000 V, nebulizer gas (N₂) 8 (arbitrary units), curtain gas (N₂) 8 (arbitrary units), collision gas (N₂) 4 (arbitrary units), declustering potential (DP) 100 V, focusing potential (FP) 300 V, entrance potential (EP) 10 V, collision energy (CE) 30 V, and drying gas (N₂) heated up to

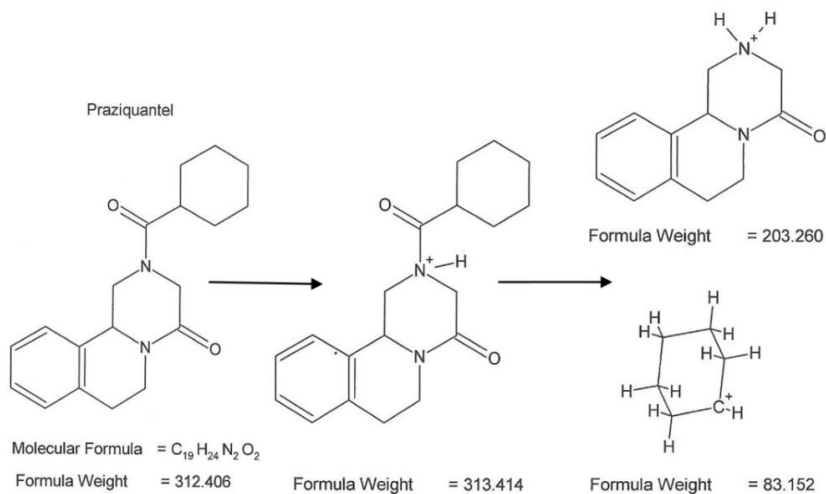


Figure 4. HPLC-MS/MS Praziquantel fragmentation: quantification transition (up) and confirmation transition (down).

350°C at a flow-rate of 5000 cm³ min⁻¹. MRM acquisition involved recording two transitions, 313.2/203.3 and 313.2/83.2, with a dwell time of 200 ms. First transition was used for quantitation purposes and the second one only for confirmation (Fig. 4), as it was more likely that the

Table 1. Calibration curves: Integrated peak areas per standard, back-calculated concentration and accuracy compliance criteria.

Methanol Standards (µg/ml)	Integrated Peak Area	Back-calculated Concentration (µg/ml)	Accuracy compliance limits ±15%	
			Lower limit	Upper limit
0,8	656225.153	0.774	0.68	1.48
1	952262.966	1.014	0.85	1.85
2	2134266.52	1.975	1.7	3.7
4	4836404.97	4.172	3.4	7.4
6	6805530.36	5.773	5.1	11.1
8	9656052.9	8.091	6.8	14.8

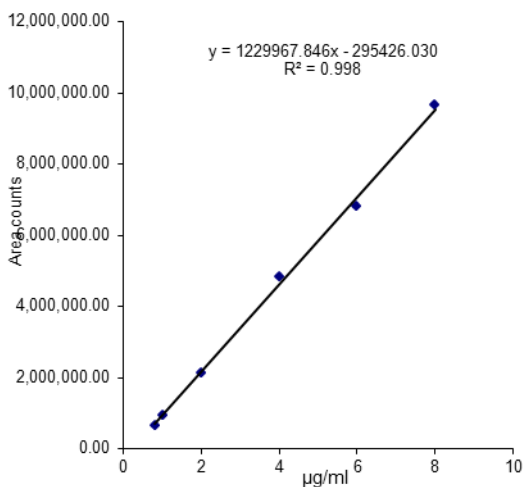


Figure 5. Calibration curve for Praziquantel-Methanol (HPLC grade) determination through HPLC-MS/MS.

Table 2. Praziquantel supplemented snail food quality control through HPLC-MS/MS analysis.

Sample	Integrated Peak Area	Experimental Concentration (µg/ml)	%
Injection 1	7282387.79	6.16	111.61
Injection 2	6924402.25	5.87	106.34
Injection 3	7326523.81	6.20	112.26
Injection 4	6923174.75	5.87	106.32
Injection 5	6786768.99	5.76	104.31
Mean concentration		5.97	108.17
Theoretical concentration		5.52	SD: ±0.20

analyzed ions were from PZQ molecules. Analyst® version 1.4 software (Sciex) on a PC was used for data acquisition and processing.

Calibration curves (Table 1 and Fig. 5) were prepared with the following standards: 0.8, 1.0, 2.0, 4.0, 6.0, and 8.0 µg/ml (PZQ/methanol HPLC grade). Each standard was prepared from a mother solution of 4 mg/ml (weighting 40 PZQmg and diluting in 10 ml of methanol). The mother solution was diluted 1:100 to obtain a 40 µg/ml working solution. The linearity was $r^2=0.998$ and accuracy compliant with all standards. The sample was analyzed through a series of 5 injections.

Integrated peak areas from analysis injection of the solution, used to extract PZQ from the snail food supplemented (see first paragraph of this section), were used in the calibration curve (Figure 5) in order to calculate the experimental concentration. In basis of the theoretical concentration, it was calculated the percentage of the experimental concentration to assess the uniformity of mass. Results over 100% indicate that the solution was more concentrated, and results under 100% indicate the opposite. If big discrepancies appear among results, the manufacturing procedure must be corrected. According to the results, the prepared lot was compliant with the ±15% acceptance value variation, with a mean value of 5.97 µg/ml, being the standard deviation (SD) ±0.20, and the calculated variation value +8.17, which easily fit the requirement ±15% (Table 2).

7. Acceptance of the snail food supplemented with Praziquantel by *C. aspersum*

PZQ taste is bitter and disgusting for humans [37]. Also, the bitterness of PZQ has been reported as a problem to achieve satisfactory treatment against monogenean parasites in the yellowtail kingfish [38]. The poor acceptance of PZQ has become of economic concern since in several livestock species satisfactory treatment was not achieved. However, poor acceptance of PZQ is not the only concern, especially in snails, were mortality rates were up to 73.4% in *Biomphalaria glabrata* after PZQ treatment [30, 34]. For this reason, the acceptance by *C. aspersum* was tested, as well as potential toxicity prior to any other step.

Taking into account that 4.14 kg of snail without shell consume daily 150 g snail food, the daily amount consumed by one specimen (4-5 g weight) without shell is about 181 mg. For the acceptance test purpose, 10 specimens of *C. aspersum* were individually disposed in plastic boxes (23 cm x 123 cm x 8 cm) covered with a net, maintained at room temperature under natural light-dark cycle, and sprayed with tap water twice in a day. An amount of 450 mg of snail food supplemented with PZQ was disposed on a small plastic plate (8.5 cm x 7.0 cm) inside each box every day along 3 days. Daily food consumption was controlled per specimen, weighting the snail food each 24 hours.

Table 3. Snail food consumption per day and daily mean (mg).

Specimen	Snail food consumption (mg)				
	Day 1	Day 2	Day 3	TOTAL	Daily mean
1	198	0	0	198	66.0
2	0	244.3	0	244.3	81.4
3	219.5	46.8	0	266.3	88.8
4	250.8	55.7	0	306.5	102.2
5	0	253	173.9	426.9	142.3
6	250.5	0	357.8	608.3	202.8
7	199.1	278.7	250.4	728.2	242.7
8	229.9	384.1	137	751	250.3
9	250	299.4	303.6	853	284.3
10	250.3	305.1	348.9	904.3	301.4

Table 4. Temperature registry: maximum, minimum and mean for snail food consumption test.

Day	Máxima (°C)	Mínima (°C)	Media (°C)
Day 1	28.9	21.2	25.1
Day 2	26.8	22.2	24.5
Day 3	24.1	22.7	23.4

The results of the acceptance test are presented in Table 3 and the registry of temperatures in Table 4.

The global daily mean consumption corresponded to 176.2 mg/day/snail being really close to the theoretically calculated 181 mg/day/snail. *C. aspersum*, apparently, did not reveal any toxic effect, since none snail consuming PZQ supplemented snail food died during the test. In regards of acceptability, the global mean consumption value was almost the theoretically calculated, suggesting that the bitter taste is not an issue for *C. aspersum*. Hereby, the mixture 11.04 PZQmg/g snail food appears to be suitable for further experiments.

8. Conclusion

In this work the most suitable way to administer PZQ to the terrestrial edible snail *C. aspersum* in a laboratory or a farm has been assessed. The oral administration of PZQ using PZQ supplemented snail food in *ad libitum* basis has been well tolerated by the snails, taking into account the average consumption of a snail per day. The manufacturing of PZQ supplemented snail food (11.04 PZQmg/g snail food) largely accomplished the acceptance value of 15% through HPLC-MS/MS analysis, assuring homogeneity of the mixture and dosage. The PZQ mixture, 11.04 PZQmg/g snail food, was accepted by *C. aspersum* despite of the bitter taste. Problems described by other species like fishes [37] did not appear. The PZQ supplemented snail food displayed an appropriated toxicological profile since mortality rates were 0% in comparison with other snails like *Biomphalaria glabrata*, which supported a mortality rate of 74.3% [30, 34]. The proposed strategy would be an easy and affordable approach to test drug efficacy in the laboratory and, in the future, in field trials.

Acknowledgements

The authors thank the ANCEC (Spanish Association for Breeding and Rearing of Snails) for providing snail food.

References

1. Gracenea, M., González-Moreno, O. 2002, *J. Parasitol.*, 88, 124.
2. Gracenea, M., González-Moreno, O., García Ruíz, R., Freixas, S., López de Arriba, M. 2009, *Acta Parasitol. Port.*, 16, 168.
3. Butcher, A. R., Talbot G. A., Norton R.E., Kirk, M. D., Cribb, T. H., Forsyth, J. R., Knight, B., Cameron, A. S. 1996, *Med. J. Aust.*, 164, 475.
4. Butcher, A. R. 1998, *Int. J. Parasitol.*, 28, 607.
5. Butcher, A. R. 2006, *ASM Aus. Soc. Micro.*, 33.
6. Sirgel, W. F., Mas-Coma, S. 2010, *Parasitol. Res.*, 106, 1443.
7. Africa, C. M., García, E. Y., de Leon, W. 1935, *Philipp. J. Public Health.*, 1, 1.
8. Belizario, V. Y., Bersabe, M. J., de Leon, W. U., Hilomen, V. Y., Paller, G. V., de Guzman, A. D., Bugayon, M. G. 2001, *South. Asian J. Trop. Med. Pub. Health.*, 32, 36.
9. Kean, B. H., Breslau, R. C. 1964, *Parasites of the human heart*, Grune and Stratton, New York, 95.
10. Meerburg, B. G., Singleton, G. R., Kijlstra, A. 2009, *Crit. Rev. Microbiol.*, 35, 22.
11. Fernández-López de Pablo, J., Badal, E., Ferrer García, C., Martínez-Ortí, A., Sanchis Serra, A. 2014, *PLoS One* 9, e104898.
12. Lubell, D.L., 2004, *XXIVe Rencontres Internationales d'Archéologie et d'Histoire d'Antibes*, 77.
13. RuralCat. 2010. Dossier Tècnic Formació i Assessorament al sector agroalimentari. Helicicultura. *La cria de caragols una opció ramadera en l'agricultura catalana*. Generalitat de Catalunya Departament d'Agricultura, Alimentació i Acció Rural 46, 19.
14. United Nations. 2015, COMTRADE database DESA/UNSD. <http://comtrade.un.org>. Accessed 26th November 2016.
15. Chevallier, H. 1985, *L'élevage des escargots: production et préparation du petit-gris*. Editions du Point Vétérinaire. Maisons-Alfort, France.
16. Bech, M. 1990, *Fauna malacològica de Catalunya. Mol·luscs terrestres i d'aigua dolça*. Treballs de la Institució Catalana d'Història Natural, Barcelona, 229.
17. Awad, A. H., Probert, A. J. 1991, *J. Helminthol.*, 65, 79.
18. Xiao, S. H., Yang, Y. Q., Shen, B. G., Xu, D. H., Yang, H. Z., Mei, J. Y., Yue, W. J. 1988, *Acta Pharmacol. Sin.*, 9, 360.
19. Gonçalves, J. P., Oliveira-Menezes, A., Maldonado Junior, A., Carvalho, T. M. U., de Souza, W. 2013, *Vet. Parasitol.*, 194, 16.
20. Lee, S. 1985, *Seoul J. Med.*, 26, 41.

21. Johansen, M. V., Monrad, J., Christensen, N. Ø. 1996, *Vet. Parasitol.*, 62, 83.
22. Shirakashi, S., Andrews, M., Kishimoto, Y., Ishimaru, K., Okada, T., Sawada, Y., Ogawa, K. 2012, *Aquacul.*, 326, 15.
23. Williams, R. E., Ernst, I., Chambers, C. B., Whittington, I. D. 2007, *Dis. Aq. Org.*, 77, 199.
24. Fei, C., Chao, F., Qiping, Z., Yang, L., Xiaoyang, W., Wenli, Z., Mi, W., Keyu, Z., Lifang, Z., Tao, L., Feiqun, X. 2013, *Vet. Parasitol.*, 198, 39.
25. Kyriakis, S. C., Tsioloyiannis, J., Vlemmas, J., Lekkas, S., Petridou, E., Sarris, K., 1997, *J. Vet. Med.*, 44, 523.
26. Michels, M. G., Bertolini, L. C. T., Esteves, A. F., Moreira, P., Franca, S. C. 2011, *Vet. Parasitol.*, 177, 55.
27. Hoflack, G., Maes, D., Mateusen, B., Verdonck, M., de Kruif, A. 2001, *J. Vet. Med.*, 48, 655.
28. Lia, R., Traversa, D., Laricchiuta, P., Dantas-Torres, F., Paradies, R., Alvinerie, M., Krecek, R. C., Otranto, D. 2010, *Vet. Parasitol.*, 169, 133.
29. Voutilainen, A. 2011, *Exp. Parasitol.*, 129, 72.
30. Riley, E. M., Chappell, L. H. 1990, *Parasitol.*, 101, 211.
31. Greenberg, R. M. 2006, *Parasitic flatworms: molecular biology, biochemistry, immunology and physiology*, A.G. Maule, and N. J. Marks (eds.). CAB International, Oxfordshire, UK, 269.
32. EMA. 1996, Committee for Veterinary Medicinal Products "Praziquantel". Summary Report (1). EMEA/MRL/141/96-FINAL. http://www.ema.europa.eu/docs/en_GB/document_library/Maximum_Residue_Limits_-_Report/2009/11/WC500015784.pdf. Accessed 20th January 2017.
33. Xiao, S., Xue, J., Xu, L., Zhang, Y., Qiang, H. 2011, *Parasitol. Res.*, 108, 723.
34. Mattos, A. C. A., Pereira, G. C., Jannotti-Passos, L., Kusel, J. R., Coelho, P. M. Z. 2007, *Act. Trop.*, 102, 84.
35. Chai, J. Y. 2013, *Infect. Chemother.*, 5, 32.
36. Council of Europe. 2017, *European Pharmacopoeia: supplement 9.2. 9th ed.* Strasbourg: Council of Europe, Oral powders and Premixes, 895.
37. Meyer, T., Sekljic, H., Fuchs, S., Bothe, H., Schollmeyer, D., Miculka, C. 2009, *PLoS Negl. Trop. Dis.*, 3, doi:10.1371/journal.pntd.0000357
38. Partridge, G. J., Michael, R. J., Thuillier, L. 2014, *Dis. Aq. Org.*, 109, 155.



Research Signpost
Trivandrum
Kerala, India

Recent Advances in Pharmaceutical Sciences VII, 2017: 115-132 ISBN: 978-81-308-0573-3
Editors: Diego Muñoz-Torrero, Montserrat Riu and Carles Feliu

8. Strategies against β -amyloid protein as therapeutics in Alzheimer's disease

Jaume Folch^{1,2}, Miren Ettcheto^{1,2,3}, Oriol Busquets^{1,2,3}, Elena Sánchez-López^{4,5}
Rubén Dario Castro-Torres^{2,6,8}, Carlos Beas-Zarate⁶, Mercè Pallàs^{2,3,5}
Jordi Olloquequi⁷, Daniela Jara³, M.L. Garcia^{4,5}, Carme Auladell^{2,8}
and Antoni Camins^{2,3,5}

¹Unitat de Bioquímica, Facultat de Medicina i Ciències de la Salut, Universitat Rovira i Virgili Reus (Tarragona), Spain; ²Centros de Investigación Biomédica en Red de Enfermedades Neurodegenerativas (CIBERNED). Instituto de Salud Carlos III. Madrid, Spain

³Unitat de Farmacologia i Farmacognòsia, Facultat de Farmàcia i Ciències de l'Alimentació Universitat de Barcelona (UB), Barcelona, Spain; ⁴Departament de Farmàcia i Tecnologia Farmacèutica i Físicoquímica, Unitat de Físicoquímica, Facultat de Farmàcia i Ciències de l'Alimentació, UB, Barcelona, Spain; ⁵Institut de Nanociència i Nanotecnologia, IN2UB Barcelona, Spain; ⁶Laboratorio de Neurobiología Celular, Universidad de Guadalajara, Zapopan Mexico; ⁷Instituto de Ciencias Biomédicas, Facultad de Ciencias de la Salud, Universidad Autónoma de Chile, Talca, Chile; ⁸Departament de Biologia Celular, Facultat de Biologia UB, Barcelona, Spain

Abstract. Alzheimer's disease (AD) is the main neurodegenerative disorder, causing total intellectual disability in patients suffering from it. It is considered an important public health problem of the 21st century due to its high global prevalence and socioeconomic impact. The amyloid hypothesis of AD proposes that β -amyloid peptide plays a key role in this disease. Several pharmacological strategies have been developed

Correspondence/Reprint request: Dr. Antoni Camins PhD., Unitat de Farmacologia i Farmacognòsia, Facultat de Farmàcia i Ciències de l'Alimentació, Universitat de Barcelona, Spain. Av. Joan XXIII, 27-31, E-08028 Barcelona, Spain. E-mail: camins@ub.edu.
Centros de Investigación Biomédica en Red de Enfermedades Neurodegenerativas (CIBERNED).

with the aim of inhibiting the formation of β -amyloid peptides, such as β -secretase and γ -secretase inhibitors. Other anti-amyloid treatments include passive and active immunotherapies focused on inhibiting β -amyloid peptide aggregation. However, the most recent phase 3 clinical trials of solanezumab, a humanized monoclonal antibody that promotes the clearance of β -amyloid in the brain, show no efficacy of this antibody in patients with mild AD, suggesting that the amyloid hypothesis of AD should be revised. In this manuscript, the current and ongoing treatments acting primarily on the β -amyloid protein are reviewed.

Introduction

Alzheimer's disease (AD) is the most frequent progressive neurodegenerative disorder that causes dementia among the world's population over 65 years (between 50 and 70% of the cases of dementia) [1]. The disease is chronic and progressive, causing deficits of multiple brain functions (mainly at the cortex and hippocampus levels) including memory, thinking, orientation, comprehension, calculation, learning ability and language [2].

Despite the great scientific and clinical advances in AD in the last 30 years, the treatments currently available are only symptomatic; thus meaning that they alleviate the symptoms of the disease by acting at different levels of the neuropathological process [2]. Although they improve the life quality of the patients, none can actually cure or delay the rapid and fatal progression of the disease.

Nowadays, there are only four drugs on the market approved for the treatment of AD. These drugs can be divided in two groups: acetylcholinesterase inhibitors (AChEI) and N-methyl-D-aspartic acid receptor (NMDAR) antagonists. AChEI includes donepezil, rivastigmine and galantamine [2, 4]. The mechanism of action of AChEI is to increase cholinergic transmission by inhibiting acetylcholinesterase in the synaptic cleft and therefore they may slightly increase the cognitive ability of patients with AD. Since in AD the levels of the neurotransmitter glutamate are pathologically elevated, memantine (MEM) is an NMDAR receptor antagonist that reduces excitotoxicity by blocking this ionotropic receptor. Both groups of drugs are indicated for the treatment of patients with moderate or severe AD [3,4]. However, it has been shown that none of these drugs actually represents a cure for the disease, since its effects are only palliative and its efficacy decrease with time.

Notwithstanding, new treatments and therapeutic strategies are being investigated in order to delay the course of the disease. These are mainly

directed to the neuropathological complexity of AD, encompassing multiple targets and are intended to be administered in the early stages of AD.

For future treatments to be effective, it will be necessary to develop new diagnostic techniques that allow an earlier diagnosis of AD in a pre-clinical phase (before symptoms appear), or even to predict the development of the disease.

The prevention of AD is a realistic challenge for researchers, but to make it possible it is necessary a better understanding of the aetiology and the extent to which environmental factors and lifestyle influence the risk of developing the disease.

1. Alzheimer's disease: Hypotheses

The cause or causes that promote the development of AD are still unknown. However, different hypotheses (Fig. 1) have been proposed thus contributing to understand the complex neurodegenerative process of this disease [5-8]. Most experts agree that it develops as a result of a combination of multiple modifiable and non-modifiable risk factors (age, sex, family history and genetics, environmental and lifestyle) rather than a single cause [9-11].

The two proposed etiological hypotheses most accepted by the scientific community currently are:

1. The hypothesis of the amyloid cascade, which suggests that the neurodegenerative process observed in the brains of patients with AD would be mainly due to the cytotoxic events triggered by the formation, aggregation and deposition of β -amyloid peptides [6,9]. This hypothesis has been strongly supported by researchers because of the genetic findings in molecular biology studies, opening new lines in the search for drugs for the treatment of AD, such as inhibitors of β and γ -secretase or enhancers of α -secretase [4]. According to this hypothesis, the initiation of AD would be triggered by the following process: APP (amyloid precursor protein) would be metabolized by the amyloidogenic route, which would cause an excess in the production of the β -amyloid peptide (β A) and / or a defect of its elimination [4,5].
2. Tau phosphorylation hypothesis. β A protein is obtained from the catabolism of APP, a membrane protein with a single domain (an intracellular and extracellular part) found in different cell types,

including neurons, glial cells, astrocytes and oligodendrocytes, [7,8]. It is encoded by a gene located on chromosome 21 which, when expressed, gives rise to 8 isoforms, with APP695 being the most abundant in the brain. This protein is cleaved by α -, β -, and γ -secretase enzymes and a complex of proteins containing the presenilin gene (PSEN1). In a physiological situation, following the non-amyloidogenic pathway, APP is catabolized by α -secretase, producing an APP α fragment (s) which remains in the extracellular space, and an 83-amino acid carboxy-terminal fragment (C83). APP α regulates neuronal excitability, improves synaptic plasticity, learning, memory and increases the resistance of neurons to oxidative and metabolic stress [5-8]. However, in a neuropathological situation, APP is metabolized by the amyloidogenic pathway, in which BACE1 (β -secretase 1) cleaves APP by the N-terminal end and the γ -secretase cleaves the C-terminal end, obtaining the fragments A β 40 / 42, which remain in the extracellular space, and a C-terminal fragment of 99 amino acids (C99), which can be transported into the cell and translocated to the nucleus, where it could induce expression of genes that promote neuronal death by apoptosis [6,7]. APP regulates neuronal survival, protection against toxic external stimuli, neurite outgrowth, synaptic plasticity and cell adhesion. Notwithstanding, when it is transformed into β A 40/42 peptides, it interferes with synapses, decreases neuronal plasticity, alters the energy metabolism and glucose, induces oxidative stress and mitochondrial dysfunction, and disrupts cellular calcium homeostasis [7]. Differential cleavage by β -secretase produces different β A peptides: β A40 is the predominant species, whereas β A42 is the major component of senile plaques. The peptide β A42 is more prone to aggregation and more neurotoxic than β A40. According to this, it has been proposed that β A is the pathogenic species in AD. In this way, β A42 is oligomerized and accumulated as senile plaques in the brain, thus exerting toxic effects on neuronal synapses. In a second stage, there would be a glial response, activation of the astrocytes and the surrounding microglia, which would release cytokines or components of the complement system leading to inflammatory responses. Likewise, oxidative stress is established in the neuron and there is an

alteration in calcium ion homeostasis, which causes hyperactivation of protein kinases and the inactivation of phosphatases. For this reason, the tau protein is hyperphosphorylated and forms the neurofibrillary tangles, which accumulate in the synapses and in the neuronal bodies causing neuronal death by apoptosis and a deficiency of neurotransmitters. All this cascade of processes ends in instituting dementia [7].

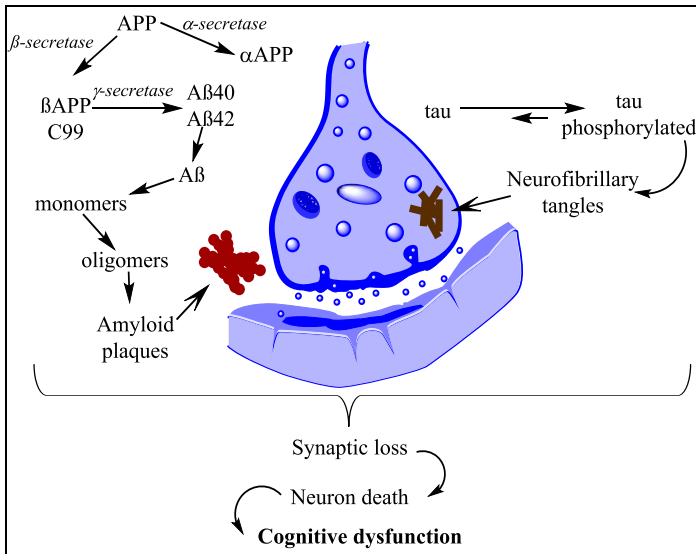


Figure 1. Alzheimer's disease hallmarks and its process.

Thus, both β A (mainly β A42) and tau proteins have been the main targets for modifying therapies of AD [4]. From this point of view, AD could be prevented or treated effectively by the decrease in the production of β A42 and the phosphorylation of the tau protein, in addition to the prevention of the aggregation or poor folding of these proteins, thus neutralizing or eliminating the toxic aggregated or poorly folded forms of these proteins, or a combination of these modalities [4-9].

Likewise, alternative hypotheses such as the alteration of mitochondrial activity, the neuroinflammatory hypothesis, the metabolic hypothesis (namely cholesterol and insulin), and the dendritic hypothesis have been also proposed [10-15]. All these lines of thought confirm the

complexity of this disease, in addition to the fact that the mechanism of neuronal death by apoptosis is not yet known at all.

2. Therapeutic strategies for the development of drugs to modify the course of Alzheimer's disease

Given the expected increase in the number of cases of AD patients in the coming decades, it is necessary to develop more effective treatments capable of modifying the course of the disease.

During the last decade, from 1998 to 2011, about 100 compounds have been evaluated with the objective of modifying the course of AD. Unfortunately, they have failed in the clinical development phase [1,3]. The reason for this failure could be explained, as already mentioned, by the multifactorial aetiology and pathophysiological complexity of the disease. Finding a suitable and effective drug in the whole population tested is a very complicated task.

Although some key aspects of the pathogenesis of AD remain to be solved, the scientific advances of the last 25 years have allowed to reasonably establishing several strategies for the development of treatments with potential to modify the course of this disease. Thus, among the different therapeutic strategies that are being investigated, those aimed at reducing the formation of β A42 and the phosphorylation of the tau protein are the most important [3]. These two types of injuries are the ones that have provided the greatest advances in the field, and could be the key to the treatment of AD in the near future.

Following the amyloid hypothesis of AD, huge efforts have been made with the aim of developing effective drugs in the treatment of AD [4, 6]. However, the multiple clinical failures of the compounds in development have led researchers to question this hypothesis. Notwithstanding, new compounds are being investigated, along with new diagnostic tools for AD. This is important, since the reason for these failures could be the lack of suitable biomarkers that would allow recruitment of patients in clinical trials before they reach a very advanced phase of the disease, in which any therapeutic intervention is useless [1].

The different anti-amyloid strategies are designed to act at different points in the metabolism of APP such as decreasing production of β A peptides. In the attempt to decrease the production of β A, the current research has focused on the modulation of the enzymatic pathways

responsible for the abnormal processing of APP, i.e. inhibition of γ and / or β -secretase and α -secretase activation.

2.1. Inhibitors of β -secretase (BACE1)

The enzyme β -secretase is responsible for initiating the amyloidogenic processing pathway of APP [7]. The development of inhibitors of this enzyme is quite challenging because, in addition to APP, β -secretase has many more substrates, among which we find neuregulin-1, involved in the myelination of the peripheral nerves [16-18]. This fact makes the non-specific inhibition of the enzyme susceptible of causing adverse effects [16]. The structure of the enzyme is another main problem. Since it belongs to the class of aspartyl proteases, the inhibitor must be a large hydrophilic molecule, which makes it difficult to cross the blood-brain barrier [19]. Currently, several compounds are being investigated to overcome these obstacles and to make some of them effective in the treatment of AD [19]. Recent studies indicate that two inhibitors of β -secretase, E2609 and MK-8931, are extremely effective in reducing the production of β A levels up to 80-90% in cerebrospinal fluid (CSF) in humans [17-19].

2.2. Inhibitors and modulators of γ -secretase

The γ -secretase enzyme is responsible for the final phase of APP processing by the amyloidogenic pathway, resulting in β A40 and β A42 peptides. Although its inhibition was a promising advance for the modification of the disease back in 2001, showing for the first time an *in vivo* decrease in the production of β A, the development of γ -secretase inhibitors shows similar problems to those of β -secretase inhibitors [19-21].

In addition to APP, γ -secretase processes multiple proteins, including the Notch protein, responsible for regulating cell proliferation, development, differentiation, communication, and cellular survival status [20,21]. For this reason, nonspecific inhibition of the enzyme results in serious adverse effects, leading to severe limitations in clinical trials.

Semagacestat (LY450139) is an example of this therapeutic group. As a functional γ -secretase inhibitor, it was shown to decrease β A levels in blood and cerebrospinal fluid in humans [22]. However, the results of this and other similar studies (NCT00762411; NCT01035138; NCT00762411)

showed that semagacestat did not decrease the slow progression of the disease and, in addition, its administration was associated with worsening cognition. Another example is avagacestat (NCT00810147; NCT00890890; NCT00810147; NCT01079819), whose pharmacokinetics and effectiveness have been evaluated in several clinical trials in AD patients [23-25].

To avoid the adverse effects derived from these γ -secretase inhibitors, the use of γ -secretase selective modulators (MSGs), which block the enzyme by altering the processing of APP without interfering with the signalling of other ways such as Notch, has been proposed [21]. The development of MSGs began with the observation that several anti-inflammatory drugs (NSAIDs) decreased β A42 peptide levels in human H4 neuroglioma cells as well as transgenic mice [26,27]. Examples of these drugs are ibuprofen, sulindac, indomethacin, and flurbiprofen. (*R*)-Flurbiprofen (tarenflurbil) inhibits cyclooxygenase-1 to a low extent, and it was tested in a clinical phase III study for the treatment of AD. However, both tarenflurbil and ibuprofen failed in their respective clinical trials [27,28].

CHF5074 is a non-steroidal anti-inflammatory derivative devoid of cyclooxygenase inhibitory activity [29]. *In vitro*, CHF5074 behaves as a β -secretase modulator, preferentially by inhibiting the production of β A42 [30,31]. As we have already mentioned, the long-term use of NSAIDs confers some protection against AD, which led to the widespread study of NSAIDs against the production of β A42. However, negative results observed in NSAID clinical trials suggest that protection against AD is not a general benefit provided by all these drugs.

An example of these MSGs is NIC5-15, a molecule of natural origin. Specifically, NIC5-15 is pinitol, a natural cyclic sugar alcohol [32]. Interestingly, pinitol also acts as an insulin sensitizer. This compound modulates β -secretase and reduces the production of β A without affecting the cleavage of the Notch- β -secretase substrate [32,33]. It has been suggested that the compound improves function deficit and memory in preclinical models of AD neuropathology [33]. Studies in animals and human trials have shown that NIC5-15 is safe and also acts as a sensitizer for insulin actions [32]. In preclinical studies, at doses higher than those previously studied in clinical trials, NIC5-15 was found to interfere with β A accumulation. This data suggest that NIC5-15 may be a suitable therapeutic agent for the treatment of AD mainly for three reasons: it is a

secretory inhibitor preserving Notch and, in addition, it is potentially an insulin sensitizer and is being investigated as an inhibitor of the inflammatory process particularly inhibiting the activation of microglia.

2.3. Activation of α -secretase

Activation of the α -secretase enzyme leads to the processing of APP by the non-amyloidogenic pathway, thereby decreasing the amount of APP available for the amyloidogenic pathway. The result is the formation of a soluble β A, which has been shown to play a neuroprotective and synaptogenic stimulatory role.

Thus, the activation of α -secretase is an attractive strategy for the development of disease modifying drugs. Different compounds related with the non-amyloidogenic pathway have been investigated, such as agonists of muscarinic acetylcholine receptors, glutamatergic receptors, serotonergic receptors, and activators of protein kinase C (PKC). However, not many compounds have been found that effectively modulate this pathway in animal models, so not many of these compounds can be found in clinical trials.

Epigallocatechin gallate (EGCG) is a polyphenolic flavonoid extracted from green tea leaves and it is considered its key bioactive ingredient. It has been reported to have beneficial clinical effects ranging from anti-tumour, anti-inflammatory and neuroprotective action, and it may also have a beneficial effect on cognitive function [34]. It has been proposed that EGCG inhibits the formation of toxic β A oligomers, in addition to activating α -secretase. A clinical trial (NCT00951834) is currently being conducted to evaluate the efficacy of EGCG in early stages of AD.

Briostatine 1 is a modulator of PKC which also seems to have immunomodulatory effects. There is preclinical data showing that this compound increases cognitive ability [35].

Etazolate (EHT0202) stimulates the neurotrophic action of α -secretase and also inhibits neuronal death induced by β A, thus providing symptomatic relief and further modifying disease progression. In a recent phase IIa clinical study in 159 patients with mild to moderate AD, EHT0202 has been shown to be safe and generally well tolerated [36]. These early encouraging results further support the development of EHT0202 to assess its clinical efficacy and confirm its tolerability in a large cohort of patients with AD in a longer period of time [36].

Moreover, acitretin is a retinoid that acts as a retinoic acid receptor agonist. It is primarily used to treat severe psoriasis [37]. In preclinical models, it increases the expression of ADAM-10, an α -secretase of the human amyloid precursor protein (APP) [37-39]. Acitretin has been reported to activate the non-amyloidogenic pathway of APP in neuroblastoma cells and to reduce β A levels in APP / PS1 transgenic mice. [37-39].

2.4. Amyloid antiaggregants

The extensive evidence on the neurotoxic and synaptotoxic activity of amyloid aggregates, constitute the scientific basis for the development of inhibitors of the aggregation of β A peptides.

The only inhibitor of β A aggregation to reach phase III is the 3-amino acid synthetic 1-propanesulfonic acid (3APS, Alzhemed, tramiprosate) [40,41]. This drug was designed to interfere with or antagonize the interaction of β A with endogenous glycosaminoglycans. Glycosaminoglycans have been shown to promote β A aggregation by interfering with the formation of amyloid fibrils and by stabilizing plaque deposition [41]. However, the disappointing results of the phase III trial in 2007 led to the suspension of the European Phase III trial.

Colostrinin, a proline-rich polypeptide complex derived from ovine colostrum, inhibits β A aggregation and its neurotoxicity in cellular assays, and improves cognitive performance in preclinical animal models [42]. Although a Phase II trial showed slight improvements in the Mini Mental State assessment in patients with mild AD over a 15-month treatment period, this beneficial effect was not maintained for another 15 months of additional continuous treatment.

The compound called scyllo-inositol is capable of stabilizing the oligomeric aggregates of β A and inhibiting β A toxicity in the mouse hippocampus. An 18-month clinical trial in the search for dose, safety and efficacy of scyllo-inositol (ELND005) in mild to moderate AD patients was carried out. Three doses of ELND005 (250, 1000, and 2000 mg) were evaluated, being 250 mg the most adequate. Future long-term clinical studies should be performed to elucidate if there is enough evidence to support or rule out an ELND005 benefit in AD.

Several compounds with an antiaggregating effect, such as PBT1 (clioquinol) and PBT2, have been evaluated. Clioquinol was investigated as a treatment for AD since it blocks the interaction between metals and β A in the brain [45]. It has been proposed that increased levels of bioactive metals

in aging brain accelerate the formation of amyloid plaques, as well as neurotoxic oxidative processes. The fundamental reason for the evaluation of clioquinol was that it would prevent accumulation of β A and, in addition, restore homeostasis of cellular levels of ions such as copper and zinc. Unfortunately, these compounds failed during clinical trial phases II and III due to lack of efficacy.

2.5. Compounds favouring the elimination of amyloid aggregates and deposits

Another amyloid-directed strategy is based on promoting the clearance of aggregates and amyloid deposits. To achieve this, three different strategies have been evaluated:

1) Activation of enzymes responsible for degrading amyloid plaques

Amyloid aggregates and plaques are degraded by different proteases, including neprilysin, insulin degrading enzyme (IDE), plasmin, endothelin-converting enzyme, angiotensin-converting enzyme, and metalloproteinases [9,46,47]. In AD, the levels of these enzymes decrease, thus contributing to the formation and accumulation of amyloid plaques [46]. Despite being an attractive anti-amyloid strategy for the development of disease-modifying drugs, no protease activator has been evaluated so far due to the lack of specificity of these compounds.

2) Modulation of β A transport from the brain to the peripheral circulation

The transport of β A between the central nervous system (CNS) and the peripheral circulation is regulated by; 1) apolipoproteins, with APOE ϵ 4 promoting the passage of β A from the blood to the brain; 2) low density lipoprotein receptor (LRP)-related protein, which increases the outflow of β A from the brain into the blood and; 3) the receptor for advanced glycation end products (RAGE), which facilitates β A entry into the CNS [48-51].

Although different strategies -like peripheral LRP administration- have been proposed to increase β A transport from the brain to the peripheral circulation, only compounds aimed at inhibiting / modulating RAGE have reached clinical development. These include PF-0449470052, which failed in the Phase II clinical trial, and TTP4000, currently in Phase I clinical trials (NCT01548430). The study ended in February 2013, and no results have been published so far.

3) Specific anti-amyloid immunotherapy

This is the most studied strategy with the aim of reducing amyloid burden in AD. There are two types of anti-amyloid immunotherapy:

a) Active immunotherapy: Active immunization (vaccination) with either β A42 (the predominant form of β A in the amyloid plaques of AD) or other synthetic fragments has been successfully evaluated in transgenic AD mouse models. The assays are generally based on the stimulation of T-cells, B-cells, and the immune response by activating the phagocytic capacity of the microglia. The results of the initially promising trials have been partially suspended due to the appearance of meningoencephalitis in some patients. When the first vaccine (AN1792, consisting of 42 amino acid peptide) was tested on patients, it was found to give rise to neurological inflammatory processes, such as aseptic meningoencephalitis, as a result of an anti-AN1792 autoimmune response. These adverse effects forced the discontinuation of Phase II clinical trials [53].

In order to avoid the non-specific immune response derived from immunization with complete β A ($A\beta$ 42) peptides, a second generation of vaccines has been designed by using shorter segments of β A ($A\beta$ 1-6) peptide, which favored a humoral response to a cellular immune response. CAD 106, designed by Novartis, was the first second generation vaccine that reached the clinical stages of development [54]. It has recently completed Phase II clinical trials, where a specific response of β A antibodies was observed in 75% of the patients tested, without giving rise to inflammatory adverse responses. ACC-001 has recently completed some Phase II trials (NCT01284387 and NCT00479557). Although there is another Phase II trial in process (NCT01227564), the pharmaceutical company has declined to continue the investigation. There are currently other vaccines in preclinical stages of development, such as the peptide ACI-24, β A1-15 tetra-palmitoylate reconstituted in a liposome, MER5101 and AF205 [55-57].

b) Passive immunization: It consists of passive -intravenous-administration of monoclonal or polyclonal antibodies directed against β A in the patient. Thus, an anti- β A immune response is achieved without the need for a pro-inflammatory reaction mediated by T cells [57]. Transgenic animal studies have demonstrated that passive immunization, in addition to reducing neuronal amyloid burden, improves cognitive deficits even before

the elimination of neuronal amyloid plaques [58]. This could be attributed to the neutralization of soluble amyloid oligomers, which are increasingly believed to play a fundamental role in the pathophysiological cascade of AD [57,58].

Bapineuzumab and solanezumab, the two monoclonal antibodies that have reached the most advanced stages of clinical development, failed in 2012 in two phase III clinical trials as they did not show the expected benefits in patients with mild-moderate AD. Bapineuzumab is a humanized monoclonal antibody against the N-terminal end of β A ($A\beta$ 1-5), while solanezumab is a humanized monoclonal antibody designed to bind to the central portion of β A ($A\beta$ 12-28) [59,60]. It is noteworthy that, despite the reduction of key AD biomarkers, such as amyloid brain plaques and phosphorylated tau protein in the cerebrospinal fluid, bapineuzumab failed to produce significant cognitive improvements in two clinical trials [61,62].

New phase III clinical trials with solanezumab are currently underway (NCT01127633 and NCT01900665), assessing its efficacy and safety in patients with mild AD (NCT02051608), with prodromal AD (NCT01224106), and in elderly asymptomatic population at high risk of losing memory (NCT02008357) [62]. Another monoclonal antibody, gantenerumab, is being tested with the aim of evaluating its modifying potential in people at risk of developing AD due to an autosomal dominant mutation of the DIAN-TI gene (NCT01760005) [63,64]. Gantenerumab is a fully human IgG1 antibody designed to bind with high affinity to a conformational epitope on β A fibers [63,64]. The therapeutic basis for this antibody is that it acts by degrading the amyloid plaques by a process of recruitment of the microglia and activation of phagocytosis. Experimental studies in transgenic mice support this hypothesis [65]. In parallel, a number of phase III clinical trials evaluating gantenerumab are being performed.

Specifically, in a phase III clinical trial, infusions of 400 mg of solanezumab or placebo once a month for 80 weeks were administered to patients with mild to moderate AD. The results seem to indicate a tendency to improve cognition with solanezumab in people with mild AD, but it does not appear to be statistically significant. Thus, we should be cautious and wait for more results.

Crenezumab (MABT5102A), is another humanized monoclonal antibody in phases of clinical development [66]. In April 2014, a phase II

clinical trial was completed to evaluate its efficacy and safety in patients with mild-moderate AD (NCT01343966), although the results are not yet available. Currently, two phase II trials with crenezumab are underway. The most recent began in 2013 in order to evaluate their efficacy and safety in asymptomatic patients with the autosomal dominant PSEN1 mutation (NCT01998841).

Other monoclonal antibodies against β A developed so far include PF-04360365 (ponezumab), which targets the free C-terminal of β A (specifically β A34-41); MABT5102A, which binds to monomers, oligomers, β A and fibrils with equally high affinity; and GSK933776A, which, similarly to bapineuzumab, targets the N-terminal sequence of β A [66]. In addition, other passive immunotherapies, such as those assessing GSK933776A, NI-101, SAR-228810 and BAN-2401 are being developed, most of which are in Phase I clinical trials.

Finally, gammagard™ is an antibody preparation from human plasma. Concerning this preparation, a safety record for human use has been established for certain autoimmune conditions. Gammagard™ has also been evaluated for the treatment of AD in a small number of patients (NCT00818662). These intravenous immunoglobulin mixtures contain a small fraction of polyclonal antibodies directed against the β A peptide, which is believed to counterbalance the synaptic toxicity caused by β A [67-69]. In addition, this intravenous IgG immunoglobulin has immunomodulatory effects, besides favoring the phagocytosis of the microglia [69].

3. Conclusion

Several attempts have been made to treat AD by reducing cerebral β A levels. Overall results obtained so far suggest that anti-amyloid drugs, as a specific group, could have a detrimental effect on the symptoms of the disease. On the other hand, the investigators argued in favor of carefully differentiating between these therapeutic approaches according to the underlying mechanism, rather than grouping them all together as anti-amyloid treatments. In addition, alternative approaches have been proposed to explain the failure of the amyloid hypothesis. Specifically, the adaptive response hypothesis proposes that β A may accumulate by an adaptive response to chronic stress stimuli in the brain [9]. According to this, stress stimuli are the pathogenic triggering signals/pathways of the late onset of AD and, therefore, would be suitable candidates for

therapeutic intervention in the disease. Such stimuli would include oxidative stress, metabolic dysregulation (cholesterol homeostasis, insulin resistance, etc.), genetic factors, and inflammatory response. Each of these stimuli is capable of eliciting a response in which more β A would be generated, and the nature of this response would determine the clinical progression of AD. Following this line of thought, acting on these stress stimuli could be an adequate pharmacological treatment to curb AD. Accordingly, intranasal insulin is recently being evaluated as a promising strategy for the treatment of AD. Positive results could confirm that β A is not the only noxious agent responsible for AD.

Acknowledgements

This work was supported by the Spanish Ministry of Economy and Competitiveness MAT 2014-59134-R project, SAF-2016-33307, PI2016/01 and the European Regional Development Funds. Research teams belongs to 2014SGR-1023 and 2014SGR-525 from Generalitat de Catalunya. The author, ESL, acknowledges the support of the Spanish Ministry for the PhD scholarship FPI-MICINN (BES-2012-056083).

References

1. Thies, W., Bleiler, L. 2013, *Alzheimers Dement.*, 9, 208.
2. Chiang, K., Koo, E.H. 2014, *Annu. Rev. Pharmacol. Toxicol.*, 54, 381.
3. Francis, P.T., Nordberg, A., Arnold, S.E., 2005. *Trends Pharmacol. Sci.*, 26, 104.
4. Huang, Y., Mucke, L., 2012, *Cell.*, 148, 1204.
5. Hardy, J., Selkoe, D.J., 2002, *Science*, 297, 353.
6. Hardy, J.A., Higgins, G.A., 1992, *Science*, 256, 184.
7. Haass, C., Kaether, C., Thinakaran, G., Sisodia, S., 2012, *Cold Spring Harb. Perspect. Med.*, 2:a006270.
8. Mucke, L., Selkoe, D.J., 2012, *Cold Spring Harb. Perspect. Med.*, 2:a006338.
9. Castello, M.A., Soriano, S., 2013, *Ageing Res. Rev.*, 12, 282.
10. Castello, M.A., Soriano, S., 2014, *Ageing Res. Rev.*, 13, 10.
11. Drachman, D.A., 2014, *Alzheimers Dement.*, 10, 372.
12. Ferreira, S.T., Clarke, J.R., Bomfim, T.R., De Felice, F.G., 2014, *Alzheimer's Dement.* 10 (1 Suppl), S76.
13. De Felice, F.G., Ferreira, S.T., 2014, *Diabetes*, 63, 2262.
14. De Felice, F.G., 2013, *J. Clin. Invest.*, 123, 531.
15. Cochran, J.N., Hall, A.M., Roberson, E.D., 2014, *Brain Res. Bull.*, 103, 18.
16. Vassar, R., Kandalepas, P.C., 2011, *Alzheimer's Res. Ther.*, 3, 20.
17. Menting, K.W., Claassen, J.A., 2014, *Front Aging Neurosci.*, 6, 165.

18. Chiang, K., Koo, E., 2014, *Annu. Rev. Pharmacol. Toxicol.*, 54, 381.
19. Imbimbo, B.P., Giardina, G.A., 2011, *Curr. Top. Med. Chem.*, 11, 1555.
20. Wolfe, M.S., 2012, *Adv. Pharmacol.*, 64, 127.
21. Doody, R.S., Raman, R., Siemers, E., Iwatsubo, T., Vellas, B., Joffe, S., Kiebertz, K., He, F., Sun, X., Thomas, R.G., Aisen, P.S., 2013, *N. Engl. J. Med.*, 369, 341.
22. Coric, V., Van Dyck, C.H., Salloway, S., Andreasen, N., Brody, M., Richter, R.W., Soininen, H., Thein, S., Shiovitz, T., Pilcher, G., Colby, S., Rollin, L., Dockens, R., Pachai, C., Portelius, E., Andreasson, U., Blennow, K., Soares, H., Albright, C., Feldman, H.H., Berman, R.M., 2012, *Arch. Neurol.*, 69, 1430.
23. Dockens, R., Wang, J.S., Castaneda, L., Sverdlov, O., Huang, S.P., Slemmon, R., Gu, H., Wong, O., Li, H., Berman, R.M., Smith, C., Albright, C.F., Tong, G., 2012, *Clin. Pharmacokinet.*, 51, 681.
24. Tong, G., Castaneda, L., Wang, J.S., Sverdlov, O., Huang, S.P., Slemmon, R., Gu, H., Wong, O., Li, H., Berman, R.M., Smith, C., Albright, C., Dockens, R.C., 2012, *Clin. Drug Investig.*, 32, 761.
25. Jaturapatporn, D., Isaac, M.G., McCleery, J., Tabet, N., 2012, *Cochrane Database Syst Rev.* 2, CD006378.
26. Eriksen, J.L., Sagi, S.A., Smith, T.E., Weggen, S., Das, P., McLendon, D.C., Ozols, V.V., Jessing, K.W., Zavitz, K.H., Koo, E.H., Golde, T.E., 2003, *J. Clin. Invest.*, 112, 440.
27. Pasqualetti, P., Bonomini, C., Dal Forno, G., Paulon, L., Sinforiani, E., Marra, C., Zanetti, O., Rossini, P.M., 2009, *Aging Clin. Exp. Res.*, 21, 102.
28. Ross, J., Sharma, S., Winston, J., Nunez, M., Bottini, G., Franceschi, M., Scarpini, E., Frigerio, E., Fiorentini, F., Fernandez, M., Sivilia, S., Giardino, L., Calza, L., Norris, D., Cicirello, H., Casula, D., Imbimbo, B.P., 2013, *Curr. Alzheimer Res.*, 10, 742.
29. Imbimbo, B.P., Frigerio, E., Breda, M., Fiorentini, F., Fernandez, M., Sivilia, S., Giardino, L., Calzà, L., Norris, D., Casula, D., Shenouda, M., 2013, *Alzheimer Dis. Assoc. Disord.*, 27, 278.
30. Ronsisvalle, N., Di Benedetto, G., Parenti, C., Amoroso, S., Bernardini, R., Cantarella, G., 2014, *Curr. Alzheimer Res.*, 11, 714.
31. Lee, B.H., Lee, C.C., Wu, S.C., 2014, *J. Sci. Food Agric.*, 94, 2266.
32. Pitt, J., Thorner, M., Brautigam, D., Larner, J., Klein, W.L., 2013, *FASEB J.*, 27, 199.
33. Obregon, D.F., Rezaei-Zadeh, K., Bai, Y., Sun, N., Hou, H., Ehrhart, J., Zeng, J., Mori, T., Arendash, G.W., Shytle, D., Town, T., Tan, J., 2006, *J. Biol. Chem.*, 281, 16419.
34. Etcheberrigaray, R., Tan, M., Dewachter, I., Kuipéri, C., Van der Auwera, I., Wera, S., Qiao, L., Bank, B., Nelson, T.J., Kozikowski, A.P., Van Leuven, F., Alkon, D.L., 2004, *Proc. Natl. Acad. Sci. U. S. A.*, 101, 11141.
35. Vellas, B., Sol, O., Snyder, P.J., Ousset, P.J., Haddad, R., Maurin, M., Lemarié, J.C., Désiré, L., Pando, M.P., 2011, *Curr. Alzheimer Res.*, 8, 203.
36. Holthoewer, D., Endres, K., Schuck, F., Hiemke, C., Schmitt, U., Fahrenholz, F., 2012, *Neurodegener. Dis.*, 10, 224.

37. Tippmann, F., Hundt, J., Schneider, A., Endres, K., Fahrenholz, F., 2009, *FASEB J.*, 23, 1643.
38. Endres, K., Fahrenholz, F., Lotz, J., Hiemke, C., Teipel, S., Lieb, K., Tüscher, O., Fellgiebel, A., 2014, *Neurology*, 83, 1930.
39. Gauthier, S., Aisen, P.S., Ferris, S.H., Saumier, D., Duong, A., Haine, D., Garceau, D., Suh, J., Oh, J., Lau, W., Sampalis, J., 2009, *J. Nutr. Health Aging*, 13, 550.
40. Aisen, P.S., Gauthier, S., Ferris, S.H., Saumier, D., Haine, D., Garceau, D., Duong, A., Suh, J., Oh, J., Lau, W.C., Sampalis, J., 2011, *Arch. Med. Sci.*, 7, 102.
41. Bilikiewicz, A., Gaus, W., 2004, *J. Alzheimers Dis.*, 6, 17.
42. Aytan, N., Choi, J.K., Carreras, I., Kowall, N.W., Jenkins, B.G., Dedeoglu, A., 2013, *Exp. Neurol.*, 250, 228.
43. Salloway, S., Sperling, R., Keren, R., Porsteinsson, A.P., van Dyck, C.H., Tariot, P.N., Gilman, S., Arnold, D., Abushakra, S., Hernandez, C., Crans, G., Liang, E., Quinn, G., Bairu, M., Pastrak, A., Cedarbaum, J.M., 2011, *Neurology*, 77, 1253.
44. Matlack, K.E., Tardiff, D.F., Narayan, P., Hamamichi, S., Caldwell, K.A., Caldwell, G.A., Lindquist, S., 2014, *Proc. Natl. Acad. Sci. U. S. A.*, 111, 4013.
45. Nalivaeva, N.N., Fisk, L.R., Belyaev, N.D., Turner, A.J., 2008, *Curr. Alzheimer Res.*, 5, 212.
46. Higuchi, M., Iwata, N., Saido, T.C., 2005, *Biochim. Biophys. Acta*, 1751, 60.
47. Deane R.J., 2012, *Fut. Med Chem.*, 4, 915.
48. Baranello, R.J., Bharani, K.L., Padmaraju, V., Chopra, N., Lahiri, D.K., Greig, N.H., Pappolla, M.A., Sambamurti, K., 2015, *Curr. Alzheimer Res.*, 12, 32.
49. Deane, R., Sagare, A., Zlokovic, B.V., 2008, *Curr. Pharm. Des.*, 14, 1601.
50. Bates, K.A., Verdile, G., Li, Q.X., Ames, D., Hudson, P., Masters, C.L., Martins, R.N. 2009, *Mol. Psychiatry*, 14, 469.
51. Galasko, D., Bell, J., Mancuso, J.Y., Kupiec, J.W., Sabbagh, M.N., van Dyck, C., Thomas, R.G., Aisen, P.S., 2014, *Neurology*, 82, 1536.
52. Gilman, S., Koller, M., Black, R.S., 2005, *Neurology*, 64, 1553.
53. Wiessner, C., Wiederhold, K.H., Tissot, A.C., Frey, P., Danner, S., Jacobson, L.H., Jennings, G.T., Lüönd, R., Ortmann, R., Reichwald, J., Zurini, M., Mir, A., Bachmann, M.F., Staufenbiel, M., 2011, *J. Neurosci.*, 31, 9323.
54. Muhs, A., Hickman, D.T., Pihlgren, M., Chuard, N., Giriens, V., Meerschman, C., van der Auwera, I., van Leuven, F., Sugawara, M., Weingertner, M.C., Bechinger, B., Greferath, R., Kolonko, N., Nagel-Steger, L., Riesner, D., Brady, R.O., Pfeifer, A., Nicolau, C., 2007, *Proc. Natl. Acad. Sci. U. S. A.*, 104, 9810.
55. Liu, B., Frost, J.L., Sun, J., Fu, H., Grimes, S., Blackburn, P., Lemere, C.A., 2013, *J. Neurosci.*, 33, 7027.
56. Panza, F., Solfrizzi, V., Imbimbo, B.P., Logroscino, G., 2014, *Expert Opin. Biol. Ther.*, 14, 1465.
57. Panza, F., Solfrizzi, V., Imbimbo, B.P., Tortelli, R., Santamato, A., Logroscino, G., 2014, *Expert Rev. Clin. Immunol.*, 10, 405.

58. Salloway, S., Sperling, R., Fox, N.C., Blennow, K., Klunk, W., Raskind, M., Sabbagh, M., Honig, L.S., Porsteinsson, A.P., Ferris, S., Reichert, M., Ketter, N., Nejadnik, B., Guenzler, V., Miloslavsky, M., Wang, D., Lu, Y., Lull, J., Tudor, I.C., Liu, E., Grundman, M., Yuen, E., Black, R., Brashear, H.R., 2014, *N. Engl. J. Med.*, 370, 322.
59. Doody, R.S., Thomas, R.G., Farlow, M., Iwatsubo, T., Vellas, B., Joffe, S., Kieburtz, K., Raman, R., Sun, X., Aisen, P.S., Siemers, E., Liu-Seifert, H., Mohs, R. 2014, *N. Engl. J. Med.*, 370, 311.
60. Tacey, H.O., Murray, E.D., Price, B.H., Tarazi, F.I., 2013, *Expert Opin. Biol. Ther.*, 13, 1075.
61. Panza, F., Solfrizzi, V., Imbimbo, B.P., Logroscino, G., 2014, *Expert Opin. Biol. Ther.*, 14, 1465.
62. Novakovic, D., Feligioni, M., Scaccianoce, S., Caruso, A., Piccinin, S., Schepisi, C., Errico, F., Mercuri, N.B., Nicoletti, F., Nisticò, R., 2013, *Drug Des. Devel. Ther.*, 7, 1359.
63. Bohrmann, B., Baumann, K., Benz, J., Gerber, F., Huber, W., Knoflach, F., Messer, J., Oroszlan, K., Rauchenberger, R., Richter, W.F., Rothe, C., Urban, M., Bardroff, M., Winter, M., Nordstedt, C., Loetscher, H., 2013, *J. Alzheimers Dis.*, 28, 49.
64. Jacobsen, H., Ozmen, L., Caruso, A., Narquizian, R., Hilpert, H., Jacobsen, B., Terwel, D., Tanghe, A., Bohrmann, B., *J. Neurosci.*, 34, 11621.
65. Jindal, H., Bhatt, B., Sk, S., Singh Malik, J., 2014, *Hum. Vaccin. Immunother.*, 10, 2741.
66. Dodel, R., Rominger, A., Bartenstein, P., Barkhof, F., Blennow, K., Förster, S., Winter, Y., Bach, J.P., Popp, J., Alferink, J., Wiltfang, J., Buerger, K., Otto, M., Antuono, P., Jacoby, M., Richter, R., Stevens, J., Melamed, I., Goldstein, J., Haag, S., Wietek, S., Farlow, M., Jessen, F., 2013, *Lancet Neurol.*, 12, 233.
67. Relkin, N.R., Szabo, P., Adamiak, B., Burgut, T., Monthe, C., Lent, R.W., Younkin, S., Younkin, L., Schiff, R., Weksler, M.E., 2009, *Neurobiol. Aging*, 30, 728.
68. Szabo, P., Mujalli, D.M., Rotondi, M.L., Sharma, R., Weber, A., Schwarz, H.P., Weksler, M., E., Relkin, N., 2010, *J. Neuroimmunol.*, 227, 167.



Research Signpost
Trivandrum
Kerala, India

Recent Advances in Pharmaceutical Sciences VII, 2017: 133-165 ISBN: 978-81-308-0573-3
Editors: Diego Muñoz-Torrero, Montserrat Riu and Carles Feliu

9. Fighting the Influenza A virus. New scaffolds and therapeutic targets

Marta Barniol-Xicota and Santiago Vázquez

Laboratori de Química Farmacèutica (Unitat Associada al CSIC), Facultat de Farmàcia i Ciències de l'Alimentació, and Institute of Biomedicine (IBUB), Universitat de Barcelona, Av. Joan XXIII, s/n, Barcelona E-08028, Spain

Abstract. Influenza A virus is a major threat to human health and a potential biowarfare pathogen. The M2 proton channel protein, essential for virus viability, contains a single transmembrane domain that forms a homo-tetrameric pore, targeted by Amantadine. The emergence of resistance to drugs poses major health risk as most of Influenza virus isolates are now Amantadine-resistant. Although only a handful of mutations are tolerated in transmissible viruses, V27A, S31N and L26F, they are enough to jeopardize public health. Aiming to overcome drug resistance, we are preparing new polycyclic small molecules which putatively will inhibit the wild-type and the mutant M2 channels.

1. The Influenza A virus

The influenza A virus, commonly known as the Flu virus, is a coated virus of the *Orthomyxoviridae* family, which has a multipartite, negative-sense,

Correspondence/Reprint request: Dr. Marta Barniol-Xicota, Laboratory of Chemical Biology, Department of Cellular and Molecular Medicine, KU Leuven, Herestraat 49, box 802, 3000 - Leuven, Belgium. E-mail: marta.barniolxicota@kuleuven.be

Dr. Santiago Vázquez, Laboratori de Química Farmacèutica (Unitat Associada al CSIC), Facultat de Farmàcia i Ciències de l'Alimentació, and Institute of Biomedicine (IBUB), Universitat de Barcelona, Av. Joan XXIII, s/n, Barcelona E-08028, Spain. E-mail: svazquez@ub.edu

single-stranded RNA genome that codes for 11 viral proteins. From the exterior to the interior of the virus, we find the following proteins: the hemagglutinin (HA) and the neuraminidase (NA), which are antigenic glycoproteins found in the lipid membrane of the virus; the M2 protein, which crosses the lipid coating in the form of a proton selective channel. In the viral interior, we find the nucleoprotein (NP), the matrix protein M1, the viral polymerase complex formed by the PA, PB1 and PB2, subunits, the non-structural protein NS1 and the nuclear export protein (NEP) [1].

The standard nomenclature of the viral strains includes: viral type/specie from isolation (in case of non-human)/ isolation place/ number of isolate/ year of isolation/ hemagglutinin type/ neuraminidase type [2]. For example A/Panama/2007/1999(H3N2) indicates an Influenza A virus found in humans in Panama, that is the number of isolate 2007 of the year 1999 and that has a HA type 3 and a NA type 2.

The two most relevant traits of the Influenza A virus are its high infectivity, which is responsible for its easy transmission through the airborne route or via hands-mouth, and its ability to mutate [3]. The viral mutations occur through two mechanisms: the antigenic drift, which consists in point mutations in the viral structure, that allow a slight variation of the viral properties and is responsible, for example, of the drug resistance mechanism. The other mutation path is the antigenic shift, which consists in the genetic rearrangement between two or more different influenza A viral strains, giving place to a new strain with mixed properties. For example, through this mechanism, an animal virus can acquire the capacity to infect humans [4].

2. The viral cycle

Viral entry. The cycle starts when the virus enters in the organism and recognizes the sialic acids located on the surface of the host's respiratory system epithelial cells, to which is attached thanks to the surface protein HA [5].

Endocytosis. Following, the virus enters into the cells through a receptor-mediated endocytosis, usually by clathrin, even alternative internalization routes as macropinocytosis [6] have been reported. The virus, hence, is internalized in a primary endosome with a pH around 6.

Fusion. The primary endosome is transported giving place to a late endosome in which the pH is again lowered thanks to the vacuolar ATPase (V-ATPase). This promotes an irreversible conformational change of the

HA, in which the N-terminus of the HA2 subunit, known as fusion peptide [7-8], is expelled. This fusion peptide will be inserted in the endosomal membrane, giving place to the fusion of both membranes, the viral and the endosomal one. The same pH shift also activates the M2 channel, which starts conducting protons, acidifying the viral interior. This will give place to the dissociation of the M1 protein from the viral ribonucleoprotein complex (vRNP), allowing the release of the vRNP to the cytoplasm from where they will be imported to the nuclei through the nuclear import factors. On another hand, the M1 protein will complex in late endosomes to be, in a similar way, imported to the nuclei [9].

Viral replication and transcription. Once in the nuclei the viral polymerase catalyzes the synthesis of one copy in positive sense of the viral RNA – the so-called complementary RNA, which will be copied to produce big quantities of viral RNA (vRNA) and the synthesis of a messenger RNA, of positive sense. The new vRNA will be encapsulated by the nucleoprotein and thanks to the NEP, the nuclear export complex will be formed; this will allow the crossing of one of the nucleoproteins to the cytoplasm. On another side, the mRNA will attach to the nucleoprotein to be exported through the nuclear export factor 1 (NXF1), which is the machinery that the host cell uses for its own RNA.

Translation. The mRNA highjacks the host cell translation mechanisms thanks to the NS1 protein, avoiding the response mechanisms of the host [10]. Once released from the NP, the mRNA are translated for viral proteins in the ribosomes. The NP, NS1, NEP and the M1 protein return to the nuclei to give place to more viral RNA. In contrast the NA, HA and the M2 protein will be transported to the endoplasmic reticulum and the Golgi apparatus where post-translational modifications will take place, giving mature proteins. Worthy of mention, during the transit through the Golgi apparatus – which has an acidic pH – the M2 protein is responsible of increasing the pH in the interior of the transport vesicles, to avoid the HA conformational change [11].

Packaging, virion formation and release of mature virus. Once the maturation process of the surface proteins HA, NA and the transmembrane protein M2 are completed, those proteins aggregate in the plasma membrane lipid rafts. Following, the viral RNA will attach to the HA, thanks to the action of the M1 protein. The high concentration of HA and NA, will alter the membrane curve, allowing the polymerization of the protein M1, in order to continue with the formation of the new virion. Simultaneously the M2 protein passes to the neck of this virion, altering

once again the plasma membrane, until this is separated from the virion [12] which will remain attached to the host cell uniquely by bonds of the HA with the sialic acid receptors. Finally, thanks to the scission of this bond by the NA, the newly formed influenza virus will be released [13].

As can be deduced from the viral cycle, all the Influenza A proteins play a paramount role. Hence, the malfunction or inhibition of any of those, will allow stopping the infection; consequently, all of them are subject to be used as anti-influenza A drug targets [14].

3. The M2 channel

3.1. Structure

The M2 viroporin of the Influenza A virus is a 97 amino acid transmembrane protein that assembles in tetramers to give place to a channel across the viral membrane. Each strand consists in two α -helices with a left-handed parallelism respect the *N*-terminal region. This deviation is due to a slight tilt of 30-35° nearby the Gly 34 [15]. The following regions can be distinguished in each strand:

Residues 1 to 24 – *N*-terminus: Extracellular unstructured region, which function is the incorporation of the protein into the virion.

Residues 25 to 46 – Transmembrane domain [16]: Tetramer of α -helices, which is responsible for the proton conduction. The drug-binding site is located in this region.

Residues 47 to 61 – Amphipathic cytoplasmic region: Intracellular, α helix structured domain that is responsible for the stabilization of the M2 protein and the release and scission of the newly formed virions.

Residues 62 to 97 – *C*-terminus: Intracellular unstructured region where the interaction with the matrix viral protein M1 takes place [17].

Since the structure of the M2 protein was solved in 2008 – by solution NMR [18] and X-Ray crystallography [19] - up to 15 different structures can be found in the Protein Data Bank (PDB). Nevertheless was not until 2014 that the M2 was assessed as a 2-fold symmetric tetramer, which can be better described as a dimerization of functional dimers [20-21].

3.2. Function

The main function of the M2 channel is to allow the proton flow in a controlled manner [15]. It acts as a pH regulator in order to allow, during the viral life cycle: i) the *proton diffusion to the interior of the endosome*,

where the virus is contained to reach a mature state, allowing the fusion of the viral membrane in the endosome and the right unpacking of the viral genome of the protein M1 [22] and, ii) the *delay of the acidification of the transport vesicles* in the Golgi apparatus to ensure the correct formation and the later release of the virus [23].

The transmembrane domain of the channel (residues 25 – 46) is the functional unit, as it contains the essential residues for the proton conduction. These are: the histidines in position 37 (**His37**), the pKa of which controls the conduction rate [24-25]; the tryptophans in position 41 (**Trp41**), which ensure the unidirectional proton flow [26]; the valine in position 27 (**Val27**), which forms a small valve to control the proton entrance to the channel, and the aspartic acid in position 44 (**Asp44**), which forms an indirect hydrogen bond with the NH group of the indole ring of Trp41 through a water net, at the end of the channel. Hence, meanwhile the motif HxxxW formed by H37 and W41 is the functional core of the channel, the V27 and the D44 are the gates veiling it.

The M2 is a slow channel as at physiological pH (pH=7.4) conducts at a rate of 10^2 - 10^3 protons per second, considered slow with respect of the constant of proton conduction through an aqueous pore of similar dimensions: 10^8 protons per second [27]. This fact is due that at physiological pH the concentration of protons is low, around one order of magnitude below the diffusion rate, however, when the external pH is lowered below the viral internal pH ($\text{pH}_{\text{out}} < \text{pH}_{\text{in}}$), this rate becomes much higher, until multiplying the diffusion rate by a second order rate constant. Hence, the conduction peak is found at low pHs [28]. This behaviour is the responsible for the sigmoidal dependence of the pH by conduction of protons through the M2 channel.

The mechanism through which the proton conduction occurs has been object of controversy in the last years [15, 29-33]. Despite this, the determination of the double dimeric structure has allowed a plausible explanation [20-21]. The protons enter the channel through the V27 gate. Once in the hydrophilic interior the protons are transported through an intermolecular translocation, thanks to the proximity of the hydrophilic residues that are facing the pore.

On a first instance the protons attach to the more N-terminal H37 and after to the more C-terminal one of the dimers which are forming an H_2 bond between the nitrogens δ i ϵ respectively. Following, the proton transfer

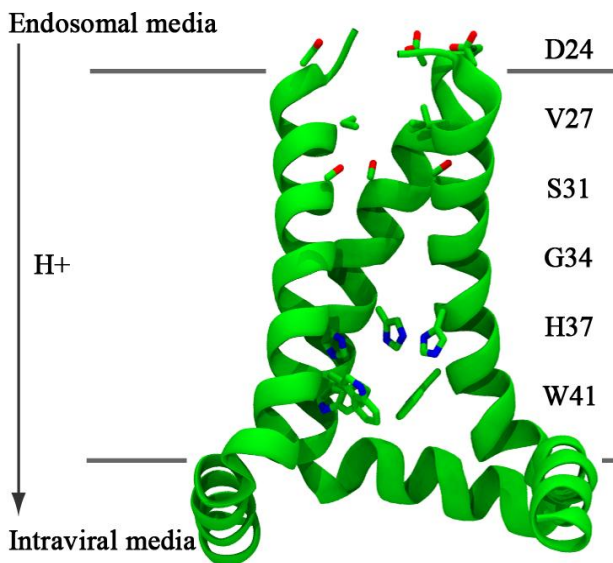


Figure 1. Schematic representation of the TM domain of the influenza A M2 channel. The side chains of the relevant residues V27, N31, H37 and W41 are shown. For clarity, only three of the four chains are shown.

from the His to the Trp occurs and the proton is then released to the viral interior. Thanks to a His37 tautomerism, the protein returns to the original state. Hence, each of the dimers that form the channel is functional for the proton conduction [33]. It is important to highlight that the proximity between the H37 and the W41 – which form a stable net of cation- π interactions inside the helix and between neighbouring helices - is the responsible of the protein tetramerization.

4. Related diseases

The influenza disease, commonly known as the flu, consists in an incubation period of two days, after which the signs and symptoms appear giving: high fever, headache, muscle and joint pain, general malaise and respiratory symptoms. Medical attention to recover from the flu for otherwise healthy patients is not usual, as symptoms normally disappear within a week. However, it can be especially aggressive giving fatal complications, among high-risk groups (children younger than two years

old, the elders and the immunosuppressed) or by a high virulent strain. Seasonal influenza outbreaks occur every year during autumn and winter in temperate regions, as there are the suitable conditions of relative humidity and temperature. Worldwide, these annual epidemics result in about 3 to 5 million cases of severe illness and about 250.000-500.000 deaths, being a clear public health treat [34]. In addition, the flu can cause serious economic losses arising from work absenteeism, productivity decrease, and saturation of health clinics during the peak illness periods [35].

However, the most important concern is the capacity of this virus to generate pandemics. These can occur through the antigenic shift, through which an especially infectious strain can combine with a highly transmissible one, giving place to a lethal unstoppable pandemic, as happened in 1918 with the Spanish Flu. The 1918 pandemic terminated with 40 million of lifes around the globe, being the most devastating of humankind history [36]. Taking this into account and knowing that those pandemics have a periodicity, the need to develop drugs to fight this virus is of vital urgency.

5. M2 channel- drug Pipeline

The M2 channel is the target of two clinically approved drugs: amantadine (Symmetrel[®], Mantadix[®]) and rimantadine (Flumadine[®]).

The mechanism of action of amantadine (Amt) was object of debate in the past [37], however, nowadays it is acknowledged that only one Amt molecule binds the interior of the pore, between the residues Val27 and

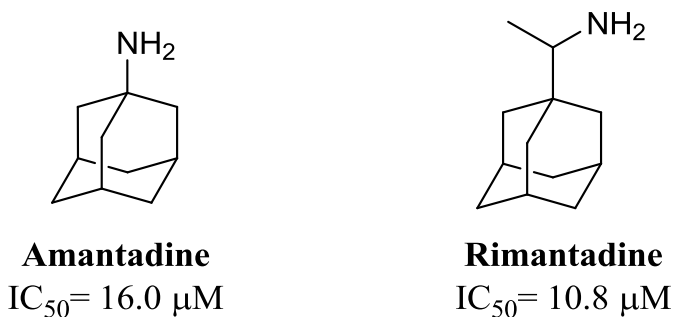


Figure 2. Commercial drugs targeting the M2 channel and corresponding IC_{50} .

Gly34 (called pore binding site), when the channel is in the open state, under acidic pH. The mechanism through which these adamantane structures inhibit the channel activity, responds to a physical blockade in which the drug occludes the pore avoiding: the proton transfer, the conformational change of the protein and the protein tetramerization.

The orientation of the polar group of the adamantane in the M2 channel had been debated as well. The two main theories were: the binding occurs in the down form [38], in which the hydrophobic cage is interacting through van der Waals forces with the methyl groups of the Val27 and Ala30, meanwhile the polar group is directed to the interior of the pore. Contrarily, in the second modality or up binding mode, the polar group is pointing the Val27 gate, being better solvated. The debate ended after proving that these two binding modes fluctuate depending on the protonation state of the M2 [39].

6. M2 as a therapeutic target

Nowadays the appearance of resistant strains together with the secondary effects in the central nervous system of Amt – known as NMDA receptor antagonist – have prompted the use of these drugs to be discouraged [40]. Surprisingly instead of causing a desertion of the M2 channel, has unchained a strong research on this protein, as it is the ideal candidate to be a drug target, presenting:

Well known biology. Nowadays the M2 channel is the best-known channel, being an ideal candidate for the rational drug design.

Essential for the viral cycle. As aforementioned, M2 channel is responsible for pH regulation in several events of the viral cycle. If the proton flow is stopped by a suitable inhibitor, the virus is no longer able to replicate.

Low mutation rate. Despite the flu virus has a high mutagenicity rate, in the case of the M2 channel, a very limited number of mutants that are both, infective and viable are known. In fact, in the circulating strains we mainly find the following 3 types [41]:

V27A (Valine → Alanine)

In this mutant channel in the position 27 the valine, which side chain is an isopropyl group, is replaced by an alanine, with a methyl group as a side chain. This destroys the entrance gate of the channel, increasing the proton conduction rate and weakening the α helix packing, which gives place to a 2 Å wider channel, respect the wild-type (*wt*). Hence, despite the inhibitors are able to bind the pore, there is not enough energetic resistance to avoid

their exit, provoking the fast drug release from the channel and restarting the proton flow. Worthy of note, the V27A is the only mutant arising from the drug selection pressure [42-43].

L26F (Leucine \rightarrow Phenylalanine)

The replacement of the leucine, with an isobutyl group, by a phenylalanine, with a benzyl group, which is placed in the interhelical interface, destabilizes the general structure of the channel. As a result, the packaging of the pore will be less compact, increasing its diameter by 0.5 Å. The widening effects are similar to those of the V27A mutation.

S31N (Serine \rightarrow Asparagine)

The S31N mutant is clinically the most relevant [44] as it is found in a 95% of the currently circulating strains. The serine (-CH₂OH) of the *wt* channel is replaced by an asparagine (-CH₂CONH₂) giving place to a bigger change than in the previous cases: the channel widens 0.5 Å nearby the Val27 gate and narrows on 1.5 Å in the mutation site (Asn31). In the *wt*, the Ser31 is oriented towards the membrane lipids, conformation that is not adopted in the mutant channel, as the Asn31 methylcarboxamide side chain, is longer and more hydrophilic, giving place to unfavourable interactions. This fact provokes a global restructuring of the channel that

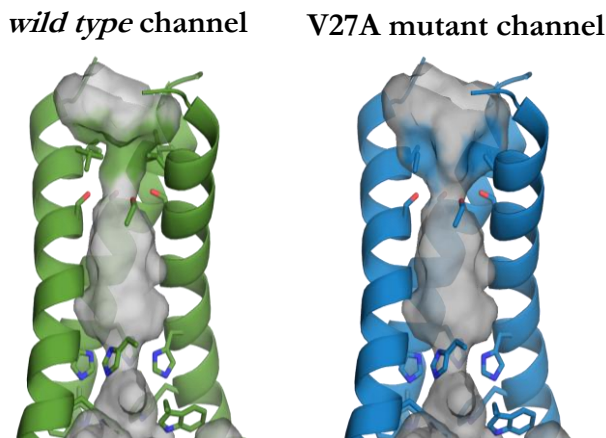


Figure 3. Schematic representation of the TM domain of the wild-type M2 channel vs its V27A mutant. Note the cavity expansion at the top in the V27A mutant M2 channel.

destroys the Amt binding site. In the case that Amt enters the channel, it will establish destabilizing interactions with the Asn31 methylcarboxamide side chain, oriented towards the pore in the S31N. Despite this will justify the resistance mechanism of S31N it needs to be mentioned that the full mechanism has not yet been elucidated and there are other hypotheses [19, 45-46].

7. Our M2 oriented research line

Since the introduction of Amt in clinics in 1966 [47], hundreds of analogues have been synthesized and evaluated. In 2011, we reviewed the earlier synthetic efforts carried out before the existence of the recent functional, structural and computational studies that have provided a solid basis for structure-based drug design [48]. More recently, in 2015, Wang *et al.* updated this topic, with focus on the rationally-designed inhibitors [49].

During the past years, our group has synthesized several polycyclic Amt analogues containing different scaffolds including ring-contracted, ring-rearranged and 2,2-dialkyl derivatives of Amt. Thanks to the growing knowledge of the M2 structure and function, the rational design of new inhibitors against the resistant strains is starting to bear fruit. In the following sections we will review our own work on M2 inhibitors, with focus on four generations of inhibitors (Figure 4).

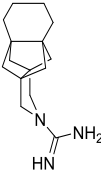
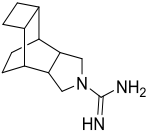
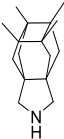
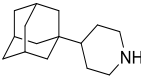
	Amantadine	1 st generation	2 nd generation	3 rd generation	4 th generation
					
IC ₅₀ (μM)					
wt	16	3.4	2.1	18	4.1
V27A	>100	0.3	22.6	0.7	3.6
L26F	>100	NT	NT	8.6	NT
S31N	>100	>100	>100	>100	>100
	Obsolete drug	Dual inhibitor Long synthesis	Dual inhibitor Short synthesis	Triple inhibitor New binding mode	Potency balance Insights in the mechanism of action

Figure 4. Summary of our M2 research line.

8. First Generation inhibitors

The first inhibitors prepared in our research group [50] stem from amine **1**, which was found to be an Influenza A compound in a wide pharmacological activity assay of Amt ring-contracted analogues prepared in the group [51]. In this early project, several ring expanded and ring contracted derivatives of Amt were synthesized and evaluated with the aim to explore the effect of modifying the inhibitor's size in the different M2 channels (at the time of unknown structure).

Resulting from this first work, several inhibitors against the *wt* channel of Influenza A virus were identified. Moreover it could be seen that the ring expanded analogues, featuring the 3-azahexacyclo[7.6.0.0^{1,5}.0^{5,12}.0^{6,10}.0^{11,15}] pentadecane scaffold (**5** and **6**) were able to show marginal inhibition values against the mutant V27A. More interesting was the ring contracted analogue **2**, which was able to mildly inhibit the three relevant channels of the virus [50].

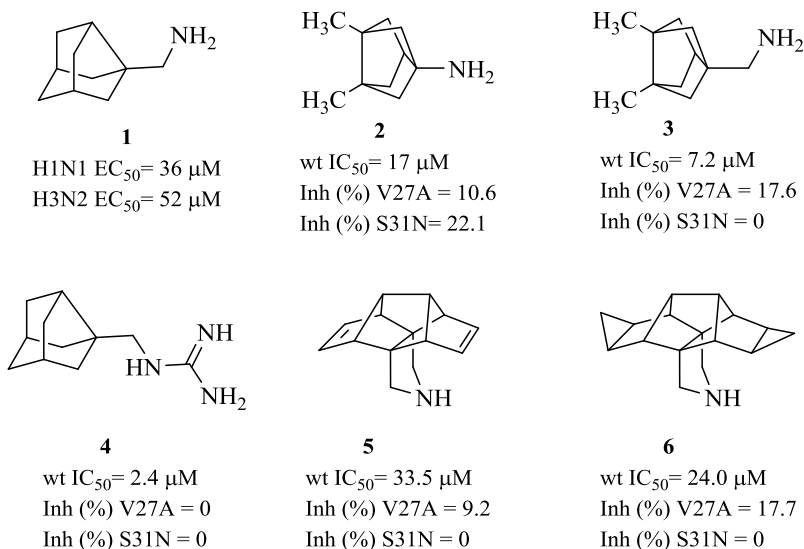


Figure 5. Ring contracted and ring expanded analogues prepared in a previous project. Antiviral EC₅₀ values are shown for **1**. For compounds **2-6**, IC₅₀ values are shown for *wt* M2 channel, while % of inhibition of the channel function by 100 μM of inhibitor for 2 min, are given for A/V27A and A/S31N mutant channels.

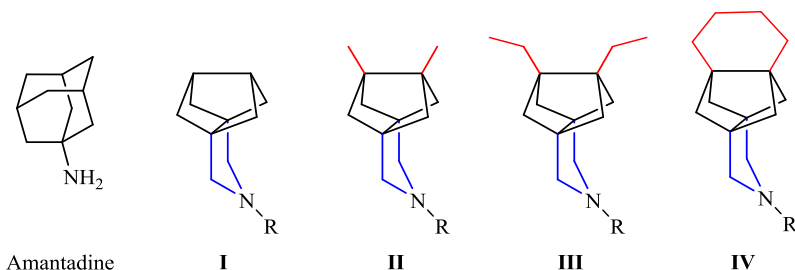


Figure 6. Analogues prepared in this project. From the bisnoradamantane scaffold (black), the length is increased in both directions with a pyrrolidine ring (blue) and with a variety of alkyl substituents (red), which confer greater length and bulkiness to the basic centre distal side.

These results promoted a further exploration of the ring contracted analogues of Amt [52]. With the aim to target the three main channels we envisaged a series of bisnoradamantane-like scaffolds, 3-azatetracyclo[5.2.1.1^{5,8}.0^{1,5}]undecanes, which were modified to be greater in length than Amt –feature that had been seen beneficial when targeting the wider V27A- but with a slight width reduction compared to this commercial drug –thought to be required to inhibit the narrower mutant S31N (Figure 6).

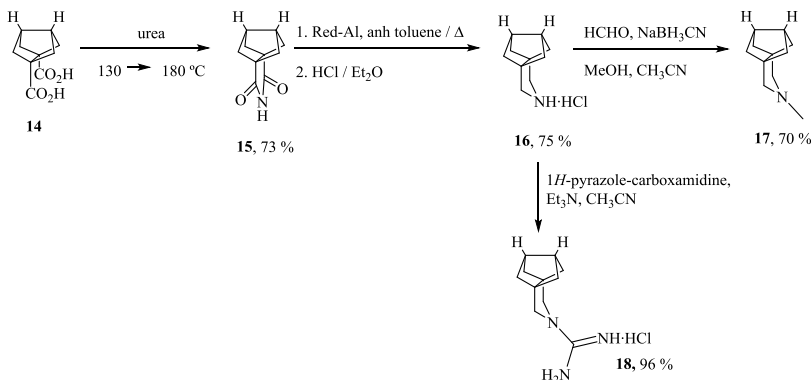
In addition, for this family of derivatives, the basic centre was introduced in a pyrrolidine scaffold. This modification had three main purposes: i) to increase the compound's length in the basic centre proximal site; ii) to confer a fixed orientation to this basic centre, and iii) to reduce the conformational freedom of the basic centre.

8.1. Synthetic route

We will exemplify the synthesis of compounds of general structure I-IV using the smaller analogues **16-18** (Scheme 2) [52]. To access dicarboxylic acid **14**, key precursor of the depicted compounds, a synthetic route previously described in the group was followed [53-54] (Scheme 1).

The synthesis started with a Weiss reaction [55-56], which implies the condensation of the α -dicarbonylic compound glyoxal with two equivalents of dimethyl 1,3-acetonedicarboxylate, in basic media. Interestingly this unique reaction consists in two aldol condensations, two dehydrations and two Michael reactions that afford the bicyclic adduct **7** in

A final hydrolysis in basic media furnished the desired bisnoradamantane diacid **14**, upon which we started the envisaged 3-step synthetic route towards our first 3-azatetracyclo[5.2.1.1^{5,8}.0^{1,5}]undecane product (Scheme 2).



Scheme 2. Route towards compounds **16**, **17** and **18**.

The reaction of **23** with urea at 180 °C furnished the imide **15**, which was reduced using Red-Al[®] to **16**. From this amine **16**, the guanidine derivative **18** and the tertiary amine **17** were easily synthesized using standard procedures.

Starting from a suitably substituted diketone analog of **8**, compounds featuring scaffolds **II-IV** were accessed in an analogous way [52].

8.2. Pharmacological evaluation

After pharmacological testing, this work showed that, starting from compounds active only against the *wt* A/M2 channel, it is possible to design compounds active against both the *wt* and the V27A mutant A/M2 channels. In fact, some of them inhibit both channels more effectively than Amt inhibits the *wt*. For example, while amine **16** and guanidine **18** were only active against the *wt* A/M2 channel (IC₅₀ = 11.7 and 1.05 μM, respectively), the corresponding analogues derived from series **IV** were endowed with dual inhibition of the *wt* (e.g., IC₅₀ = 3.4 μM for the guanidine), and the V27A mutant (e.g., IC₅₀ = 0.3 μM for the guanidine) A/M2 channels. Of note, the low micromolar antiviral activity of the three dual inhibitors identified, amine from series **IV** and guanidines from series

II and **IV**, was confirmed by an influenza virus yield assay [52]. Interestingly, *these were the first non-adamantane compounds endowed with this dual activity reported in the literature*, opening the way to the design of novel M2 inhibitors structurally based on non-adamantane scaffolds.

9. Second and third generation inhibitors

The endeavour described herein has its origins in our previous project (see above) in which we observed that the polycyclic amines, which were greater in length but featured a reduction in the polycyclic core width in respect to amantadine, were endowed with dual activity against the *wt* and the V27A mutant channels from Influenza A virus.

With the objective of further exploring this strategy and taking into account that:

- Several structures of the M2 *wt* channel were available at the time [19, 29,58], which allowed a tailoring of our compounds to the binding site.
- The structure of the V27A mutant had been disclosed, reporting wider diameters of the pore [59].
- Our hypothesis that, in order to target the V27A mutant, greater lengths might be required. Presumably this would allow the basic centre of our molecules to establish interactions with the Gly34 in the lower binding site of the channel, disrupting the deeper water clusters and blocking the pore [60].
- Coming from a resource consuming synthetic route of 12 steps, which included challenging reactions and the use of hazardous reagents to reach the first bioactive compound, this time we aimed for ready-access compounds, this is, the new bioactive polycycles should be prepared in few synthetic steps [61].

The following three polycyclic scaffolds: 4-azatetracyclo[5.3.2.0^{2,6}.0^{8,10}]dodecanes (**V**), 4-azatetracyclo[5.4.2.0^{2,6}.0^{8,11}]tridecane (**VI**) and 7,8,9,10-tetramethyl-3-azapentacyclo[7.2.1.1^{5,8}.0^{1,5}.0^{7,10}]tridecane (**VII**), were envisaged at the start of this work (Figure 7).

These structures were meeting the sought criteria, being greater in length than our previous family of compounds and the first bioactive compound of each series was accessible in only 2 synthetic steps in the case of **V** and **VI** or 5 steps in the case of **VII**. In addition, these scaffolds offered diverse chemically modifiable points, which allowed us to prepare a family of derivatives for each series.

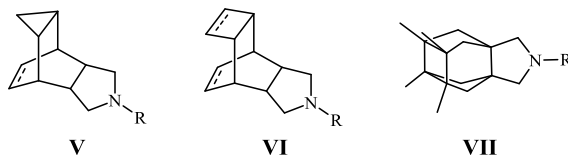
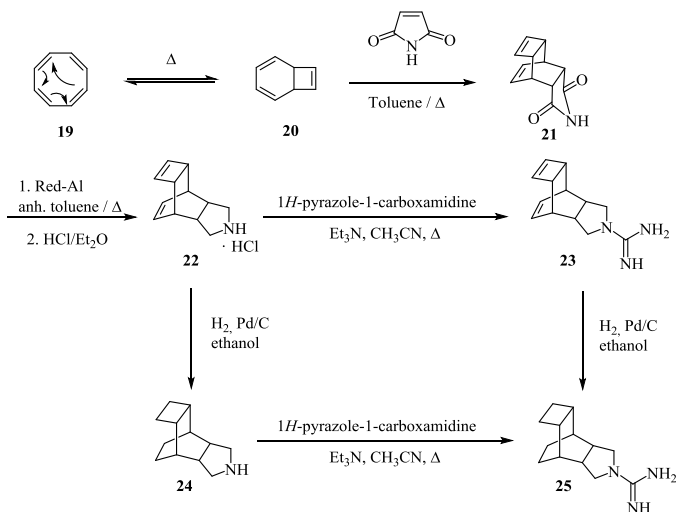


Figure 7. Designed polycycles with putative anti-influenza A activity.

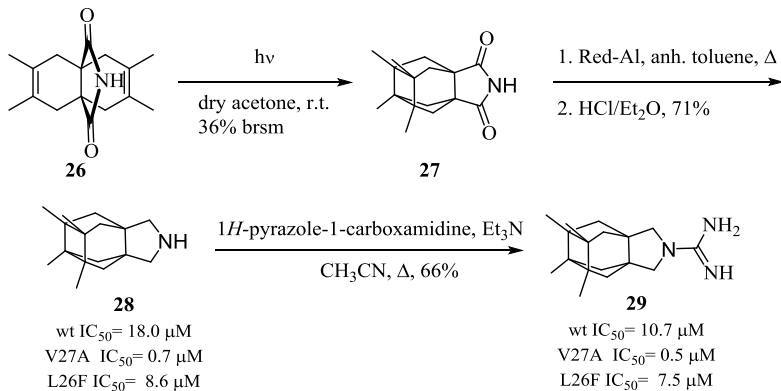
9.1. Synthetic route

The **V** and **VI** families were synthesized in parallel [61]. The synthesis started with the reaction of maleimide with either cycloheptatriene (for the preparation of **V**) or cyclooctatetraene (for the preparation of **VI**) in a heated sealed tube. Interestingly, in this reaction –previously reported by Abou-Gharbia and co-workers [62], the cyclooctatetraene, **19**, under high temperatures, isomerizes to its valence isomer bicyclo[4.2.0]octa-2,4,7-triene, **20**, by means of a thermal $6e^-$ electrocyclic pericyclic reaction [63-65]. This *in situ* formed specie is the diene that reacts with the dienophile maleimide in the subsequent Diels-Alder reaction, yielding the tetracyclic *endo*-adduct **21**.



Scheme 3. Synthetic route to 4-azatetracyclo[5.4.2.0^{2,6}.0^{8,11}]tridecane derivatives with antiviral activity. The ring-contracted analogues derived from **V** were synthesized using the same synthetic route but starting from cycloheptatriene [61].

A double reduction of the imide **21** carbonyl groups using Red-Al[®], lead to the first bioactive product, the pyrrolidine **22**. From this key intermediate **22** the desired saturated derivative, **24**, and their corresponding guanidines, **23** and **25**, were easily accessed through an hydrogenation with Pd/C as catalyst and a reaction with 1*H*-pyrazole-1-carboxamide, respectively.



Scheme 4. Synthesis of the third generation: **28** and **29**, triple inhibitors of the wt, V27A and L26F mutant channels of influenza A [61].

We were aiming to improve our previous results and, for this, in our third generation we designed a structurally unrelated scaffold which was wider and longer in respect to amantadine's structure. Following this idea the family **VII** was prepared. Starting from the known imide **26**, this molecule gave access to the new pentacyclic core in only one step, which involved a [2+2] photocycloaddition under UV light. Even the 36% yield of this step was relatively low, the rapid access to the desired **VII** scaffold shift the balance positively towards this synthetic strategy. Upon isolation of imide **26**, the usual synthetic path yielded amine **28** and guanidine **29**.

9.2. Pharmacological evaluation

The inhibitory activity of the compounds was tested on A/M2 channels expressed in *Xenopus* oocytes using the two-electrode voltage clamp (TEVC) technique. Regarding the second-generation compounds (scaffolds

V and **VI** in Figure 7), the four derivatives of scaffold **VI** (amines **22** and **24** and guanidines **23** and **25**) and their corresponding analogues derived from scaffold **V** were low micromolar inhibitors of the *wt* channel (e.g., $IC_{50} = 16.0$ and $1.2 \mu\text{M}$ for Amt and **24**, respectively). Regarding the activity against the V27A M2 mutant channel, three trends were found, i.e., guanidine performed better than its corresponding amine, the fully saturated compounds were more potent than their corresponding unsaturated analogues, and the derivatives of **V** were less potent than the ring-expanded derivatives of **VI**. Not unexpectedly, the larger compound from this series, guanidine **25**, was the more promising compound, being more potent than Amt against the *wt* M2 channel ($IC_{50} = 2.1 \mu\text{M}$) and endowed with fair activity against the V27A mutant channel ($IC_{50} = 22.6 \mu\text{M}$). Overall, this second generation compounds led to dual inhibitors in very short synthetic routes [61].

The next challenge, to be able to target more mutant channels while keeping very short synthetic sequences, was achieved with the third generation of inhibitors (scaffold **VII**, Figure 7 and Scheme 4). Strikingly, we could report, for the first time in the literature, potent triple inhibitors lacking the adamantane scaffold. Thus, our new compounds **28** and **29** were able to potently inhibit at once three different M2 channels: the *wt* and the mutants V27A and L26F. On the top of that, **28** and **29** were equipotent to amantadine for the *wt* and clear superior inhibitors of the V27A and the L26F mutant.

In addition, this unforeseen activity prompted an in-depth study of **28** binding mode by Prof. F. J. Luque and co-workers. Through molecular dynamics simulations, a clear difference between the binding of this amine **28** in the *wt* or in the V27A mutant channel could be spotted. Meanwhile in the *wt* the binding occurred with the basic group pointing towards the viral interior –the so called *down* binding mode- paralleling the one that Amt displays; in the case of the V27A this compound is found in equilibria between the *down binding mode* and the *up binding mode* – where the basic moiety points towards the viral exterior. The key feature for this compound to be stabilized in the *up binding mode*, preventing its rapid release to the cytoplasm, was found to be the four methyl substituents placed in the upper part of the molecule [61].

The presented families show the feasibility of designing easily accessible compounds able to successfully inhibit the *wt* and the V27A and L26F variants of the A/M2 channels of influenza A virus. In fact, some of the newly designed compounds inhibit the three channels similarly or even

more effectively than Amt inhibits the *wt* proton channel. In particular, amine **28** and guanidine **29** emerged as promising compounds, being low micromolar inhibitors against the *wt* channel and the L26F mutant, while being endowed with submicromolar IC_{50} against the V27A variant. Furthermore, compound **28** showed strong activity against the A/PR/8/34 strain, an A/H1N1 virus with two mutations (S31N and V27T) in the M2 protein. However, taking into account that this compound was devoid of activity against the S31N M2 mutant channel, this activity must be related with an alternative mechanism of action, as we and others have comprehensively discussed [66-67]. Overall, these results suggest that compounds **28** and **29** are suitable templates to explore novel candidates against influenza virus.

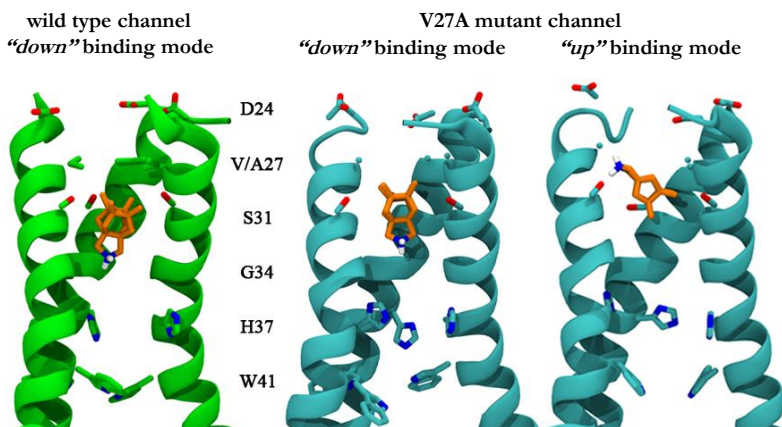


Figure 8. Amine **28** bound to the *wt* ("down" bonding mode) and the V27A mutant channels ("down" and "up" binding modes). For clarity, only 3 chains are shown.

10. Fourth generation inhibitors

Regardless our previous efforts in the anti-influenza research line had been mainly oriented to replace the adamantane scaffold by a more suitable polycycle [50,52,61], the disclosure of several M2 channel structures with bound amantadine [19,58,68] or adamantane containing compounds [69], provided new detailed insights of the binding mode of adamantane-like molecules. Hence, we decided to take advantage of this recent knowledge to, building up on our expertise, design adamantane related compounds with improved features to display an upgraded inhibition profile.

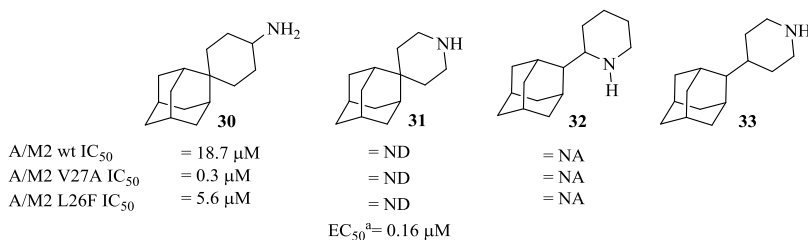


Figure 9. Anti-influenza adamantyl compounds: spiro compound **30**, piperidines **31** and **32** and the novel envisaged analogue **33**. ^aEC₅₀ determined in the influenza A/HongKong/7/87/H3N2 strain, which carries a *wt* channel.

In line with this, DeGrado's group disclosed in 2011 the spiro compound **30**, which shows an outstanding activity against the V27A, the L26F mutant and the *wt* M2 channels [70]. Worthy of note, Kolocouris *et al.* had previously reported the synthesis of **32**, an adamantyl piperidine related to **30** [71], which failed to show activity against an Influenza strain carrying an Amt-resistant S31N mutant M2 channel (A/X31, H3N2), and its isomeric piperidine **31** [72-73] that was found to be active against a strain containing a *wt* M2 channel (A/HongKong/7/87/H3N2). They also showed that the lowest energy conformation of **32**, resulted in a geometry quite different that the one shown by the amines **30** and **31**. These facts made us question the importance of the basic centre position in the molecule; hence, in our new designs we orientated this polar group towards the terminal histidines and perpendicular to the protein backbone, analogously to **30** (Figure 9).

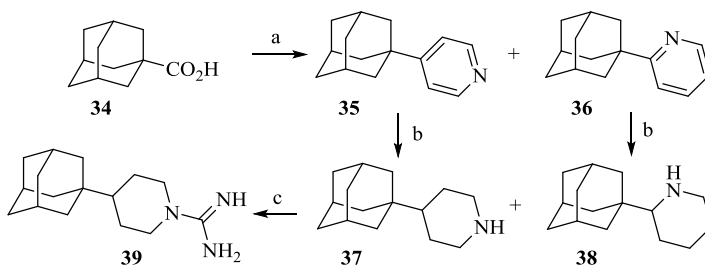
To further address the basic centre orientation remark, besides modifying the position of the nitrogen atom in the piperidine ring, we decided to investigate which was the most suitable anchoring point for this ring, in the adamantane scaffold. For this we prepared two series of adamantyl piperidine analogues bearing the heterocycle in the adamantane C1 (as in amantadine) or C2 (as in the triple inhibitor **30**) positions [74]. Our designs were first studied *in silico* by Luque's group. Their theoretical calculations indicated that our compounds were very similar to **30**, so their increased length with respect to Amt could provide an improvement of the inhibitory activity.

In light of those predictions we decided to prepare an extra series of C-2 analogues featuring a methylene group between the lipophilic core and the ring, displaying even longer scaffolds.

10.1. Synthesis

First we undertook the synthesis of the C-1 series. Paralleling the work of Togo and coworkers [75], the isomeric mixture of the pyridine derivatives **44** and **45** was readily obtained after the radical decarboxylation of the carboxylic acid **43** in the presence of pyridine. In this reaction the first step is the acid-base exchange between the 1-adamantane carboxylic acid and the pyridine. Next, the [bis(trifluoroacetoxy)iodo]benzene reacts with the *in situ* generated adamantane carboxylate, displacing the trifluoroacetate moieties, to give [bis(1-adamantanecarboxyl)iodo]benzene. This species undergoes a radical decarboxylation to generate an adamantyl radical, which adds to the pyridinium cation that finally, rearomatizes to yield the desired addition products **35** and **36**.

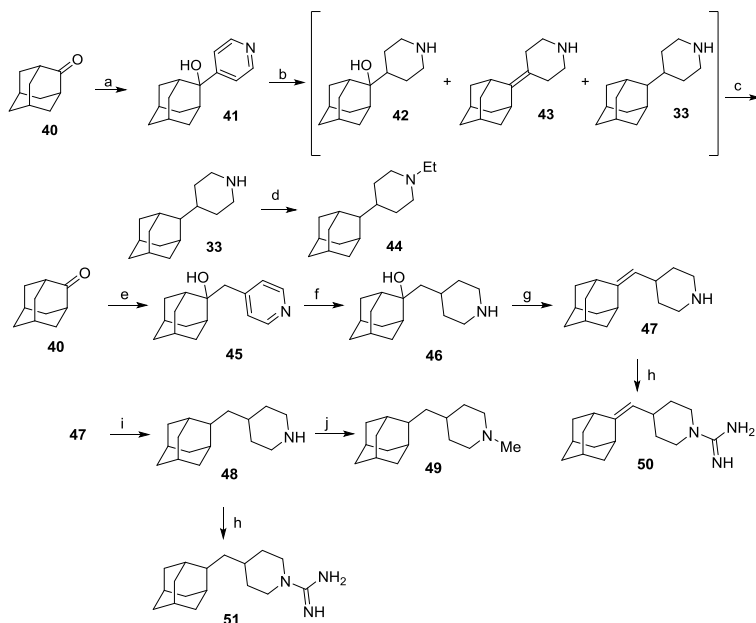
After a simple chromatography separation of both isomers, a catalytic hydrogenation with platinum oxide (IV) as catalyst, yielded the desired piperidines **37** and **38**. The usual guanidine derivative was built up for **37**, in a 76% yield. Despite our several attempts, the analogous reaction over the piperidine **38** was repeatedly unsuccessful, presumably reflecting the greater steric congestion around this nitrogen atom (Scheme 5).



Scheme 5. Synthesis of 4-(1-adamantyl)piperidines. ^aReagents and conditions: a: pyridine, [bis(trifluoroacetoxy)iodo]benzene, anh. benzene, reflux, overnight, **35**, 9%; **36**, 27%; b: H₂, PtO₂, MeOH, 30 atm, 97% yield for **37**; 99% yield for **38**; c: 1*H*-pyrazole-1-carboxamide hydrochloride, anh. Et₃N, acetonitrile, reflux, 6 h, 76% yield.

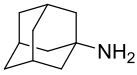
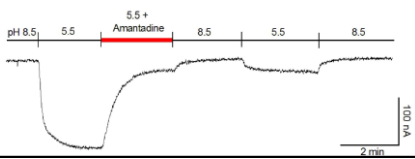
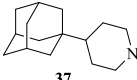
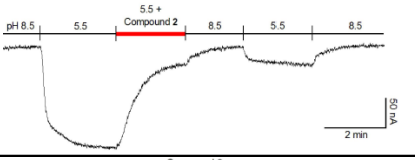
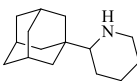
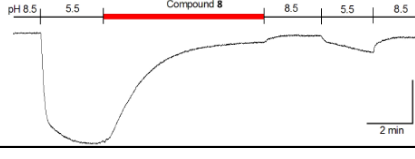
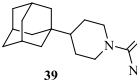
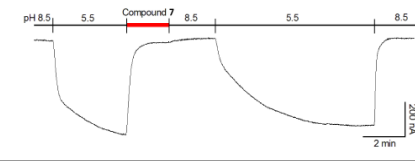
After this, the compounds belonging to the C-2 series were prepared (Scheme 6). The preparation of both series was envisaged through the same synthetic sequence starting with the addition to 2-adamantanone of the corresponding *in situ* generated organolithium reagent, 4-pyridyl lithium or 4-picolinyl lithium, respectively. The formed adamantyl pyridine species

was then hydrogenated using platinum oxide as catalyst, to give the first bioactive compound (**33** and **46**). The tertiary alcohol group of **46** was eliminated to yield olefin **47** that was further hydrogenated using 10% palladium over active charcoal as catalyst to give the saturated analogue **48**. The saturated compounds, **33** and **48** were converted to tertiary amines through a reductive alkylation reaction with acetaldehyde or formaldehyde, to furnish **44** and **49**, respectively. Finally, amines **47** and **48** reacted with 1*H*-pyrazole-1-carboxamide hydrochloride furnishing the guanidine derivatives **50** and **51**, respectively [74].



Scheme 6. Synthetic route for the preparation of the adamantyl piperidine C-2 series. Reagents and conditions: **a**: 4-pyridyl lithium; Et₂O/THF, -65 °C to rt, 70% yield; **b**: 1 atm H₂, PtO₂, ethanol, rt, 24 h, 93% yield of a mixture of **42**, **43** and **33**; **c**: 1) SOCl₂, pyridine, anh. CH₂Cl₂, -60 °C, 30 min, 2) 1 atm H₂, Pd/C, methanol, HCl, rt, 2 h, 63% overall yield; **d**: acetaldehyde, NaCNBH₃, AcOH, methanol, rt, 24 h, 76% yield; **e**: 4-picolone, anh THF, *n*-BuLi, 2 h, rt, 90% yield; **f**: 1 atm H₂, PtO₂, HCl, methanol, 5 days, > 99% yield; **g**: SOCl₂, pyridine, anh. CH₂Cl₂, -60 °C, 30 min, > 99% yield; **h**: 1*H*-pyrazole-1-carboxamide hydrochloride, anh Et₃N, acetonitrile, 70 °C, 6 h, 88% yield for **50**, 64% yield for **51**; **i**: 1 atm H₂, Pd/C, methanol, HCl, rt, 2 h, 68% yield; **j**: formaldehyde (37% aqueous solution), NaCNBH₃, AcOH, rt, 18 h, 73% yield.

Table 1. Pharmacological assays in M2/*wt* wrap up. ^aIsochronic (2 min) values for IC₅₀ are given. ^bTEVC technique in *Xenopus* oocytes. ^cEC₅₀ based on 72-h compound exposure time.

Influenza A <i>wt</i>	IC ₅₀ μM ^a	Kinetics ^b	EC ₅₀ μM ^c
 Amt	16.0		0.2 
 37	4.1		0.2 
 38	ND		0.8 
 39	1.9		>50

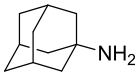
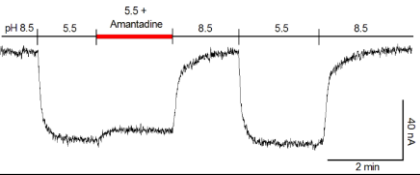
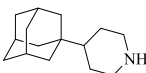
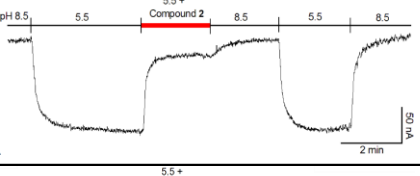
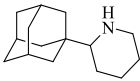
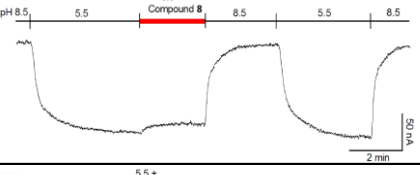
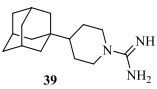
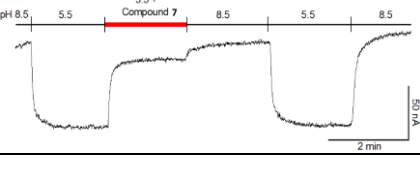
10.2. Pharmacological evaluation

As in previous series, the antiviral activities and the channel blocking abilities of the new compounds were measured; this time, however, further TEVC assays, to assess the kinetics of the M2 channel inhibitors were carried out (Table 1 and Table 2) [74]. From these results a lack of correlation was observed between those coming from the isochronic inhibition assays, in which several compounds displayed potent M2 blockade (both on the *wt* and the V27A M2 mutant channel), and the antiviral activity assays, in which a reduced number of our molecules were identified as antivirals. Steaming from these observations we could

experimentally prove the V27A resistance mechanism previously proposed *in silico* and through NMR studies.

In table 1 it can be seen that only the compounds with slow K_{off} (as Amt, **37** and **38**) display antiviral activity, regardless their channel blocking ability. The importance of slowly leaving the channel before the rate of binding to it, can be seen when comparing **39**, which displays M2 blockade at 2 min but not antiviral activity, and **38**, that does not block the channel upon short exposure, due to a slow K_{on} , but displays antiviral activity (because of slow K_{off}).

Table 2. Pharmacological assays in M2/V27A wrap up. ^aIsochronic (2 min) values for IC_{50} are given. ^bTEVC technique in *Xenopus* oocytes. ^c EC_{50} based on 72-h compound exposure time. NA = Not active. ND = EC_{50} not determined.

Influenza A V27A	IC_{50} μM^a	Kinetics ^b	EC_{50} μM^c
 Amt	> 500		NA 
 37	3.6		ND 
 38	> 500		NA 
 39	16.2		NA 

The main evidence for the mechanism of resistance of the V27A mutant M2 channel is the behaviour of amine **37**. This compound is able to block both the *wt* ($IC_{50} = 4.1 \mu\text{M}$) and the V27A mutant ($IC_{50} = 3.6 \mu\text{M}$) M2 channels in the typical TEVC experiments (2 min). However, for the V27A mutant, the block is only maintained for a short time, because weak binding affinity facilitates dissociation during washing with drug-free pH 8.5 buffer, after which the blocker is released from the channel that becomes functional again. This fact explains why **37** is active as antiviral against a strain carrying the *wt* channel but lacks activity against a strain carrying the V27A mutant M2 channel (compare Table 1 and 2) [74]. Our new experimental evidence for V27A drug resistance reinforces the previous computational [76-80] and structural [59] hypothesis and may lead to a more profound comprehension on how Influenza A virus acquires resistance, to eventually shed light to drug design.

11. Conclusion

Overall our research has allowed to move from Amt, inactive against the three main mutants, to potent dual inhibitors with a complex synthesis (first generation) which was later on simplified reaching potent dual inhibitors in only two synthetic steps (second generation). Following the most potent triple inhibitor at the time, was accessed in few synthetic steps and featuring an unforeseen polycyclic scaffold (third generation). Finally with the fourth generation the *in silico* predicted drug resistance mechanism of the V27A mutant channel, could be demonstrated.

We hope that all these findings, along with the recent paramount advances on the understanding of the proton conductance mechanisms [81-85] and mutant M2 channels structure [86-87] will bring the antiinfluenza A drug research closer to the discovery of a suitable drug to fight the virus [88-93].

Finally is worth mentioning the combined antiviral therapy has raised great interest as a strategy to fight the influenza virus [94-95]. Similar to the antiretroviral therapy, this will consist in the administration of a drug cocktail that will target different steps of the viral cycle. We believe that the drugs targeting the viral protein HA will be excellent allies to the M2 blockers for this purpose [96].

Acknowledgements

The authors are grateful to all the colleagues that have contributed to this research endeavor. Our experimental work on new anti-influenza compounds has been supported by Project Grants (CTQ2008-03768, CTQ2011-22433 and SAF2014-57094-R) from the Spanish *Ministerio de Ciencia e Innovación* and *Ministerio de Economía y Competitividad*.

References

1. Ghedin, E., Sengamalay, N. A., Shumway, M., Zaborsky, J., Feldblyum, T., Subbu, V., Spiro, D. J., Sitz, J., Koo, H., Bolotov, P., Dernovoy, D., Tatusova, T., Bao, Y., St George, K., Taylor, J., Lipman, D. J., Fraser, C. M., Taubenberger, J. K., Salzberg, S. L. Large-scale sequencing of human influenza reveals the dynamic nature of viral genome evolution. 2005, *Nature*, 437, 1162.
2. WHO. Bull. A revision of the system of nomenclature for influenza viruses: a WHO Memorandum. 1980, *World Health Organ.*, 58, 585.
3. Centers for Disease Control and Prevention: <http://www.cdc.gov/flu/about/viruses/change.htm> (10 Jun 2017).
4. Bouvier, N. M., Palese, P. The biology of influenza viruses. 2008, *Vaccine*, 26, D49.
5. Skehel, J. J., Wiley, D. C. Receptor binding and membrane fusion in virus entry: the influenza hemagglutinin. 2000, *Annu. Rev. Biochem.*, 69, 531.
6. de Vries, E., Tscherne, D. M., Wienholts, M. J., Cobos-Jiménez, V., Scholte, F., García Sastre, A., Rottier, P. J. M., de Haan, C. A. M. Dissection of the influenza A virus endocytic routes reveals macropinocytosis as an alternative entry pathway. 2011, *PLoS Pathog.*, 7, e1001329.
7. Lin, X., Noel, J. K., Wang, Q., Ma, J., Onuchic, J. N. Lowered pH Leads to Fusion Peptide Release and a Highly Dynamic Intermediate of Influenza Hemagglutinin. 2016, *J. Phys. Chem. B.*, 5, 6775.
8. Carr, C. M., Kim, P. S. A spring-loaded mechanism for the conformational change of influenza hemagglutinin. 1993, *Cell*, 73, 823.
9. Samji, T. Influenza A: Understanding the viral life cycle. 2009, *Yale J. Biol. Med.*, 82, 153.
10. Krug, R. M. Functions of the influenza A virus NS1 protein in antiviral defense. 2015, *Curr. Opin. Virol.* 12, 1.
11. Takeuchi, K., Lamb, R. A. Influenza virus M2 protein ion channel activity stabilizes the native form of fowl plague virus hemagglutinin during intracellular transport. 1994, *J. Virol.*, 68, 911.
12. Schmidt, N. W., Mishra, A., Wang, J., DeGrado, W.F., Wong, G. C. Influenza virus A M2 protein generates negative Gaussian membrane curvature necessary for budding and scission. 2013, *J. Am. Chem. Soc.*, 135, 13710.

13. Palese, P., Tobita, K., Ueda, M., Compans, R. W. Characterization of temperature sensitive influenza virus mutants defective in neuraminidase. 1974, *Virology*, 61, 397.
14. Das, K., Aramini, J.M., Ma, L., Krug, R. M., Arnold, E. Structures of influenza A proteins and insights into antiviral drug targets. 2010, *Nat. Str. Mol. Bio.*, 17, 530.
15. Wang, J., Qiu, J. X., Soto, C., DeGrado, W. F. Structural and dynamic mechanisms for the function and inhibition of the M2 proton channel from influenza A virus. 2011, *Curr. Opin. Struct. Biol.*, 21, 68.
16. Wang, J., Kim, S., Kovacs, F., Cross, T. A. Structure of the transmembrane region of the M2 protein H(+) channel. 2001, *Protein Sci.*, 10, 2241.
17. Martin, K., Helenius, A. Nuclear transport of influenza virus ribonucleoproteins: The viral matrix protein (M1) promotes export and inhibits import. 1991, *Cell*, 67, 117.
18. Schnell, J. R., Chou, J. J. Structure and mechanism of the M2 proton channel of influenza A virus. 2008, *Nature*, 451, 591.
19. Stouffer, A. L., Acharya, R., Salom, D., Levine, A. S., Di Costanzo, L., Soto, C. S., Tereshko, V., Nanda, V., Stayrook, S., DeGrado, W. F. Structural basis for the function and inhibition of an influenza virus proton channel. 2008, *Nature*, 451, 596.
20. Kawano, K., Yano, Y., Matsuzaki, K. A dimer is the minimal proton-conducting unit of the influenza a virus M2 channel. 2014, *J. Molec. Bio.*, 426, 2679.
21. Andreas, L. B., Reese, M., Eddy, M. T., Gelev, V., Ni, Q. Z., Miller, E. A., Emsley, L., Pintacuda, G., Chou, J., Griffin, R. G. Structure and Mechanism of the Influenza A M218-60 Dimer of Dimers. 2015, *J. Am. Chem. Soc.*, 137, 14877.
22. Helenius, A. Unpacking the incoming influenza virus. 1992, *Cell*, 69, 577.
23. Sakaguchi, T., Leser, G. P., Lamb, R. A. The ion channel activity of the influenza virus M2 protein affects transport through the Golgi apparatus. 1996, *J. Cell. Biol.*, 133, 733.
24. Hu, F., Schmidt-Rohr, K., Hong, M. NMR Detection of pH-Dependent Histidine–Water Proton Exchange Reveals the Conduction Mechanism of a Transmembrane Proton Channel. 2012, *J. Am. Chem. Soc.*, 134, 3703.
25. Hu, J., Fu, R., Nishimura, K., Zhang, L., Zhou, H. X., Busath, D. D., Vijayvergiya, V., Cross, T. A. Histidines, heart of the hydrogen ion channel from influenza A virus: toward an understanding of conductance and proton selectivity. 2006, *Proc. Natl. Acad. Sci. USA*, 103, 6865.
26. Tang, Y., Zaitseva, F., Lamb, R. A., Pinto, L. H. The gate of the influenza virus M2 proton channel is formed by a single tryptophan residue. 2002, *J. Biol. Chem.*, 277, 39880.
27. Decoursey, T. E. Voltage-gated proton channels and other proton transfer pathways. 2003, *Physiol. Rev.*, 83, 475.
28. Ma, C., Polishchuk, A. L., Ohigashi, Y., Stouffer, A. L., Schon, A., Magavern, E., Jing, X., Lear, J.D., Freire, E., DeGrado, W. F., Lamb, R. A. Identification of the

- functional core of the influenza A virus A/M2 proton-selective ion channel. 2009, *Proc. Natl. Acad. Sci. USA*, 106, 12283.
29. Acharya, R., Carnevale, V., Fiorin, G., Levine, B. G., Polishchuk, A. L., Balannik, V., Samish, I., Lamb, R. A., Pinto, L. H., DeGrado, W. F., Klein, M. L. Structure and mechanism of proton transport through the transmembrane tetrameric M2 protein bundle of the influenza A virus. 2010, *Proc. Natl. Acad. Sci. USA*, 107, 15075.
 30. Phongphanphanee, S., Rungrotmongkol, T., Yoshida, N. Proton Transport through the Influenza A M2 Channel: Three-Dimensional Reference Interaction Site Model Study. 2010, *J. Am. Chem. Soc.*, 9, 9782–9788
 31. Ivanovic, T., Rozendaal, R., Floyd, D. L., Popovic, M., Van Oijen, A. M., Harrison, S. C. Kinetics of Proton Transport into Influenza Virions by the Viral M2 Channel. 2012, *PLoS One*, 7, e31566, 1-9.
 32. Okada, A., Miura, T., Takeuchi, H. Protonation of histidine and histidine-tryptophan interaction in the activation of the M2 ion channel from influenza A virus. 2001, *Biochemistry*, 40, 6053-60.
 33. Carnevale, V., Fiorin, G., Levine, B. G., DeGrado, W. F., Klein, M. L. Multiple Proton Confinement in the M2 Channel from the Influenza A Virus. 2010, *J. Phys. Chem. C*, 114, 20856.
 34. <http://www.who.int/mediacentre/factsheets/fs211/en/> (26 May 2017).
 35. Molinari, N. A. M., Ortega-Sanchez, I. R., Messonnier, M. L., Thompson, W. W., Wortley, P. M., Weintraub, E., Bridges, C. B. The annual impact of seasonal influenza in the US: measuring disease burden and costs. 2007, *Vaccine*, 25, 5086.
 36. Taubenberger, J. K., Morens, D.M. 1918 Influenza: the Mother of All Pandemics. Centers for Disease Control and Prevention. 2006.
 37. Kozakov, D., Chuang, G., Beglov, D., Vajda, S. Where does amantadine bind to the influenza virus M2 proton channel? 2010, *Trends Biochem. Sci.*, 35, 471.
 38. Cady, S. D., Wang, J., Wu, Y., DeGrado, W. F., Hong, M. Specific Binding of Adamantane Drugs and Direction of Their Polar Amines in the Pore of the Influenza M2 Transmembrane Domain in Lipid Bilayers and Dodecylphosphocholine Micelles Determined by NMR Spectroscopy. 2011, *J. Am. Chem. Soc.*, 2, 4274.
 39. Khurana, E., Devane, R. H., Dal Peraro, M., Klein, M. L. Computational study of drug binding to the membrane-bound tetrameric M2 peptide bundle from influenza A virus. 2011, *Biochim. Biophys. Acta.*, 1808, 530.
 40. Hubsher, G., Haider, M., Okun, M. S. Amantadine: the journey from fighting flu to treating Parkinson disease. 2012, *Neurology*, 78, 1096.
 41. Leonov, H., Astrahan, P., Krugliak, M., Arkin, I. T. How Do Aminoadamantanes Block the Influenza M2 Channel, and How Does Resistance Develop? 2011, *J. Am. Chem. Soc.*, 133, 9903.
 42. Furuse, Y., Suzuki, A., Kamigaki, T., Oshitani, H. Evolution of the M gene of the influenza A virus in different host species: large-scale sequence analysis. 2009, *J. Virol.*, 6, 67.

43. Furuse, Y., Suzuki, A., Oshitani, H. Large-scale sequence analysis of M gene of influenza A viruses from different species: Mechanisms for emergence and spread of amantadine resistance. 2009, *Antimicrob. Agents Chemother.*, 53, 4457.
44. Dong, G., Peng, C., Luo, J., Wang, C., Han, L., Wu, B., Ji, G., He, H. Adamantane-resistant influenza A viruses in the world (1902-2013): frequency and distribution of M2 gene mutations. 2015, *PLoS One.*, 10, e0119115.
45. Pielak, R. M., Oxenoid, K., Chou, J. J. Structural investigation of rimantadine inhibition of the AM2-BM2 chimera channel of influenza viruses. 2011, *Structure*, 19, 1655.
46. Can, T. V., Sharma, M., Hung, I., Gor'kov, P. L., Brey, W. W., Cross, T. A. Magic Angle Spinning and Oriented Sample Solid-State NMR Structural Restraints Combine for Influenza A M2 Protein Functional Insights. 2012, *J. Am. Chem. Soc.*, 134, 9022.
47. Hay, A. J., Wolstenholme, A. J., Skehel, J. J., Smith, M. H. 1985, *EMBO J.*, 4, 3021.
48. Duque, M. D.; Valverde, E.; Barniol, M.; Guardiola, S.; Rey, M.; Vázquez, S. Inhibitors of the M2 channel of the influenza A virus. In *Recent Advances in Pharmaceutical Sciences*; Muñoz-Torrero, D., Ed.; Transworld Research Network: Kerala, India, 2011; pp 35–64.
49. Wang, J.; Li, F.; Ma, C. Recent progress in designing inhibitors that target the drug resistant M2 proton channels from the influenza A viruses. 2015, *Biopolymers*, 104, 91.
50. Duque, M. D., Ma, C., Torres, E., Wang, J., Naesens, L., Juárez-Jiménez, J., Camps, P., Luque, F. J., DeGrado, W. F., Lamb, R. A., Pinto, L. H., Vázquez, S. Exploring the size limit of templates for inhibitors of the M2 ion channel of influenza A virus. 2011, *J. Med. Chem.*, 54, 2646.
51. Camps, P., Duque, M. D., Vázquez, S., Naesens, L., Clercq, E. De, Sureda, F. X., López-Querol, M., Camins, A., Pallàs, M., Prathalingam, S. R., Kelly, J. M., Romero, V., Ivorra, M. D., Cortés, D. Synthesis and pharmacological evaluation of several ring-contracted amantadine analogs. 2008, *Bioorg. Med. Chem.*, 16, 9925.
52. Rey-Carrizo, M., Torres, E., Ma, C., Barniol-Xicota, M., Wang, J., Wu, Y., Naesens, L., DeGrado, W.F., Lamb, R. A., Pinto, L. H., S. Vázquez. 3-Azatetracyclo [5.2.1.1^{5,8}.0^{1,5}]undecane derivatives: from wild-type inhibitors of the M2 ion channel of influenza A virus to derivatives with potent activity against the V27A mutant. 2013, *J. Med. Chem.*, 56, 9265.
53. Camps, P., Iglesias, C., Rodríguez, M. J., Grancha, M. D., Gregori, M. E., Lozano, R., Miranda, M. A., Figueredo, M., Linares, A. A short synthesis of dimethyl tricyclo[3.3.0.0^{3,7}]octane-1,5-dicarboxylate and its 3,7-dimethyl derivative. A new route to the tricyclo[3.3.0.0^{3,7}]octane skeleton. 1988, *Chem. Ber.*, 121, 647.
54. Camps, P., Font-Bardia, M., Pérez, F., Solans, X., Vázquez, S. Synthesis, Chemical Trapping, and Dimerization of 3,7-Dimethyltricyclo[3.3.0.0^{3,7}]oct-

- 1(5)-ene: [2+2] Retrocycloaddition of the Cyclobutane Dimer. 1995, *Angew. Chem., Int. Ed. Engl.*, 34, 912.
55. Fu, X., Cook, J. M. 1992, *Aldrichimica Acta.*, 25, 43.
 56. Gupta, A. K., Fu, X., Snyder, J. P., Cook, J. M. General approach for the synthesis of polyquinenes via the Weiss reaction. 1991, *Tetrahedron*, 47, 3665.
 57. Bertz, S. H., Cook, J. M., Gawish, A., Weiss, U. *Org. Synth. Coll. Vol. VII*, Wiley: New York, 1990, 50.
 58. Cady, S. D., Schmidt-Rohr, K., Wang, J., Soto, C. S., DeGrado, W. F., Hong, M. Structure of the amantadine binding site of influenza M2 proton channels in lipid bilayers. 2010, *Nature*, 463, 689.
 59. Pielak, R. M., Chou, J. J. Solution NMR structure of the V27A drug resistant mutant of influenza A M2 channel. 2010, *Biochem. Biophys. Res. Commun.*, 401, 58.
 60. Hong, M., DeGrado, W. F. Structural basis for proton conduction and inhibition by the influenza M2 protein. 2012, *Protein Sci.*, 21, 1620.
 61. Rey-Carrizo, M., Barniol-Xicotá, M., Ma, C., Frigolé-Vivas, M., Torres, E., Naesens, L., Llabrés, S., Juárez-Jiménez, J., Luque, F. J., DeGrado, W. F., Lamb, R. A., Pinto, L. H., Vázquez, S. Easily accessible polycyclic amines that inhibit the wild-type and amantadine-resistant mutants of the M2 channel of influenza A virus. 2014, *J Med Chem.*, 57, 5738.
 62. Abou-Gharbia, M., Patel, U. R., Webb, M. B., Moyer, J. A., Andree, T. H., Muth, E. A. Polycyclic aryl- and heteroarylpiperazinyl imides as 5-HT_{1A} receptor ligands and potential anxiolytic agents: synthesis and structure-activity relationship studies. 1988, *J. Med. Chem.*, 31, 1382.
 63. Huisgen, R., Mietzsch, F. The Valence Tautomerism of Cyclooctatetraene. 1964, *Angew. Chem., Intl. Ed. Engl.*, 3, 83.
 64. Vogel, E., Kiefer, H., Roth, W. R. Bicyclo[4.2.0]octa-2,4,7-triene. 1964, *Angew. Chem., Intl. Ed. Engl.*, 3, 442.
 65. Huisgen, R., Konz, W. E., Gream, G. E. Evidence for different valence tautomers of bromocyclooctatetraene. 1970, *J. Am. Chem. Soc.*, 92, 4105.
 66. Torres, E., Duque, M. D., Vanderlinden, E., Ma, C., Pinto, L. H., Camps, P., Froeyen, M., Vázquez, S., Naesens, L. Role of the viral hemagglutinin in the anti-influenza virus activity of newly synthesized polycyclic amine compounds. 2013, *Antiviral Res.* 99, 281.
 67. Kolocouris, A., Tzitzoglaki, C., Johnson, F. B., Zell, R., Wright, A. K., Cross, T. A., Tietjen, I., Fedida, D., Busath, D. D. Aminoadamantanes with persistent in vitro efficacy against H1N1(2009) influenza A. 2014, *J. Med. Chem.*, 57, 4629.
 68. Cady, S. D., Mishanina, T. V., Hong, M. Structure of amantadine-bound M2 transmembrane peptide of influenza A in lipid bilayers from magic-angle-spinning solid-state NMR: the role of Ser31 in amantadine binding. 2009, *J. Mol. Biol.*, 385, 1127.
 69. Wu, Y., Canturk, B., Jo, H., Ma, C., Gianti, E., Klein, M. L., Pinto, L. H., Lamb, R. A., Fiorin, G., Wang, J., DeGrado, W. F. Flipping in the pore: discovery of dual inhibitors that bind in different orientations to the wild-type versus the

- amantadine-resistant S31N mutant of the influenza A virus M2 proton channel. 2014, *J. Am. Chem. Soc.*, 136, 17987.
70. Wang, J., Ma, C., Fiorin, G., Carnevale, V., Wang, T., Hu, F., Lamb, R. A., Pinto, L. H., Hong, M., Klein, M. L., DeGrado, W. F. Molecular dynamics simulation directed rational design of inhibitors targeting drug-resistant mutants of influenza A virus M2. 2011, *J. Am. Chem. Soc.*, 133, 12834.
 71. Kolocouris, A., Tataridis, D., Fytas, G., Mavromoustakos, T., Foscolos, G. B., Kolocouris, N., De Clercq, E. Synthesis of 2-(2-adamantyl)piperidines and structure anti-influenza virus A activity relationship study using a combination of NMR spectroscopy and molecular modeling. 1999, *Bioorg. Med. Chem. Lett.*, 9, 3465.
 72. Kolocouris, N., Zoidis, G., Foscolos, G. B., Fytas, G., Prathalingham, S. R., Kelly, J. M., Naesens, L., De Clercq, E. Design and synthesis of bioactive adamantane spiro heterocycles. 2007, *Bioorg. Med. Chem. Lett.*, 17, 4358.
 73. Kolocouris, A., Spearpoint, P., Martin, S. R., Hay, A. J., Lopez-Querol, M., Sureda, F. X., Padalko, E., Neyts, J., De Clercq, E. Comparisons of the influenza virus A M2 channel binding affinities, anti-influenza virus potencies and NMDA antagonistic activities of 2-alkyl-2-aminoadamantanes and analogues. 2008, *Bioorg. Med. Chem. Lett.*, 18, 6156.
 74. Barniol-Xicota, M., Gazzarrini, S., Torres, E., HU, Y., Wang, J., Naesens, L., Moroni, A., Vázquez, S. Slow but Steady Wins the Race: Dissimilarities among New Dual Inhibitors of the Wild-Type and the V27A Mutant M2 Channels of Influenza A Virus. 2017, *J. Med. Chem.* 60, 3727.
 75. Togo, H., Aoki, M., Kuramochi, M., Yokoyama, M. Radical decarboxylative alkylation onto heteroaromatic bases with trivalent iodine compounds. 1993, *J. Chem. Soc., Perkin Trans. 1*, 2417.
 76. Gu, R.-X., Liu, L. A., Wang, Y.-H., Xu, Q., Wei, D.-Q. Structural comparison of the wild-type and drug-resistant mutants of the influenza A M2 proton channel by molecular dynamics simulations. 2013, *J. Phys. Chem. B*, 117, 6042.
 77. Gu, R.-X., Liu, L. A., Wei, D.-Q. Structural and energetic analysis of drug inhibition of the influenza A M2 proton channel. 2013, *Trends Pharm. Sci.*, 34, 571.
 78. Gu, R.-X., Liu, L. A., Wei, D. Drug inhibition and proton conduction mechanisms of the influenza A M2 proton channel. 2015, *Adv. Exp. Med. Biol.*, 827, 205.
 79. Van Nguyen, H., Nguyen, H. T., Le, L. T. Investigation of the free energy profiles of amantadine and rimantadine in the AM2 binding pocket. 2016, *Eur. Biophys. J.*, 45, 63.
 80. Llabrés, S., Juárez-Jiménez, J., Masetti, M., Leiva, R., Vázquez, S., Gazzarrini, S., Moroni, A., Cavalli, A., Luque, F. J. Mechanism of the pseudoirreversible binding of amantadine to the M2 proton channel. 2016, *J. Am. Chem. Soc.*, 138, 15345.
 81. Liang, R., Swanson, J. M. J., Madsen, J. J., Hong, M., DeGrado, W. F., Voth, G. A. Acid activation mechanism of the influenza A M2 proton channel. 2016, *Proc. Natl. Acad. Sci. USA*, 113, E6955.

82. Fu, R., Miao, Y., Qin, H., Cross, T. A. Probing hydronium ion histidine NH exchange rate constants in the M2 channel via indirect observation of dipolar-dephased ^{15}N signals in magic-angle-spinning NMR. 2016, *J. Am. Chem. Soc.* 138, 15801.
83. Jeong, B.-S., Dyer, R. B. Proton transport mechanism of M2 proton channel studied by laser-induced pH jump. 2017, *J. Am. Chem. Soc.* 139, 6621.
84. Lin, C.-W., Mensa, B., Barniol-Xicotà, M., DeGrado, W. F., Gai, F. Activation pH and gating dynamics of influenza A M2 proton channel revealed by single-molecule spectroscopy. 2017, *Angew. Chem. Int. Ed.*, 56, 5283.
85. Mandala, V. S.; Liao, S. Y., Kwon, B., Hong, M. Structural basis for asymmetric conductance of the influenza M2 proton channel investigated by solid-state NMR spectroscopy. 2017, *J. Mol. Biol.*, 429, 2192.
86. Thomaston, J. L., Alfonso-Prieto, M., Woldeyes, R. A., Fraser, J. S., Klein, M. L., Fiorin, G., DeGrado, W. F. High-resolution structures of the M2 channel from influenza A virus reveal dynamic pathways for proton stabilization and transduction. 2015, *Proc. Natl. Acad. Sci. USA*, 112, 14260.
87. Thomaston, J. L., DeGrado, W. F. Crystal structure of the drug-resistant S31N influenza M2 proton channel. 2016, *Protein Sci.*, 25, 1551.
88. Hu, Y., Musharrafieh, R., Ma, C., Zhang, J., Smee, D. F., DeGrado, W. F., Wang, J. An M2-V27A channel blocker demonstrates potent in vitro and in vivo antiviral activities against amantadine-sensitive and -resistant influenza A viruses. 2017, *Antiviral Res.*, 140, 45.
89. Li, F., Ma, C., DeGrado, W. F., Wang, J. Discovery of highly potent inhibitors targeting the predominant drug-resistant S31N mutant of the influenza A virus M2 proton channel. 2016, *J. Med. Chem.*, 59, 1207.
90. Ma, C., Zhang, J., Wang, J. Pharmacological characterization of the spectrum of antiviral activity and genetic barrier to drug resistance of M2-S31N channel blockers. 2016, *Mol. Pharmacol.*, 90, 188.
91. Li, F., Hu, Y., Wang, Y., Ma, C., Wang, J. Expedient lead optimization of isoxazole-containing influenza A virus M2-S31N inhibitors using the Suzuki-Miyaura cross-coupling reaction. 2017, *J. Med. Chem.*, 60, 1580.
92. Tzitzoglaki, C., Wright, A., Freudenberger, K., Hoffmann, A., Tietjen, I., Stylianakis, I., Kolarov, F., Fedida, D., Schmidtke, M., Gauglitz, G., Cross, T. A., Kolocouris, A. Binding and proton blockage by amantadine variants of the influenza M2_{WT} and M2_{S31N} explained. 2017, *J. Med. Chem.*, 60, 1716.
93. Hu, Y., Wang, Y., Li, F., Ma, C., Wang, J. Design and expeditious synthesis of organosilanes as potent antivirals targeting multidrug-resistant influenza A viruses. 2017, *Eur. J. Med. Chem.*, 135, 70.
94. Nguyen, J. T., Smee, D. F., Barnard, D. L., Julander, J. G., Gross, M., de Jong, M. D., Went, G. T. Efficacy of Combined Therapy with Amantadine, Oseltamivir, and Ribavirin In Vivo against Susceptible and Amantadine-Resistant Influenza A Viruses. 2012, *PLoS One*, 7, e31006.

95. Seo, S., Englund, J. A., Nguyen, J. T., Pukrittayakamee, S., Lindegardh, N., Tarning, J., Tambyah, P. A., Renaud, C., Went, G. T., de Jong, M. D., Boeckh, M. Combination therapy with amantadine, oseltamivir and ribavirin for influenza A infection: safety and pharmacokinetics. 2013, *J. Antivir. Ther.*, 18, 377.
96. Li, F., Ma, C., Wang, J. Inhibitors targeting the influenza virus hemagglutinin. 2015, *Curr. Med. Chem.*, 22, 1361.